PNA/DNA chimeras for biotechnological applications

Giovanni Roviello

Dottorato in Scienze Biotecnologiche – XVIII ciclo
Indirizzo Biotecnologie Molecolari
Università di Napoli Federico II

Dottorato in Scienze Biotecnologiche – XVII ciclo
Indirizzo Biotecnologie Molecolari
Università di Napoli Federico II

PNA/DNA chimeras for biotechnological applications

Giovanni Roviello

Dottorando:	Giovanni Roviello
Relatore:	prof. Ettore Benedetti
Correlatore:	Dr. Enrico Bucci
Coordinatore:	Prof. Gennaro Marino

Alla mia famiglia

INDEX

Summary

Among the oligonucleotides analogues Peptide Nucleic Acids (PNAs) are the most powerful, with a *N*-(2-amino-ethyl)-glycine unit replacing the sugar-phosphate backbone.[1] They show strong and sequence specific hybridisation to complementary single stranded DNA and RNA[2] as well as to double stranded DNA by triplex formation.[3] In addition, this kind of DNA mimic is not degraded by nucleases and proteases[4] and was shown to have both good antisense and antigene activity.[5]
Although they have truly remarkable binding properties, pure PNAs present some problems: a limited water solubility and the inability to interact with DNA-binding proteins.

On the other hand chimeric molecules composed of a DNA region protected by a PNA moiety at 3' and/or 5' end (PNA/DNA chimeras) retain a good water solubility and the ability of DNA to interact with DNA-binding proteins; moreover, like PNAs, they are resistant to the exonuclease degradation.

PNA-DNA chimeras can be recognized by the DNA polymerase and can be used as primers for PCR reactions[6]; furthermore, double stranded molecules based on PNA-DNA chimeras bind to transcription factors in a sequence-dependent manner[7]
Despite their interesting characteristics, *in vivo* biological studies of PNA-DNA chimeras have been so far limited because of the difficulties associated with obtaining them in good amount, due to the synthetic problems in the routes to the monomers, linkers and oligomers. In the first part of my PhD thesis, I address this problem, as furthermore discussed in the next sections.
The second part of my thesis deals with the resolution of a different problem related to the usage of PNA/DNA chimeras in diagnostic applications. Specifically, the addressed problem is the production of a chimera which retains its diagnostic power, without risking of acting an antisense in the cellular contest. The selected diagnostic approach is that of the molecular beacons.

---

[1] a) Nielsen, P. E.; Egholm, M.; Berg, R. M.; Buchardt, O. Science 1991, 254, 1497; b) Egholm, M.; Buchardt, O.; Nielsen, P. E.; Berg, R. H. J Am Chem Soc 1992, 114, 1895; c) Nielsen, P. E.; Egholm, M.; Buchardt, O. Bioconjug Chem, 1994, 5, 3; d) Uhlmann, E.; Peyman, A.; Breipohl, G.; Will, D. W. Angew Chem Int Ed 1998, 37, 2796.
[2] Egholm, M.; Buchardt, O.; Christensen, L.; Behrens, C.; Freier, S. M.; Driver, D. A.; Berg, R. H.; Kim, S. K.; Norden B.; Nielsen, P. E. Nature 1993, 365, 566.
[3] Nielsen, P. E.; Egholm, M.; Buchardt, O. J Mol Recognit 1994, 7, 165.
[4] Demidov, V. V.; Potaman, V. N.; Frank-Kamenetskii, M. D.; Egholm, M.; Buchard, O.; Sonnichsen, S. H.; Nielsen, P. E. Biochem Pharmacol 1994, 48, 1310-3.
[5] a) Buchardt, O.; Egholm, M.; Berg R. H.; Nielsen, P. E. Trends in Biotechnology 1993, 11, 384-6; b) Nielsen, P. E.; Egholm, M.; Berg, R. H.; Buchardt, O. Anti-Cancer Drug Design 1993, 8, 53; c) Nielsen, P. E.; Egholm, M. Curr Issues Mol Biol 1999, 1, 89. Gambari, R. Curr Pharm Des 2001, 7, 1839; d) Nielsen, P. E. Curr Opin Mol Ther 2000, 2, 282; e) Ray, A.; Norden, B. Faseb J 2000, 14, 1041.
[6] Uhlmann, E.; Will, D. W.; Breipohl, G.; Langner, D.; Ryte, A. Angew Chem Int Ed 1996, 35, 2632.
[7] Uhlmann, E. Biol Chem 1998, 379, 1045.

A molecular beacon[8] is a DNA single strand composed of a loop region with a sequence complementary to the target DNA and a stem region in which the nucleotides are paired in a double strand. On the 5'- or 3'-terminus, respectively, a fluorophore and a quencher are linked. Fluorescence is quenched as long as the stem region is paired in a double strand. Upon their binding to complementary targets, molecular beacons adopt an open conformation in which the labels are spatially separated. As a result, molecular beacons brightly fluoresce in the presence of nucleic acid target sequences.
In order to protect the DNA loop from exonuclease degradation and avoid non specific sequence recognition by the stem region, we propose to use an alanyl peptide nucleic acid double stranded (alanyl-PNA) as the stem of a molecular beacon keeping the DNA recognition loop. Since the alanyl-PNA pairing system is orthogonal to oligonucleotides with respect to double strand formation, the overall system will have greater specificity and no risk of inducing an antisense effect due to the stem.

[8] a) S. Tyagi, F. R. Kramer, *Nat. Biotechnol*. **1996**, *14*, 303. b) S. Tyagi, D. Bratu, F. R. Kramer, *Nat. Biotechnol*. **1998**, *16*, 49; b) G. P. Pfeifer, *Technologies for Detection of DNA damage and mutations*, Plenum, New York, **1996**; c) G. R. Taylor, *Laboratory methods for the detection of mutations and polymorphisms in DNA*, CRC Press, Boca Raton, Fla, **1997**; d) V. V. Didenko, *In situ detection of DNA damage: Methods and protocols*, Humana Press, Totowa, New Jersey, **2002**; e) W. Tan, X. Fang, J. Li, X. Liu, *Chem. Eur. J.* **2000**, *6*, 1107.

Riassunto

Questo lavoro di tesi riguarda la sintesi di molecole ibride composte da porzioni di DNA e da altre a base di Acidi Peptido Nucleici (detti PNA da *Peptide Nucleic Acids*), dette Chimere PNA-DNA, e alcune possibili applicazioni biotecnologiche di queste utili molecole nell'ambito ambito terapeutico e diagnostico.
I PNA sono analoghi oligonucleotidici basati su un'unità ripetitiva di *N*-(2-amminoetil)glicina che porta la base eterociclica legata all'atomo di azoto della glicina mediante un ponte metilencarbonilico. I PNA riconoscono DNA ed RNA complementari in maniera specifica formando complessi molto stabili obbedendo allo schema di legame ad idrogeno di Watson-Crick con un'affinità maggiore rispetto ad oligonucleotidi convenzionali. Inoltre, il loro scheletro pseudopeptidico conferisce loro stabilità chimica e resistenza a degradazione enzimatica da parte di nucleasi o proteasi.

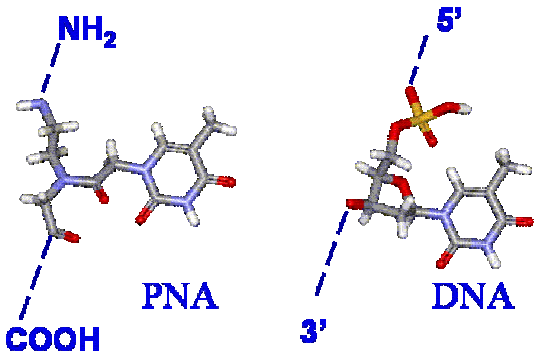

I PNA sono molto interessanti dal punto di vista biologico come agenti antisenso, per la loro capacità di inibire la traduzione riconoscendo mRNA complementari, come agenti antigene, per la modulazione della trascrizione e replicazione, come anticancro, in quanto inducono la riduzione di attività delle telomerasi. Altra applicazione consiste nell'individuazione di mutazioni genetiche, come nel caso della rivelazione del gene CFTR nella fibrosi cistica. I PNA, spostando singoli filamenti di DNA in *duplex*, permettono l'idrolisi di questi filamenti da parte di nucleasi specifiche. Si possono ottenere, perciò, degli enzimi di restrizione artificiali usando la nucleasi opportuna in combinazione con molecole di PNA. Nonostante le loro notevoli proprietà di ibridazione i PNA presentano alcuni limiti. Infatti, dato il loro carattere neutro, questi analoghi oligonucleotidici risultano scarsamente solubili in acqua. Inoltre, proteine regolative che normalmente si legno al DNA, non sono però in grado di interagire con i PNA. Infatti, come dimostrato da strudi strutturali, doppie eliche tra PNA ed acidi nucleici naturali o PNA/PNA mostrano una struttura molto diversa da quella delle corrispondenti *duplex* naturali.

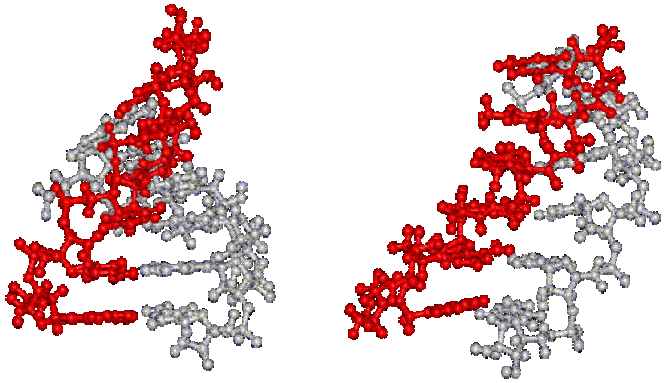

RNA duplex PNA:RNA duplex

Una possibile strategia per poter utilizzare oligonucleotidi per il legame con proteine regolative, in applicazioni *in vivo*, si basa sulla sintesi di sistemi misti in cui il DNA si trova protetto alle estremità 5' e 3' da porzioni di PNA. In questo modo si combinano la stabilità enzimatica dei PNA alla capacità del DNA di interagire con proteine, rendendo questi ibridi anche più solubili in acqua e migliorando l'*uptake* cellulare. Risultati incoraggianti provengono dall'utilizzo *in vitro* con un approccio *decoy* di duplex chimeriche PNA-DNA in grado di interagire stabilmente con il fattore nucleare NF-kB che gioca un ruolo chiave nel processo di trascrizione del genoma di HIV-1 legando la sequenza regolativa HIV-LTR (long terminal repeat). [Curr Drug Targets. 2004 Nov;5(8):735-44 Peptide nucleic acids (PNA)-DNA chimeras targeting transcription factors as a tool to modify gene expression. Borgatti M, Finotti A, Romanelli A, Saviano M, Bianchi N, Lampronti I, Lambertini E, Penolazzi L, Nastruzzi C, Mischiati C, Piva R, Pedone C, Gambari R.]

Nella prima parte della tesi si affronta l'interazione di chimere PNA/DNA con HMGB1, una proteina coinvolta in molti processi infiammatori come potente citochina e considerata, pertanto, un target terapeutico di grande interesse. HMGB1 è una proteina con una sequenza amminoacidica molto conservata tra i mammiferi ed è nota come proteina coinvolta nel mantenimento della struttura del nucleosoma e nella regolazione della trascrizione genica. La struttura di HMGB1 comprende tre domini: due domini per il legame del DNA (Box A e Box B) ed un'estremità carbossilica (coda acida). In particolare i domini Box A e Box B hanno una forma angolata (o a "L") e sono responsabili del legame di HMGB1 al *minor groove* del DNA, causando una locale distorsione della doppia elica.

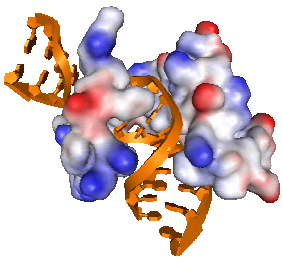

HMGB1 è secreta attivamente da monociti e macrofagi (rilascio specifico) ma è anche rilasciata passivamente da cellule necrotiche (rilascio non specifico). Questi due percorsi sono fondamentali per l'attività di HMGB1 come citochina. La secrezione di HMGB1 sembra essere indotta da due segnali ed aver luogo attraverso tre *step*: all'inizio un segnale infiammatorio promuove l'acetilazione di HMGB1, la sua rilocazione dal nucleo al citoplasma (*step* 1) ed il suo accumulo nelle vescicole secretorie presenti nel citoplasma (*step* 2); successivamente un segnale di secrezione (ATP extracellulare o lisofosfatidilcolina) promuove l'esocitosi (step 3) [Andersson et al., 2002; Scaffidi et al. 2002; Bonaldi et al., 2003; Friedman et al., 2003; Gardella et al., 2002].
Extracellularmente HMGB1 lega i recettori RAGE, TLR2 e TLR4 attivando diversi processi infiammatori. Perciò agenti terapeutici in grado di inibire il rilascio o l'azione di HMGB1 conferiscono una protezione significativa contro sepsi, endotossiemia ed artrite in modelli animali permettendo di affrontare così varie patologie infiammatorie.
La strategia presentata in questa tesi per l'inibizione di HMGB1 si basa su uno scambio di ligandi. In altre parole l'idea consiste nell'usare il ligando nucleare di HMGB1 (cioè il DNA) al di fuori della sua locazione naturale in modo da antagonizzare i ligandi extracellulari nel riconoscimento della stessa HMGB1 ed evitare gli effetti pro-infiammatori di questa citochina.

In questa strategia anti-HMGB1 inizialmente sono state considerate alcune *duplex* di DNA che presentavano una struttura preventivamente piegata in modo da trovarsi già nella condizione favorevole per l'interazione di legame con HMGB1. Sulla base di sequenze note in letteratura di DNA in legame con proteine omologhe di HMGB1, sono stati disegnate le seguenti sequenze di DNA:

24-mer 3' OH-GTTGCATTGAAAAAATTTCTTAGG-5'OH 18-mer 5'OH-CAACGTAAC - - - - - - AAAGAATCC-3'OH	6A
22-mer 3'OH-GTTGCATTGAAAATTTCTTAGG-5'OH 18-mer 5'OH-CAACGTAAC - - - -AAAGAATCC-3'OH	4A
20-mer 3'OH-GTTGCATTGAATTTCTTAGG-5'OH 18-mer 5'OH-CAACGTAAC - - AAAGAATCC-3'OH	2A
18'-mer 3'OH-GTTGCATTGTTTCTTAGG-5'OH 18-mer 5'OH-CAACGTAACAAAGAATCC-3'OH	0A

Nel caso di 6A, 4A e 2A i due filamenti, di differente lunghezza, risultano complementari a meno del tratto poliadeninico (dA_6, dA_4 e dA_2) nella parte centrale di uno dei due al fine di indurre una piegatura nella stuttura del DNA in forma *duplex* (*bent duplex*):

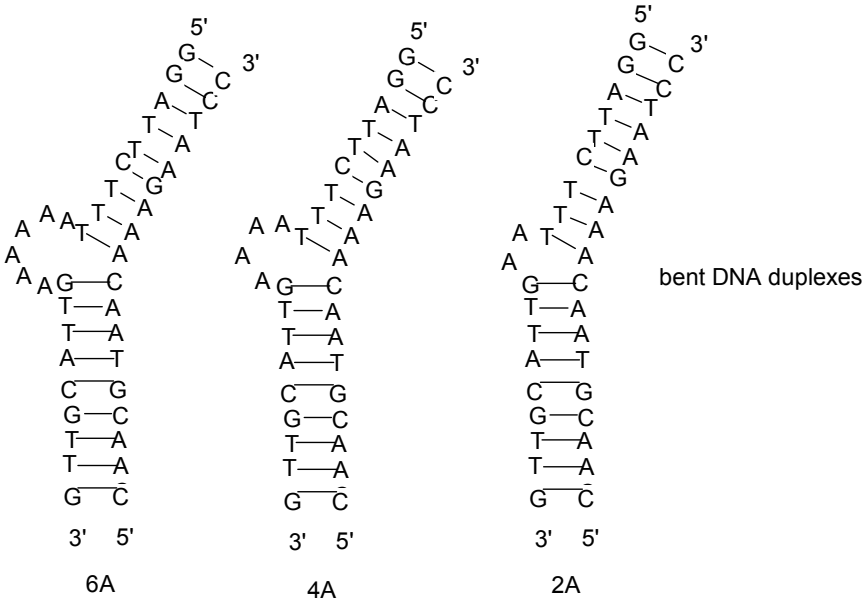

La *duplex* 0A (perfettamente complementare) è servita come riferimento in esperimenti effettuati successivamente.
Studi di *modelling* effettuati usando come dati di partenza le strutture note in letteratura di complessi di regioni omologhe a Box B con duplex di DNA sono stati eseguiti sulle 3 *bent duplex*. Da questi studi è stato evidenziato innanzitutto che la piegatura nelle *duplex* non è un effetto dovuto solo al legame con la proteina ma è già intrinsecamente dovuto alla presenza del *bulge*.

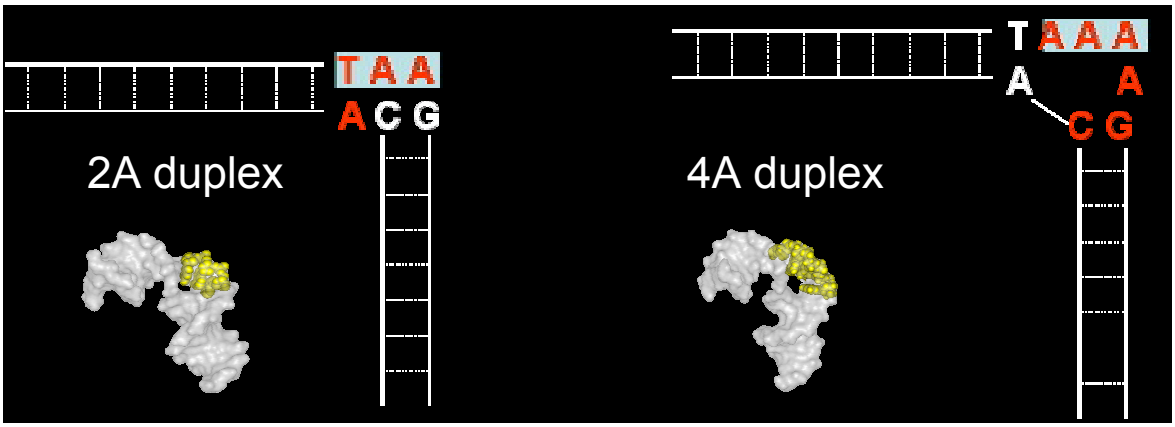

E' stato inoltre possibile rivelare una maggiore stabilità per la *duplex* 2A che presenta un maggior contributo di *stacking* per adenina contenuta nel *bulge* (nella struttura piegata del 2A si ha perdita dell'interazione tra una coppia di basi T-A, ma si ha un effetto stabilizzante di *stacking* tra le basi T-A-A impilate le une sulle altre). Nel caso di 4A solo 3 adenine su 4 nel *bulge* danno luogo allo *stacking* e si ha perdita dell'interazione tra una coppia di basi C-G (con perdita di ben 3 legami H). Nel caso del 6A non è stato possibile ottenere nessuna struttura stabile che contenesse un *bulge* con 6 adenine. In

conclusione dagli studi di *modelling* è stato possibile dedurre che la *duplex* 2A, che presenta il contributo di *stacking* per adenina maggiore, è quella più stabile.
I DNA progettati sono stati ottenuti mediante sintesi in fase solida su un sintetizzatore automatico Expedite 8909, utilizzando come supporto solido una resina CPG, funzionalizzata con il primo monomero nucleotidico all'estremità 3'. Utilizzando tali filamenti, mediante procedure di *annealing*, sono state ottenute le duplex corrispondenti.
Le *duplex* così ottenute sono state studiate mediante Dicroismo Circolare (CD) in esperimenti che hanno rivelato l'andamento di stabilità gia previsto dal *modelling* con una diminuzione della stabilità all'aumentare delle dimensioni del *bulge*. Gli "spettri dei *bulge*" sono stati, inoltre, ottenuti sottraendo lo spettro CD dello 0A a quelli relativi a 6A, 4A e 2A e normalizzando per il numero di A presenti nel *bulge*.

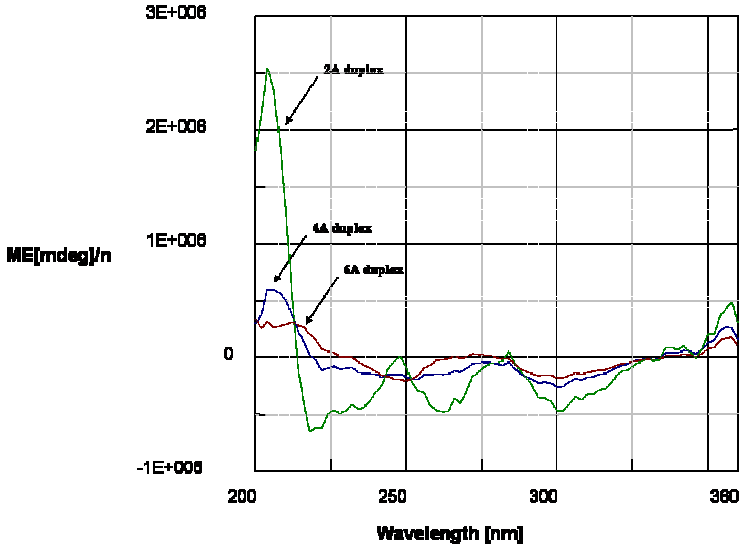

Da questi esperimenti è stato evidenziato che il contributo di *stacking* per adenina risulta più grande nel caso del 2A, come già previsto dagli studi di *modelling*.
La formazione dei complessi con la proteina per 6A, 4A e 2A è stata dimostrata dal fatto che gli spettri relativi alla somma dei contributi CD di proteina e DNA risultano differenti da quelli ottenuti dopo il mescolamento, mediante speciali *cuvette* a doppia camera.
La maggiore differenza ottenuta sottraendo i due spettri si ha nel caso del 6A che rappresenta la *bent duplex* che richiede la maggiore riorganizzazione strutturale per poter legare HMGB1.
La stabilità termica dei complessi proteina/*bent* DNA è stata ottenuta mediante esperimenti di *melting* via CD. Anche nel caso dei complessi, la stabilità diminuisce all'aumentare della lunghezza del bulge, come evidenziato dalle Tm che rispecchiano l'andamento dei DNA non legati.

	6A	4A	2A
Tm Free	31.40	34.40	36.99
Tm Comp	34.81	39.08	40.5
ΔTm	3.41	4.68	3.5

Il complesso *duplex*/HMGB1 più stabile risulta quindi essere quello relative al 2A con una Tm di 40 °C. Proprio sul 2A è stata effettuata la titolazione con la proteina per studiare la affinità di legame (K_d = 25 10^{-9} M).
Il miglior candidato per l'utilizzo terapeutico anti-HMGB1 risulta quindi essere la *duplex* piegata contenente 2 adenine. Non è però possibile utilizzare tale *duplex* formata da DNA naturale *in vivo*, in quanto verrebbe velocemente degradato. Abbiamo quindi realizzato una *duplex* chimerica PNA/DNA per ottenere maggiore resistenza all'azione degradativa delle nucleasi seriche. Tali chimere sono formate da due filamenti di DNA contenenti una porzione di PNA all'estremità 3'(5'DNA-PNA3'). Le chimere 3' risultano più resistenti alla degradazione enzimatica rispetto alle corrispondenti PNA-5'DNA3', poiché in siero le 3' esonucleasi sono più abbondanti delle 5' esonucleasi[22].
La *duplex* chimerica col *bulge* contenente 2 adenine è stata ottenuta grazie alla sintesi dei seguenti filamenti:

20-mer COOH-ctt*GCATTGAATTTCTTAGG-5'OH Chim 2A
18-mer 5'OH-GAACGTAAC - - AAAGAA*tcc-COOH

Esperimenti di spettroscopia UV e CD sono stati effettuati per verificare la formazione della *duplex* e per determinare la temperatura di *melting*. Inoltre da studi di stabilità enzimatica in siero umano è stato dimostrato che la *duplex* Chim 2A risulta 18 volte più resistente della duplex naturale corrispondente.
L'inibizione di HMGB1 da parte di Chim 2A è stata verificata mediante esperimenti cellulari (su cellule BAEC) in cui la migrazione e proliferazione cellulare indotta da HMGB1 è ridotta drasticamente in presenza di Chim 2A (IC50~10 nmol/L).
Infine migliorando i protocolli sintetici relativi all'ottenimento di monomeri di PNA tritilati(nota), compatibili con la sintesi del DNA, ed ottimizzando i protocolli per l'ottenimento di filamenti chimerici su larga scala, è stato possibile ottenere quantità di *duplex* chimeriche sufficienti per esperimenti *in vivo*, mai realizzati prima d'ora su chimere PNA/DNA.
La seconda parte di questa tesi, sviluppata presso l'Institut für Organische und Biomolekulare Chemie della Georg-August-Universität di Göttingen sotto la direzione del Prof. Dr. Ulf Diederichsen, tratta di chimere alanil PNA-DNA-alanil PNA da utilizzarsi in diagnostica molecolare in un approccio di *molecolar beacon* (nota) per la rivelazione di sequenze oligonucleotidiche.

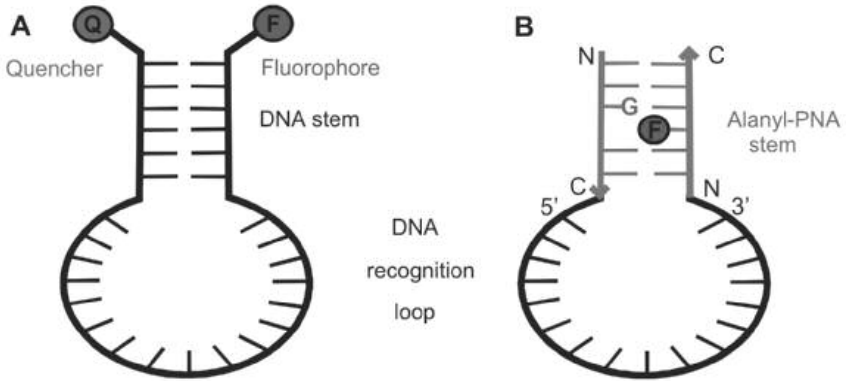

La novità rispetto ai *molecular beacon* tradizionali (a base cioè unicamente di DNA, lettera A in figura) risiede nella possibilità di evitare fenomeni di riconoscimento non specifico dovuti allo *stem* grazie al fatto che gli alanil PNA sono in grado di formare complessi stabili con alanil PNA complementari (seguendo lo schema di legame ad idrogeno di Watson-Crick), ma non ibridano sequenze oligonucleotidiche naturali complementari. In questo modo si ha apertura del *molecolar beacon,* e comparsa del fenomeno della fluorescenza, unicamente in seguito al riconoscimento di sequenze *target* da parte del *loop*.
Altre caratteristiche utili di questo sistema diagnostico innovativo sono l'utilizzo di una guanina come *quencher* e la protezione dalla degradazione nucleasica in siero del sistema dovuta alla presenza dei tratti di alanil PNA.
E' stata dunque effettuata la sintesi dei nuovi monomeri di alanil PNA (1-4) con protezioni Mmt (Monometossitritile)/acile e pertanto adatti alla sintesi di chimere alanil PNA/DNA, per tutte e quattro le basi azotate.

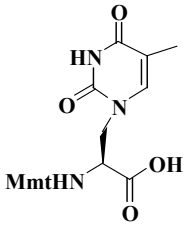

1

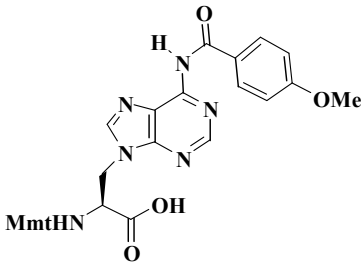

2

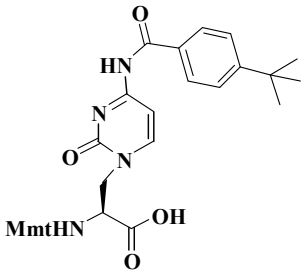

3

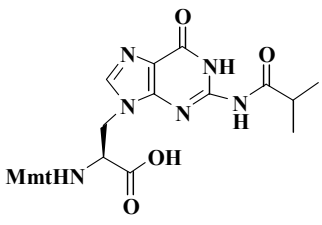

4

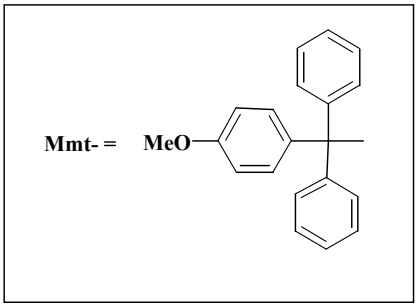

La sintesi enantioselettiva descritta in questa tesi parte dal lattone della (L)-Boc Serina e ha fornito i quattro monomeri, dopo rimozione del gruppo Boc e riprotezione con il gruppo Mmt, già pronti per la sintesi in fase solida delle chimere il cui assemblaggio è al momento in corso di realizzazione presso una azienda privata per conto dello stesso ateneo tedesco.

PART 1

PNA/DNA chimeras for the inhibition of HMGB1, a DNA-binding protein involved in inflammatory processes

1.1 The therapeutic target: HMGB1 protein

1.1.1 Introduction.

Sepsis, a lethal systemic inflammatory response to infection, is a severe illness affecting nearly 750,000 patients in the United States annually with a mortality of 30% and for this reason is among the top ten causes of death in the United States today. A series of recent discoveries showed the importance of cytokines, circulating factors produced by the innate immune system, acting as mediators of sepsis-related tissue injury and death. Many resources have been expended to elucidate the pathologic mechanisms that underlie sepsis and to develop appropriate and effective therapeutics. Unfortunately even a slight delay in administration of therapeutics targeting inflammatory mediators renders most approaches ineffective; for this reason, to date, no anti-inflammatory agent has been clinically approved for the treatment of sepsis. These and other findings, described in part in the following discussion, have suggested that successful clinical management of sepsis may be dependent on targeting, in a broader therapeutic window, those agents identified as late-acting, downstream lethal mediators. One of these candidate mediators of delayed lethality is high mobility group box 1 (HMGB1 formerly known as HMG-1), a cellular and nuclear protein that is now recognized as a cytokine and experimental therapeutic target.
Recently an improved understanding was achieved of the pathogenic mechanisms in the field of sepsis. In the early stages, for instance, bacterial endotoxins stimulate cells of the innate immune system wich release pro-inflammatory cytokines (TNF, IL-1α and IL-6). These early cytokines, in turn, induce the release of a later acting downstream mediator – identified as the known protein HMGB1 – that triggers the pathological sequelae mediated by the subsequent release of cytokines like TNF, IL-1α, IL-1β, IL-1Ra, IL-6, IL-8, etc., leading to a multisystem pathogenesis or to a lethal systemic inflammation[9]. Furthermore, other proteins belonging to the family of HMG-proteins and able to bend DNA are released together with HMGB1 in the extracellular medium. These proteins are inter alia HMGB2, HMGB3, HMG-1L10, HMG-4L and SP100-HMG. They share with HMGB1 highly homologous amino acid sequences. Like HMGB1, they trigger/sustain inflammatory pathologies interacting with the same receptors and leading to the same downstream pathways of interaction

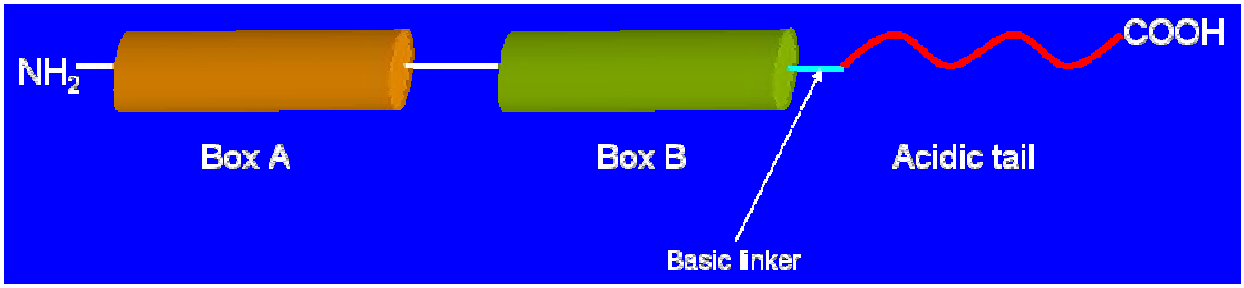

[9] Andersson, U., Erlandsson-Harris, H., Yang, H and Tracey, K.J. (2002) HMGB1 as a DNA-binding cytokine. J. Leukocyte Biol., 72:1084-1091

Figure 1: HMGB1 is made of three independent domains.

HMGB1, formerly named HMG1 but also known as amphoterin and sulphoglucuronyl carbohydrate-binding protein [SBP-1], together with homologous HMGB2 is an abundant (~10^6 molecules/cell), ubiquitous protein present in the nucleus (where it is associated with eukaryotic chromatin) and in the cytoplasm of mammalian cells. HMGB1 homologous proteins are present in organisms other than vertebrates (e.g. HMGD in *Drosophila melanogaster*, Nhp6A in *Saccharomyces cerevisiae*, HMGa in maize) and have only a single HMG box which may (as in in *Drosophila melanogaster*) or may not (as in *Saccharomyces cerevisiae*) present an acidic tail. Single HMG-box domain proteins present in plants can contain basic extensions, at N-terminus and sometimesm at C-terminus of the HMG box, and short C-terminal acidic tails. HMG boxes, in single copies and not accompanied by acidic tails, are also found in several transcription factors[10].

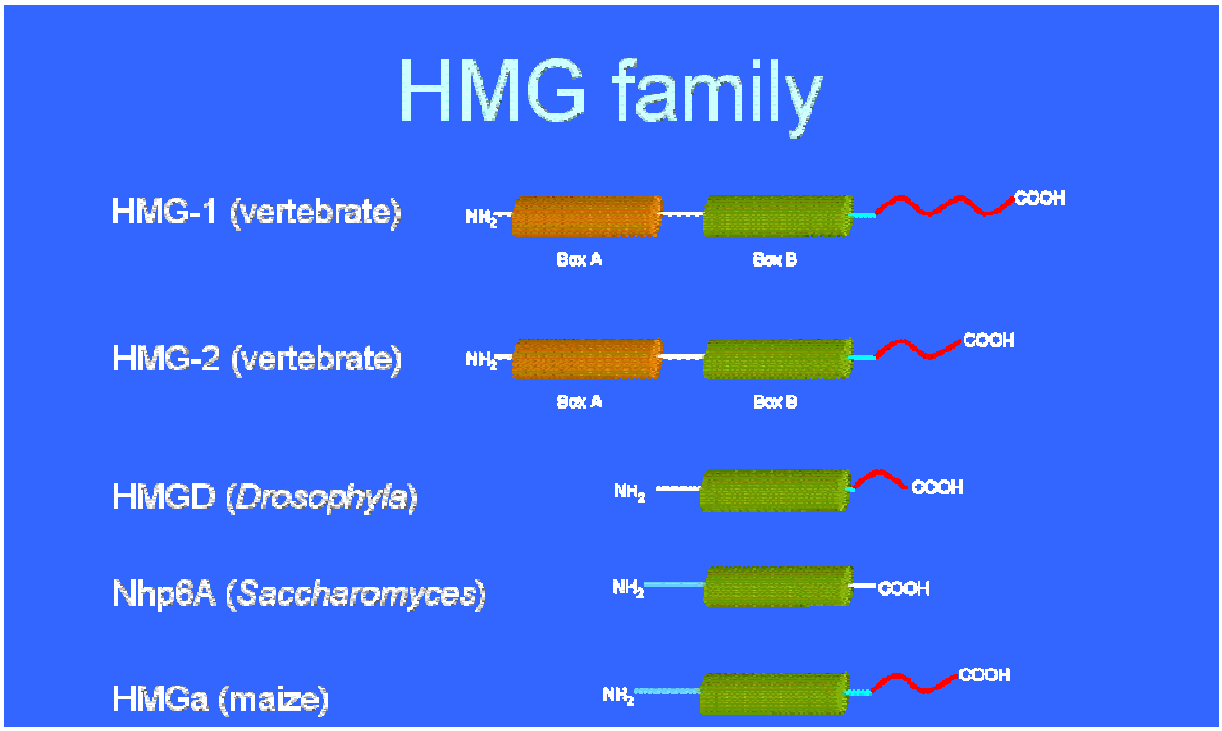

Figure 2 HMG family: HMGB1 and other homologous proteins.

[10] Biochem. Soc. Trans. (2001) 29, (395–401) HMG1 and 2: architectural DNA-binding proteins J. O. Thomas.

HMGB1 is only 10 times less abundant than core histones. It can be found in fibroblasts, neurons, hepatocytes, glia and in cells derived from hematopoietic stem cells, including monocytes/macrophages, neutrophils and platelets. HMGB1 protein is a ca. 25 kDa protein with a highly conserved sequence among mammals, whereby 2 out of 214 amino acids have conservative substitutions in all mammalian species Its name means "High Mobility group Box 1" and simply derives from its electrophoretic mobility in SDS-polyacrylamide gels. HMGB1 does not present any enzymatic activity on its own, but requires the assistance of other protein factors that in many cases show very little, if any, similarity in sequence or structure. It is traditionally known as a DNA binding protein involved in maintenance of nucleosome structure and regulation of gene transcription. HMGB1 molecule has a tripartite structure composed of three distinct domains: two DNA binding domains and an acid carboxyl terminus, making it bipolarly charged.

1.1.2 Box A and Box B domains bind DNA.

The three different domains that constitute HMGB1 structure are: two homologous DNA-binding regions called Box A and Box B, having remarkably similar three dimensional structure, and a negatively charged C terminus (Acidic Tail). The structure that these two domains adopt in the complexes with DNAs comprises three α-helices (I, II and III) connected by two loops. Interactions of helices I and II, and interactions between helix III and the N-terminal strand are stabilised by clusters of highly conserved hydrophobic residues[11].

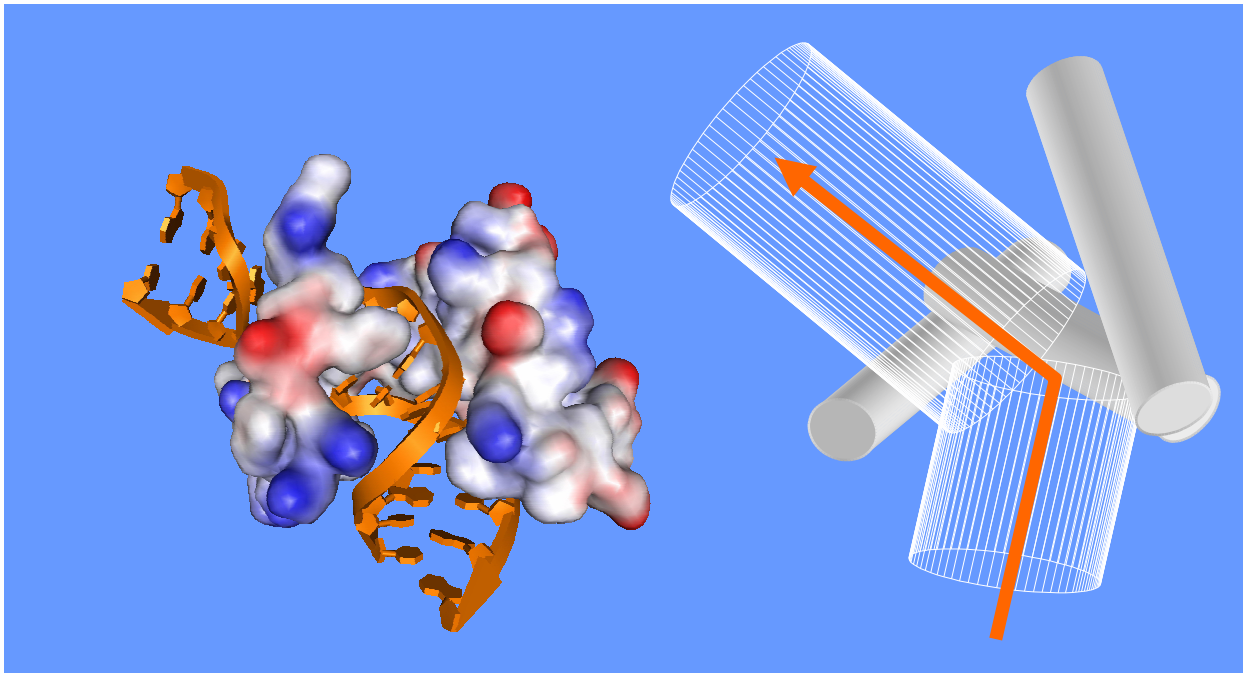

[11] *Nature* 399, 708 - 712 (17 June 1999); Basis for recognition of cisplatin-modified DNA by high-mobility-group proteins Uta-Maria Ohndorf, Mark A. Rould, Qing HE, Carl O. Pabo & Stephen J. Lippard

Figure 3a Representation of Box B-DNA binding.

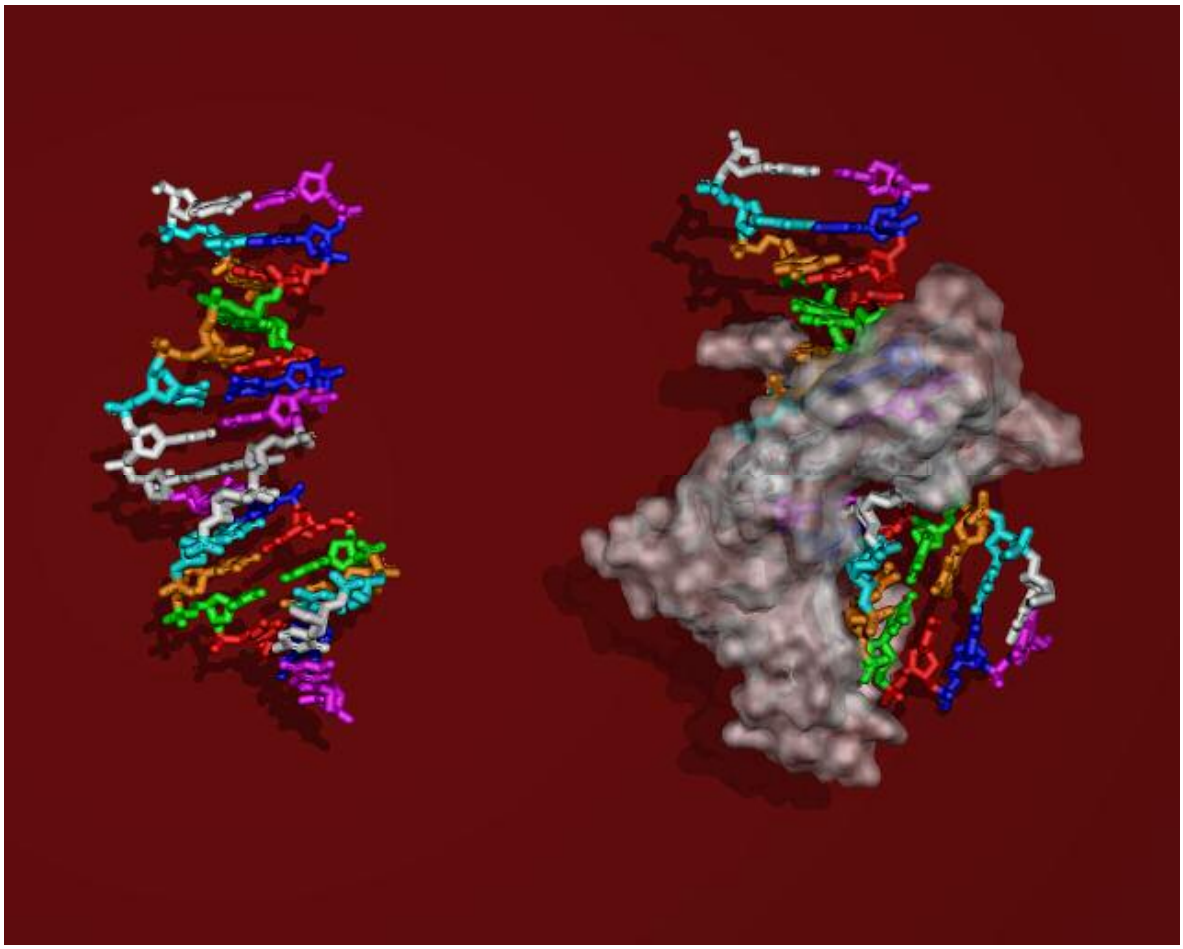

Figure 3b DNA deformation induced by Box B-DNA binding.

Every box domain shows an angular shape (or L shape) and allow HMGB1 to bind to the minor groove of DNA, causing a local distortion of the double helix.
By this interaction the protein induces a DNA bend angle of 90-120°. Binding is not sequence–specific[12]. In the Box B domain resides the proinflammatory cytokine functionality of HMGB1, whereas the DNA-binding Box A region has an anti-inflammatory effect and specifically antagonizes the activity of HMGB1.

1.1.3 The role of HMGB1 protein in nuclear processes.

For a long time, HMGB1 function was not clear and many research groups suggested different roles for this protein in nuclear processes as transcription, V(D)J recombination, DNA replication, DNA repair and nucleosome assembly. HMGB1 directly interacts with a

[12] Toshihiro Imamura, Hiroto Izumi, Gunji Nagatani, Tomoko Ise, Minoru Nomoto, Yukihide Iwamoto, and Kimitoshi Kohno J. Biol. Chem., Vol. 276, Issue 10, 7534-7540, March 9, 2001

number of proteins, including some HOX and POU domain transcription factors and the TATA-binding protein, and facilitate their binding through protein–protein interactions. HMGB1/2 were shown to enhance immunoglobulin V(D)J recombination by enforcing specific DNA recognition through their interaction with the RAG1/2 recombinase complex, and facilitating cleavage.
HMGB1 plays an architectural role in DNA bending, looping, folding and wrapping by distorting, bending or modifying complexes of DNA structures with transcription factors or histones[13].
As a nuclear protein, HMGB1 stabilizes nucleosomes and acts as a transcriptional regulatory molecule. In fact it causes DNA separation from the histone, in a mechanism seeing a key role of the Acidic Tail domain, and facilitates the binding of several transcriptional complexes.
Through its DNA-binding domains HMGB1 binds DNA in a manner that does not depends on sequence, but on the presence of certain DNA structures including four-way junctions (cruciform DNA) and undertwisted DNA. HMGB1 protein facilitates self-ligation of short DNA fragments, and can bridge linear DNA fragments thereby enhancing multimerization of longer DNAs. Together with the closely related HMGB2 protein, HMGB1 has been implicated in a number of eukaryotic cellular processes mediated by DNA recognition including gene regulation, DNA replication and recombination.

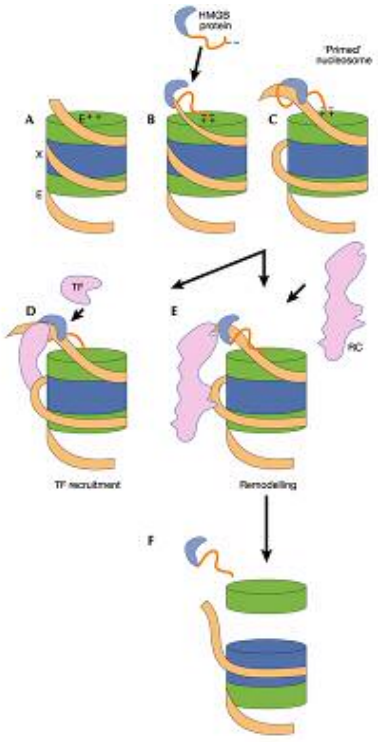

Figure 4 HMGB1-DNA interaction facilitates binding of transcription factors to DNA.

[13] a) Agresti, A. and Bianchi, M.E. (2003) HMGB-proteins and gene expression. Current Opin. In Genetics and Develop., 13: 170-178; b) Degryse, B., de Virgilio, M. (2003) The nuclear protein HMGB1, a new kind of chemokine ? FEBS Letters, 553:11-17

1.1.4 The extracellular presence of HMGB1 protein in serum.

Beyond its intracellular location, HMGB1 is also found extracellularly. HMGB1 is actively secreted by monocytes and macrophages (specific release) but is also passively released from necrotic cells from any tissue (non specific release). These two pathways are fundamental for the activity of HMGB1 as a cytokine and provide key mechanisms integrating the inflammatory response to infectious and non-infectious cell injuries. Extracellular presence of HMGB1 is due to a mechanism in which inflammatory cells sense the tissue damage by recognising the presence of nuclear proteins in the extracellular milieu. Subsequently, during the evolution of the immune system specialised cells developed a signalling system that could lead to a strong inflammatory process by releasing HMGB1 following specific events, as outlined in the next few lines. In healthy cells, HMGB1 migrates to the cytoplasm both by passive and active transport. However, all cultured cells and resting monocytes contain the vast majority of HMGB1 in the nucleus, indicating that in basal conditions import is much more effective than export. Cells might transport HMGB1 from the nucleus by acetylating lysine residues which are abundant in HMGB1, thereby neutralizing their basic charge and rendering them unable to function as nuclear localization signals as was recently suggested by Bonaldi et al[14]. Nuclear HMGB1 hyperacetylation determines the relocation of this protein from the nucleus to the cytoplasm (in the fibroblasts, for example) or its accumulation into secretory endolysosomes (for example in monocytes and macrophages stimulated by IL-1, Ifnγ, TNFα or LPS) and subsequent redirection towards release through a non-classical vesicle mediated secretory pathway. HMGB1 secretion by activated monocytes is triggered by bioactive lysophosphatidylcholine (LPC), which is generated later in the inflammation site from phosphatidylcholine through the action of the secretory phospholipase sPLA2, produced by monocytes several hours after activation. Therefore, secretion of HMGB1 seems to be induced by two signals[14] and to take place through three steps: 1) at first, an inflammatory signal promotes HMGB1 acetylation and its relocation from the nucleus to the cytoplasm (step 1) and storage into cytoplasmic secretory vesicles (step 2); then, a secretion signal (extracellular ATP or lysophosphatidylcholine) promotes exocytosis (step 3)[9,14]
HMGB1 is released from activated innate immune cells or necrotic cells and functions as an important mediator of sepsis, endotoxemia, arthritis, and local inflammation. Thus, strategies targeting HMGB1 with specific antagonists or antibodies have big importance for treating lethal systemic inflammatory diseases characterized by excessive HMGB1 release.

[14] a) Monocytic cells hyperacetylate chromatin protein HMGB1 to redirect it towards secretion Tiziana Bonaldi[1,2], Fabio Talamo[1], Paola Scaffidi[3], Denise Ferrera[4], Annalisa Porto[1,5], Angela Bachi[1], Anna Rubartelli[4], Alessandra Agresti[1,6], and Marco E. Bianchi[3,6] The EMBO Journal, Vol. 22, No. 20 pp. 5551-5560, 2003; b) Release of chromatin protein HMGB1 by necrotic cells triggers inflammation.Scaffidi, P., Misteli, T. and Bianchi, M.E. (2002) Nature, 418:191-195; c) The gesture life of high mobility group box 1. Friedman, S.G., Czura, C.J. and Tracey, K.J. (2003) Current Opinion in Clinical Nutrition and Metabolica Care, 6:283-287; d) The nuclear protein HMGB1 is secreted by monocytes via a non-classical, vesicle-mediated secretory pathway.Gardella, S., Andrei, C., Ferrera, D., Lotti, L.V., Torrisi, M.R., Bianchi, M.E. and Rubarteli, A. (2002) EMBO. Rep., 3:995-1001

Therapeutic agents that inhibit HMGB1 action or release confer significant protection against sepsis, endotoxemia, and arthritis in animal models and thus hold potential for the clinical management of various inflammatory diseases.

1.1.5 The role of HMGB1 protein as a cytokine.

Extracellular HMGB1 acts as a powerful cytokine and as an extremely powerful macrophage-stimulating factor. HMGB1 acts directly by binding to the cell membrane inducing signaling and chemotaxis, having a chemokine-like function (Yang et al., 2001), and further acting indirectly by up-regulating the expression and secretion of pro-inflammatory cytokines. This makes extracellular HMGB1 a powerful chemotactic and immunoregulatory protein, which promotes an effective inflammatory immune response.
For HMGB1 the transduction of the receptor signal occurs in part through RAGE (Receptor for Advanced Glycation End-products), that is expressed on monocytes and macrophages, neurons, endothelial cells, and smooth muscle cells. Released HMGB1 has been identified as one of the ligands binding to the RAGE receptor. This receptor is expressed at a high level mainly in endothelial cells, in vascular smooth muscle cells, in monocytes and monophages and in mononuclear phagocytes. Recognition involves the C-terminal of HMGB1. The interaction of HMGB1 and RAGE triggers a sustained period of cellular activation mediated by RAGE up-regulation and receptor-dependent signaling. In particular, the interaction of HMGB1 and RAGE activates several intracellular signal transduction pathways, including mitogen-activated protein kinases (MAPKs), Cdc-42, p21ras, Rac and the nuclear translocation factor kB (NF-kB), the transcription factor classically linked to inflammatory processes (Schmidt et al., 2001).
According to several experimental evidences, released HMGB1 may also interact with the receptors belonging to the family of the Toll-like receptors (TLR), e.g. with the subclasses TLR2, TLR4, TLR7, TLR8 or/and TLR9.
Furthermore, HMGB1 may also interact with the functional N-terminal lectin-like domain (D1) of thrombomodulin. Due to the ability of the functional D1 domain of thrombomodulin to intercept and bind circulating HMGB1, the interaction of the HMGB1 with the RAGE receptors and the Toll-like receptors is prevented.
When released *in vivo*, HMGB1 is an extremely powerful cytokine and a powerful macrophage-stimulating factor and activates *in vitro* a cascade of multiple proinflammatory cytokines (TNF, IL-1α, IL-1β, IL-1Ra, IL-6, IL-8, MIP-1α and MIP-1β) from human macrophages.
HMGB1 is a late-acting cytokine, appearing in the extracellular milieu with a peak around 10 hours after the initial response of macrophages to pro-inflammatory stimulation. Knowledge of the role that HMGB1 plays as a cytokine is important for understanding regulation of delayed innate immune responses, downstream cytokine cascades, and constitutes the basis for targeting treatment strategies towards these processes. A window of clinically relevant opportunities allowing rescue from lethal sepsis comes from the delayed but effective treatment with HMGB1 blockade up to 1 day after induction of experimental sepsis. When added to macrophage cultures, HMGB1 activates the release of other cytokines and stimulates the autocrine production of the same HMGB1 and RAGE. Furthermore, when released into the extracellular milieu, HMGB1 causes systemic inflammatory responses including acute lung injury, epithelial barrier dysfunction, and death. It was also observed that passive immunization

with anti-HMGB1 antibodies confers significant protection against lethality induced by LPS administration and sepsis caused by cecal perforation in mice. Moreover, High Mobility group Box 1 protein mediates endotoxin lethality, arthritis induction, activation of macrophages, smooth muscle cell chemotaxis, and epithelial cell barrier dysfunction.
Its observed *in vitro* pro-inflammatory effects and correlation between circulating HMGB1 levels and the development of the pathogenic sequence of systemic inflammation *in vivo* indicate that therapeutically targeting HMGB1 should be of relevant clinical value, suggesting novel therapeutic approaches by a “late” administration of antagonists/inhibitors of the extracellular activities of HMGB1.

1.1.6 HMGB1 recognition of TLR2, TLR4 and RAGE receptors.

HMGB1 potentially activates multiple membrane receptors like RAGE, TLR2, and possibly TLR4. RAGE (Receptor for Advanced Glycation End Products) is a multiligand member of the immunoglobulin superfamily of cell surface molecules that interacts with distinct molecules implicated in inflammation. RAGE stucture consists of three immunoglobulin-like regions, one "V"-type region (containing 9 β-strands connected by several loops) followed by two "C"-type domains (containing 7, or more rarely 8, β-strands connected by loops in a manner different from the case of "V"-type domain)[15].

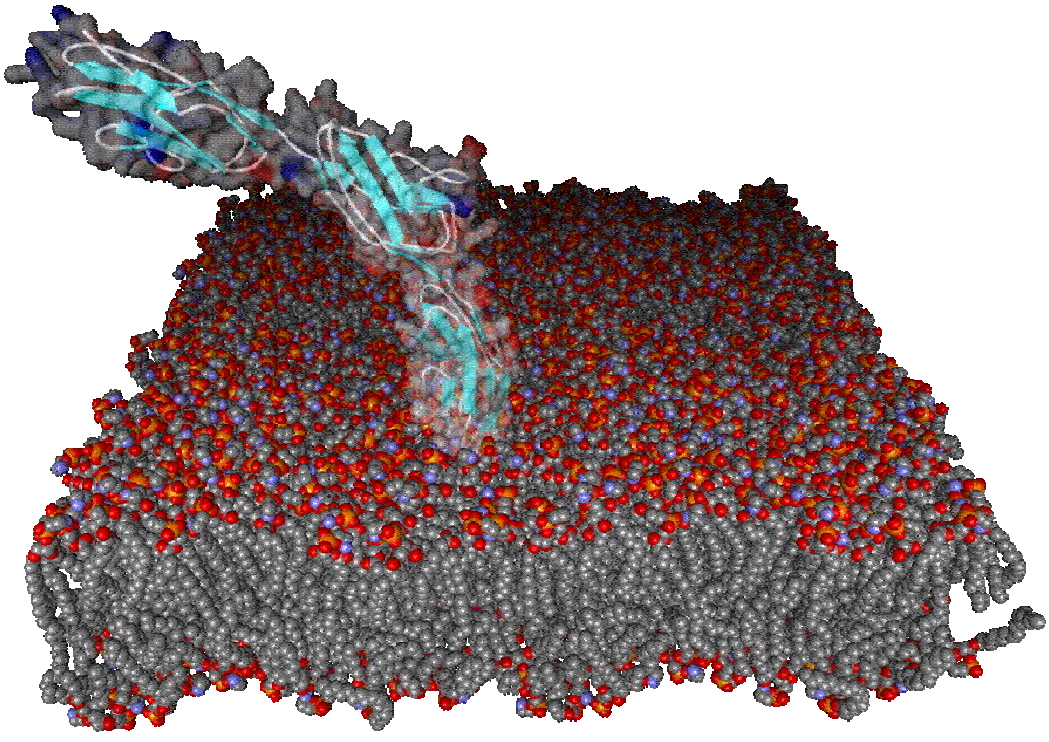

Figure 5: Representation of RAGE structure.

[15] Understanding RAGE, the receptor for advanced glycation end products; J Mol Med (2005) 83: 876–886 Angelika Bierhaus . et al.

RAGE contains a single transmembrane spanning domain and a 43 amino acid cytosolic tail. Structure-function studies suggested that V-domain is important for ligand binding, while that the cytosolic tail is essential for RAGE-mediated intracellular signalling.
HMGB1-RAGE interaction activates MAP kinases pathways, and subsequently causes the nuclear translocation of NF-κB, a central regulator of inflammatory responses. Inhibition of HMGB1-RAGE interaction suppressed activation of several MAP kinases and decreased growth of metastases *in vivo*[16].
Other HMGB1 receptors include Toll-like Receptor 2 (TLR2) and TLR4. Toll-like receptor (TLR) family members are transmembrane proteins having the function to activate immune responses by recognising molecular structures found in a variety of microbial pathogens. Some experimental evidences indicate that TLR2 leads to increased secretion of TNF-α (cytokine inducine HMGB1 release), IL-6, IL-12, and MIP-2 proinflammatory cytokines.
Activation of TLR2 and TLR4 by HMGB1 causes recruitment of IL-1 receptor associated kinase (IRAK) and MyD88, which subsequently activates the MAP kinases pathway and then NF-κB translocation[17] (ref).

1.1.7 Strategies for blocking HMGB1 chemokine-protein.

Several strategies were explored to block HMGB1 extracellular chemokine-protein. Among the many approaches it is useful to remember the administration of antibodies against HMGB1, of antibodies to RAGE, of soluble RAGE (sRAGE), of HMGB1 fragments (HMGB1 A Box) and of ethyl pyruvate (Czura et al., 2003; Lotze et al., 2003).
The passive immunization of mice by using HMGB1-neutralizing antibodies conferred a highly significant and lasting protection against lethal doses of endotoxin, even when the first doses of antibodies were given after the TNF peak had passed, and suggested that an effective treatment approach to potentially lethal sepsis resides in antagonizing HMGB1 activity late in the clinical course.
Another possibility is the administration of antibodies against the HMGB1 Box B, or its 20 amino acid relevant core which signals through RAGE[18]. Furthermore, HMGB1 Box A, one of the two DNA-binding domains in HMGB1, has been identified as a specific antagonist of HMGB1: highly purified recombinant Box A protected mice from lethal experimental sepsis even when initial treatment was delayed for 24 hours after pathology induction, further suggesting that HMGB1 antagonists may be administered successfully in a clinically relevant window wider than that one used for other known cytokines. Box A domain of HMGB1 competitively displaces the saturable binding of HMGB1 to macrophages, specifically antagonizing HMGB1 activities. As already seen for the protective activity of anti-HMGB1 antibodies, the administration of the Box A rescues mice from sepsis even when treatment initiated as late as 24 hours after surgical induction of sepsis. Moreover, saturation of circulating HMGB1 by the

[16] Blockade of RAGE-amphoterin signalling suppresses tumour growth and metastases.Taguchi A, Blood DC, del Toro G, et al. Nature. 2000;405:354-360
[17] The Cytokine Activity of HMGB1 - Extracellular Escape of the Nuclear Protein Nian-Kang Sun, PhD; Chuck C.-K. Chao Chang Gung Medical Journal REVIEW ARTICLE Vol. 28 No. 10 October 2005 673
[18] HMGB1 as a cytokine and therapeutic target; Yang H.[1]; Wang H.[1]; Czura C.J.[1]; Tracey K.J.; Journal of Endotoxin Research, Volume 8, Number 6, December 2002, pp. 469-472(4)

administration of sRAGE blocks its activities mediated by cellular RAGE. The same result can be also obtained by inhibiting RAGE itself by the administration of anti-RAGE antibodies.
Finally, a similar protective response late in the course of sepsis was obtained by administering ethy pyruvate, a stable lipophilic molecule and relatively non-toxic food additive, that attenuates the systemic inflammation of ischemia/reperfusion tissue injury and lethal hemorrhagic shock. Among its positive effects Ethyl-pyruvate inhibited HMGB1 and TNF release *in vitro* from endotoxin-stimulated murine macrophages, while *in vivo* protected mice from peritonitis-induced lethal sepsis.
However these therapeutical approaches present some problems: for example is difficult to obtain good quantities of pure Box A protein (even by recombinant approach) due to its characteristics; anti HMGB1 antibodies can recognise differently HMGB1 produced by different cells of the same organism as reported in literature in an example where anti-HMGB1 antibodies in serum did not recognize HMGB1 in neutrophils while they recognised HMGB1 produced by lymphocytes[19]. Limits for the use of ethyl piruvate come from the absence of informations about its action mechanism; furthermore, ethyl piruvate activity is also lower than that showed by anti HMGB1 antibodies[20].
Thus, a new approach was explored in this thesis based on the use of DNA or DNA like molecules effording to a significative contribute in the field of anti HMGB1 therapeutics as described in the next sections.

[19] Conformational Difference in HMGB1 Proteins of Human Neutrophils and Lymphocytes Revealed by Epitope Mapping of a Monoclonal Antibody; Ichiaki Ito, Nobuyoshi Mitsuoka, Junko Sobajima, Hiroko Uesugi, Shoichi Ozaki, Kazuhiko Ohya and Michiteru Yoshida. *J. Biochem.* 136, 155–162 (2004).
[20] Ethyl pyruvate prevents lethality in mice with established lethal sepsis and systemic inflammation PNAS Luis Ulloa, Mahendar Ochani, Huan Yang, Mahira Tanovic, Daniel Halperin, Runkuan Yang, Christopher J. Czura, Mitchell P. Fink and Kevin J. Tracey| September 17, 2002 | vol. 99 | no. 19 | 12351-12356

1.2 DNA duplexes as HMGB1 inhibitors.

1.2.1 The idea: to use the nuclear ligand for extracellulary inhibiting the activity of HMGB1 protein.

As previously described in this thesis HMGB1 binds to DNA molecules in the nucleus allowing in this way for the binding of transcriptional factors to DNA.
On the other hand HMGB1 extracellularly binds to RAGE, TLR2 and TLR4 receptors (see 1.2.7 section) activating several inflammatory processes.
The strategy presented in this thesis for inhibiting HMGB1 is based on a ligand exchange. In other words, the idea was to use the HMGB1 nuclear ligand outside its natural location to antagonise the extracellular ligands to avoid the inflammatory effects of HMGB1.
Consequently some DNA structures were firstly considered for this anti-HMGB1 strategy. In an improved approach chimeric molecules composed by PNA and DNA molecules were then realised to take advantage of the interesting enzymatic stability properties of PNA-DNA chimeras.

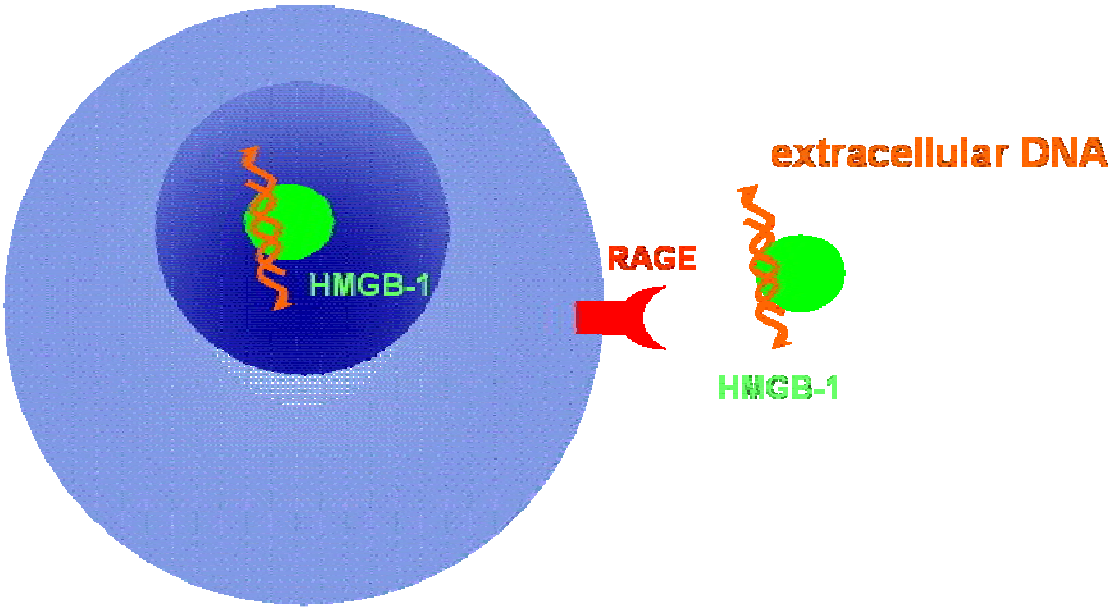

Figure 6: Ligand exchange to antagonize RAGE-HMGB1 interaction and the consequent proinflammatory effects.

1.2.2 Bent DNAs Design and Modelling

When HMGB1 binds to DNA, it causes bending of linear DNA structures. Furnishing to HMGB1 a DNA already in the conformation suitable for the binding would decrease the activation energy for the binding process. Thus, the approach described in this thesis was based on the hypothesis that bent DNA duplexes could have the right conformational requirements for binding HMGB1 at high affinity.

Five DNA strands were synthesised having the following sequences:

24-mer 3' OH-GTTGCATTGAAAAAATTTCTTAGG-5'OH 6A
18-mer 5'OH-CAACGTAAC - - - - - - AAAGAATCC-3'OH

22-mer 3'OH-GTTGCATTGAAAATTTCTTAGG-5'OH 4A
18-mer 5'OH-CAACGTAAC - - - -AAAGAATCC-3'OH

20-mer 3'OH-GTTGCATTGAATTTCTTAGG-5'OH 2A
18-mer 5'OH-CAACGTAAC - - AAAGAATCC-3'OH

18'-mer 3'OH-GTTGCATTGTTTCTTAGG-5'OH 0A
18-mer 5'OH-CAACGTAACAAAGAATCC-3'OH

The sequences of these DNA molecules were derived by a sequence already published in a paper showing the interaction between the *Drosophyla* HMGB1 homologous and a DNA duplex containing a 2 adenines asymmetric insertion[21].

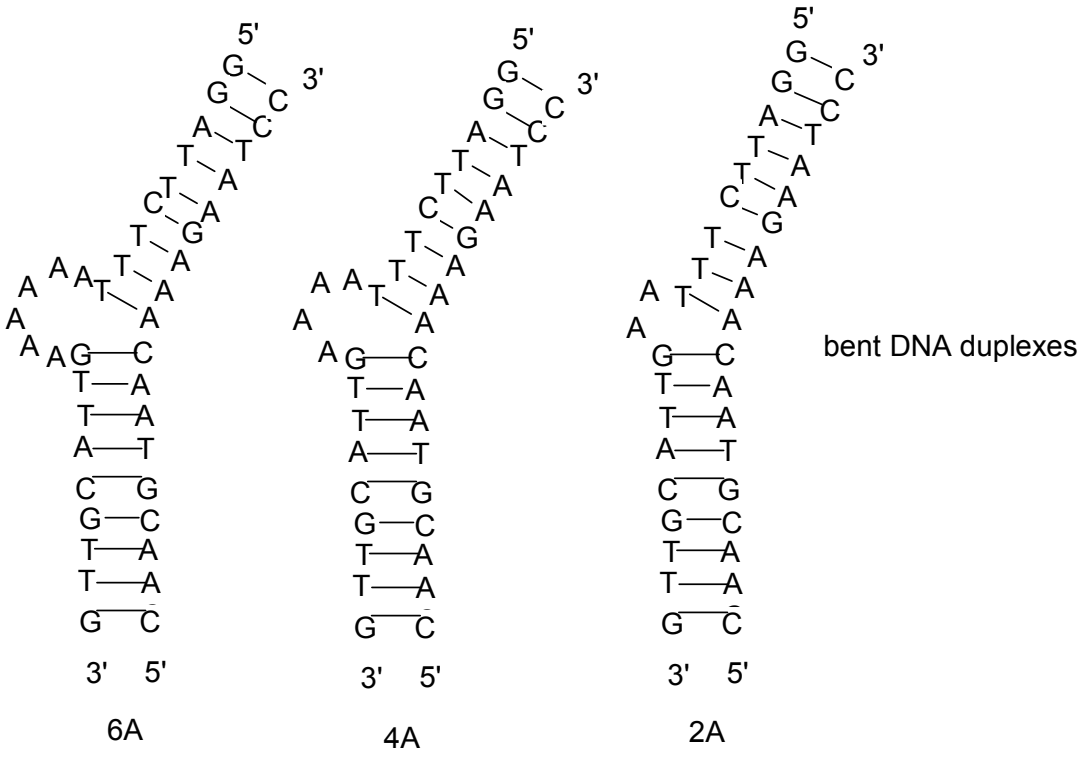

Sequences were checked for the absence of competitor target sequences in the human genome by BLAST in the EMBL sequence database[22] and for the lack of self-complementarity by the software MFOLD[23].

Afterwards, three bent structures (6A, 4A and 2A) were realised by using DNA duplexes carrying in the middle some unpaired nucleotide residues (six, four and two adenines respectively). In this way, it was possible to obtain by solid phase synthesis some structures presenting an extruding loop formed by the unpaired monomers.
In order to elucidate the role of the asymmetric bulge in inducing the DNA bending, modelling studies were performed on the three DNA duplexes by using as starting data the coordinates available from the following PDB files:

- 1E7J, corresponding to a Box B found in HMGD protein, a HMGB1 homologous present in *Drosophyla*, in complex with a DNA molecule similar to those used in this work (carrying two adenines in the asymmetrical bulge);
- 1CKT, corresponding to HMGB1 Box A in complex with a DNA bent by cisplatin;
- 1QSK, corresponding to a DNA duplex carrying an asymmetrical bulge containing 5 adenine residues.
- 1HME, corresponding to free Box B of HMGB1

These modelling studies, and particularly the comparison with the structural data from 1QSK file, showed that the asymmetrical bulge can bend the DNA duplexes designed in this work even in absence of HMGB1. In other words, bending is not an effect due to HMGB1 binding only, but is rather an intrinsic property of the used DNA duplexes, due to the unpaired region present in the middle of them.
Three-dimensional models for the complexes of HMGB1 with DNAs containing different asymmetric insertions/deletions, were obtained by homology on the basis of the 1E7J, 1HME and 1QSK PDB files. In particular, we focused on the three DNA duplexes containing an insertion of 2, 4 or 6 adenines, called duplex 2A, 4A and 6A respectively.
Models of stable DNA structures were obtained only for 2A and 4A duplexes, since it was not possible to accommodate in a defined structure all the adenines in the 6A duplex. The 2A duplex presents a continuous stacking between the 2 adenines of the insertion and the T preceding the bulge preventing H-bond formation of an A-T base pair, as shown in the picture below. Immediately after the adenines, there is a sharp bent of the DNA duplex, with stacking interruption and H-bond conservation between subsequent G-C base pair. The 4A duplex presents a continuous stacking between the first 3 adenines of the insertion. After the third adenine, there is a sharp bent, with stacking interruption. In this case the G-C base pair hydrogen bonds are lost. In summary we expected a major stability for 2A duplex because the stacking contribute per adenine is bigger than that present in 4A; in addition, a GC (3 H-bonds) base pair is retained in 2A instead of an AT (2 H-bonds). On the other hand, in 4A an AT base pair is retained a more significant GC interaction is lost.
No stable, stacked structure could accommodate a 6 adenine bulge, suggesting a lower stability for the 6A duplex.

---

[21] HMG-D complexed to a bulge DNA: An NMR model; Rachel Cerdan[1], Dominique Payet[2], Ji-Chun Yang, Andrew A. Travers and David Neuhaus; Protein Science *(2001), 10:504-518.*

[22] P. Hingamp, A. E. van den Broek, G. Stoesser, W. Baker, *Mol Biotechnol* 1999, *12*, 255.

[23] E. A. Skripkin, A. B. Jacobson, *J Mol Biol* 1993, *233*, 245.

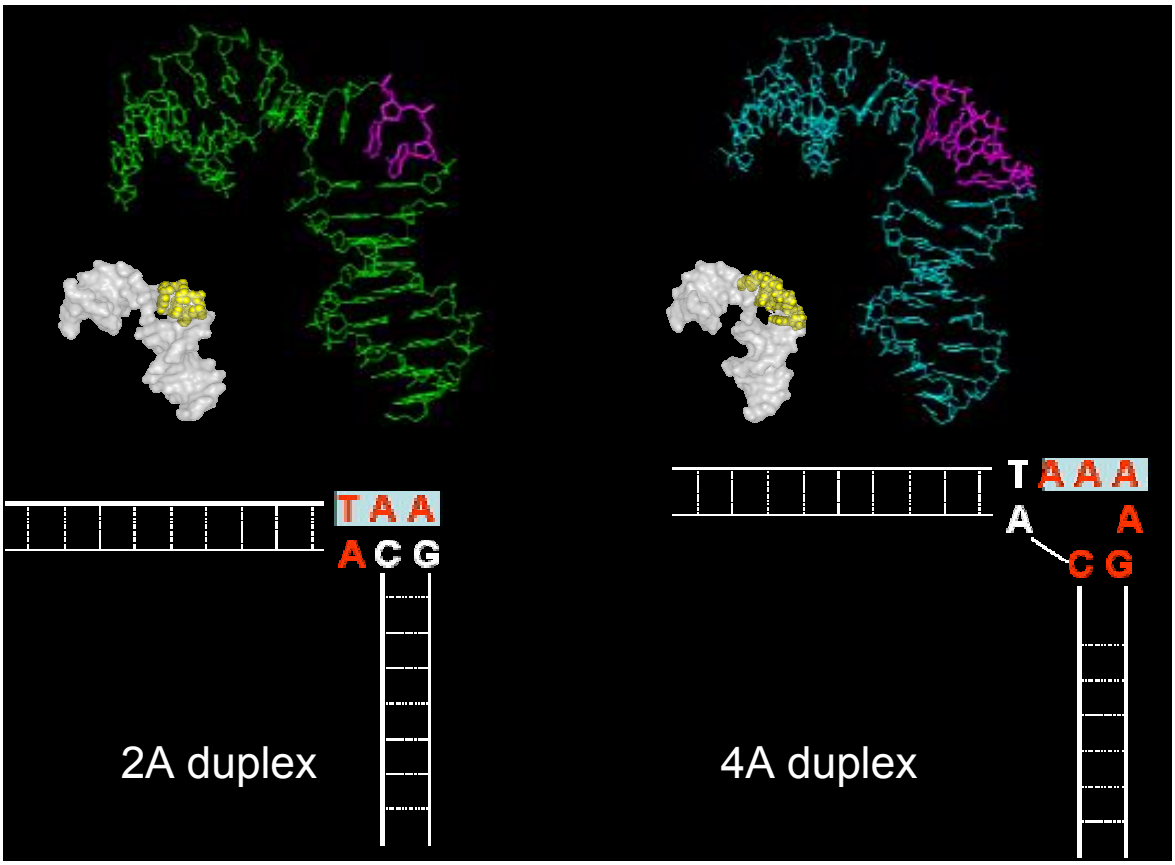

Figure 7: Modelling studies predicted the best stability for 2A DNA duplex. Bulge bases in the PDB models are purple. In the schematic representation, in grey are evidenced the bases involved in the stacking. Bases which do not participate to Watson-Crick hydrogen bond formation are red. White letters indicate bases that retain the hydrogen bond.

1.2.3 DNA Synthesis, purification and characterisation

Oligonucleotide synthesis was performed on an ABI/Perceptive Biosystems Expedite model 8909 Synthesizer that allows to synthesise not only DNA/RNA oligomers (0.02 µmol to 15 µmol scale) but also PNA (2 to 8 µmol scale) and other DNA analogues. Synthesis was accomplished on controlled pore glass supports in a 3' to 5' direction. Synthesis scale of the DNA oligomers was 1 micromole using standard protocols like that reported as an example below:

Protocol Edit Search Window Help

```
/* ------------------------------------------------------------------------------------ */
/*       Function              Mode  Amount Time(sec)        Description                 */
/*                                   /Arg1   /Arg2                                      */
/* ------------------------------------------------------------------------------------ */
$Deblocking
 144 /*Index Fract. Coll.   */ NA         1      0  "Event out ON"
   0 /*Default             */ WAIT       0    1.5  "Wait"
 141 /*Trityl Mon. On/Off   */ NA         1      1  "START data collection"
  16 /*Dblk                */ PULSE     30      0  "Dblk to column"
  16 /*Dblk                */ PULSE     70     70  "Deblock"
  38 /*Diverted Wsh A       */ PULSE     60      0  "Flush system with Wsh A"
 141 /*Trityl Mon. On/Off   */ NA         0      1  "STOP data collection"
  38 /*Diverted Wsh A       */ PULSE     60      0  "Flush system with Wsh A"
 144 /*Index Fract. Coll.   */ NA         2      0  "Event out OFF"
$Coupling
   1 /*Wsh                 */ PULSE      5      0  "Flush system with Wsh"
   2 /*Act                 */ PULSE      7      0  "Flush system with Act"
  18 /*A + Act             */ PULSE      7      0  "Monomer + Act to column"
  18 /*A + Act             */ PULSE      4     20  "Couple monomer"
   2 /*Act                 */ PULSE      5     30  "Couple monomer"
   1 /*Wsh                 */ PULSE      9     66  "Couple monomer"
   1 /*Wsh                 */ PULSE     14      0  "Flush system with Wsh"
$Capping
  12 /*Wsh A               */ PULSE     20      0  "Flush system with Wsh A"
  13 /*Caps                */ PULSE     14      0  "Caps to column"
  12 /*Wsh A               */ PULSE     10     20  "Cap"
  12 /*Wsh A               */ PULSE     20      0  "Flush system with Wsh A"
$Oxidizing
  15 /*Ox                  */ PULSE     25      0  "Ox to column"
  12 /*Wsh A               */ PULSE     25      0  "Flush system with Wsh A"
$Capping
  13 /*Caps                */ PULSE     10      0  "Caps to column"
  12 /*Wsh A               */ PULSE     50      0  "End of cycle wash"
```

1:1 | Deblocking | Step 1

DNA synthesis was based on the β-Cyanoethyl Phosphoramidite Chemistry and commercial phosphoramidites used in this thesis are successively shown.

ABI / Perceptive Biosystems Expedite model 8909

The exocyclic amines of 2'-deoxyadenosine (dA), 2'-deoxycytidine (dC) are protected by benzoyl (bz) groups at the N4 and N6 positions, respectively, while the 2' deoxyguanosine (dG) is protected at the N2 position by an isobutyryl (ibu) group. The phosphoramidite monomers are also protected at the the 5'-hydroxyl position with a DMT group and the 3'-phosphite brings β-cyanoethyl and diisopropylamine groups.

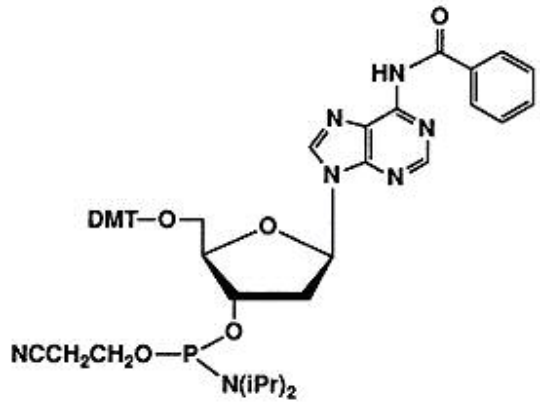

N-Benzoyl 5′-O-DMT-2′-deoxy-Adenosine-3′-(β-cyanoethyl)-Phosphoramidite

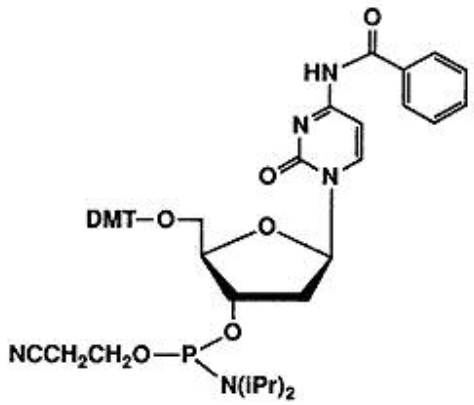

N⁴-Benzoyl-5′-O-DMT-2′-deoxy-Cytidine-3′-(β-cyanoethyl)-Phosphoramidite

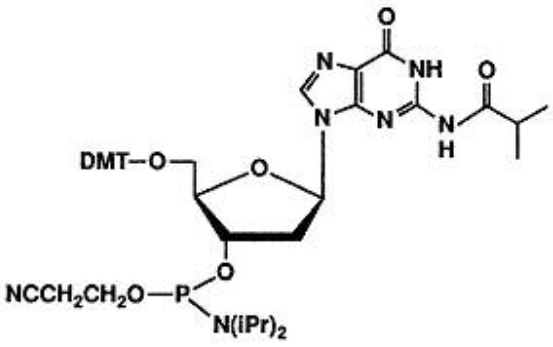

N-Isobutyrl-5′-O-DMT-2′-deoxy-Guanosine-3′-(β-cyanoethyl)-Phosphoramidite

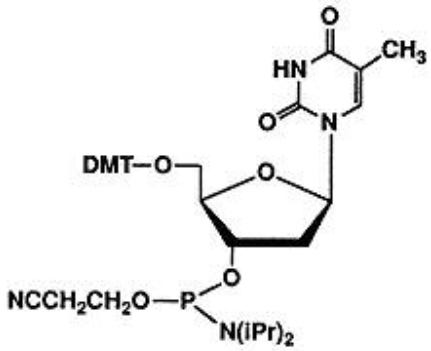

5′-O-DMT-Thymidine-3′-(β-cyanoethyl)-Phosphoramidite

DNA synthesis followed the standard cycle that begins with the 3'-hydroxyl nucleoside attached to a solid CPG (Controlled-Pore Glass) support through a long spacer linker. The first step in the synthesis is the removal of the dimethoxytrityl (DMT) group with TCA (detritylation) to free the 5'-hydroxyl for the coupling reaction. As the DNA bases are acid-labile, the detritylation step must only be as long as is necessary to ensure complete detritylation. After detritylation the next protected phosphoramidite is delivered

to the reaction column. Tetrazole is used to activate the phosphoramidite. The two reagents are premixed just prior to delivery to the reaction column. Tetrazole, acting as a weak acid, protonates the tertiary nitrogen group of the phosphoramidite and the diisopropylamine moiety, as a good leaving group, is displaced during the successive nucleophilic attack of 5'-hydroxyl group on the 3'-phosphorous the incoming activated monomer. To have a totally hydroxyl-free environment in the column dry acetonitrile is used as the general solvent, and all the reagents and solvents used are anhydrous. Under these conditions the coupling efficiencies are very high, thereby permitting synthesis of long oligonucleotides. Unreacted 5'-hydroxyl groups (1-2%) are capped by acetylation to avoid further elongation in the the next cycles. This is achieved using acetic anhydride and N-mehtyllimidazole as activated acetylating agent. The internucleotide linkage is then converted from the less stable phosphite to the phosphotriester in the oxidation step. Iodine is used as the oxidizing agent and water as the oxygen donor. After oxidation, the DMT group is removed with trichloroacetic acid and the cycle is repeated until chain elongation is complete. Coupling efficiency has been estimated spectrophotometrically by measuring DMT cation released during the detrytilation step. An example of trytil monitoring during the synthesis is shown in figure 8

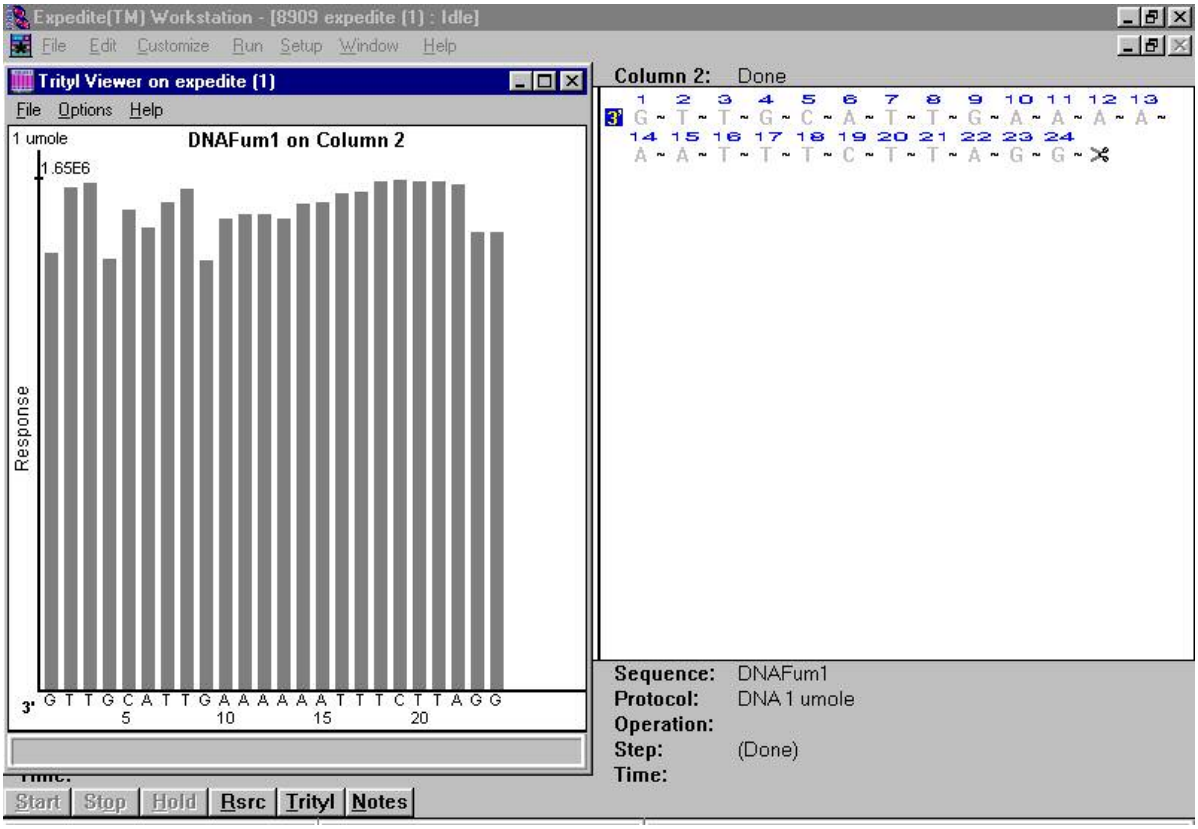

Fig.8: On-line trytil monitoring of DNA with 6 adenines in the bulge (24-mer).

The oligos is then cleaved from the solid support with concentrated ammonium hydroxide at 65 °C. Ammonia treatment also deprotects the phosphorus by β-elimination of the cyanoethyl group. After cleavage/deprotection, the resulting crude mixture contains the oligonucleotide, the truncated failure sequences with free 5'-hydroxyl ends, by-products of deprotection (benzamide, isobutyramide, acrylonitrile, and acetamide), and silicates from hydrolysis of the glass support. Anion exchange HPLC separate oligonucleotides by length. Normally the product is longer than the failure sequences.

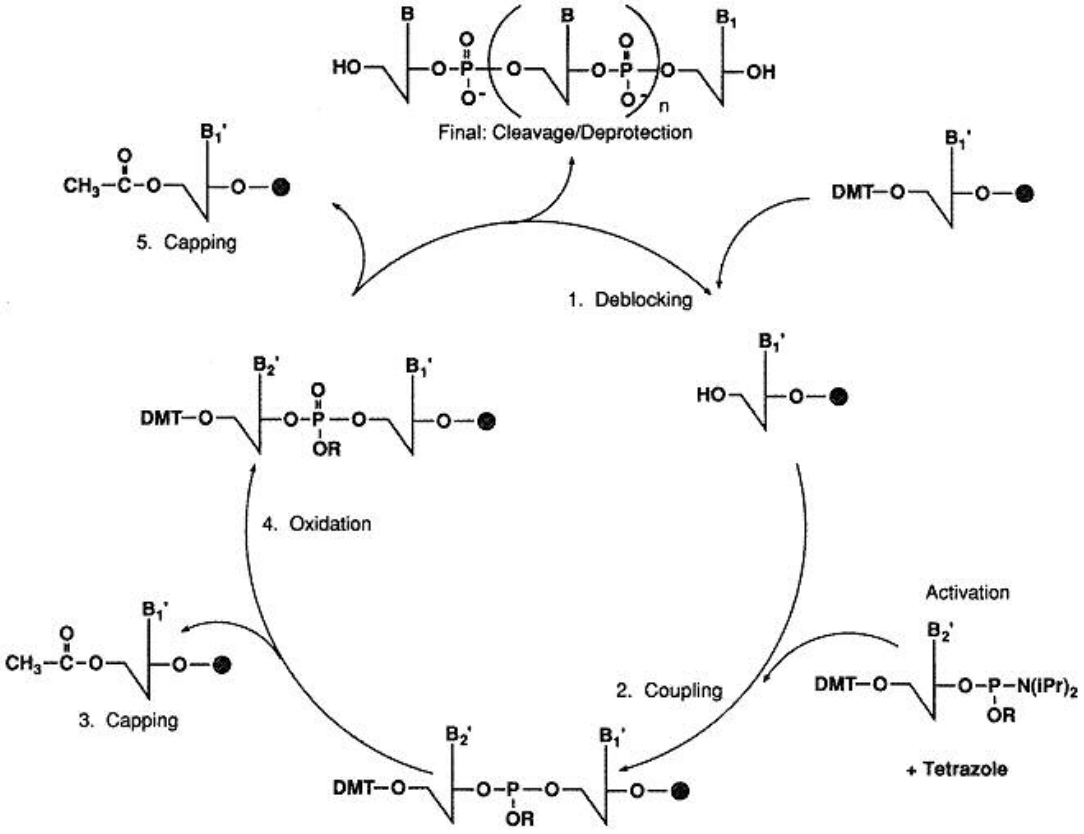

Chromatographic separation was performed using a Waters 600 Controller, equipped with the diode array detector Waters 996 and with Millennium software. A Nucleogel SAX column (Machery Nagel SAX 1000-8 4.6x50 mm) was used for this procedure. Solvent A was made up of 20 mM K_2HPO_4, pH 7.0, 20% CH_3CN and solvent B of 1 M KCl in 20 mM K_2HPO_4, pH 7.0, 20% CH_3CN. Oligos were separated by using a linear gradient of B in A at a flow rate of 1 ml min^{-1}. Detection was performed at 260 nm.

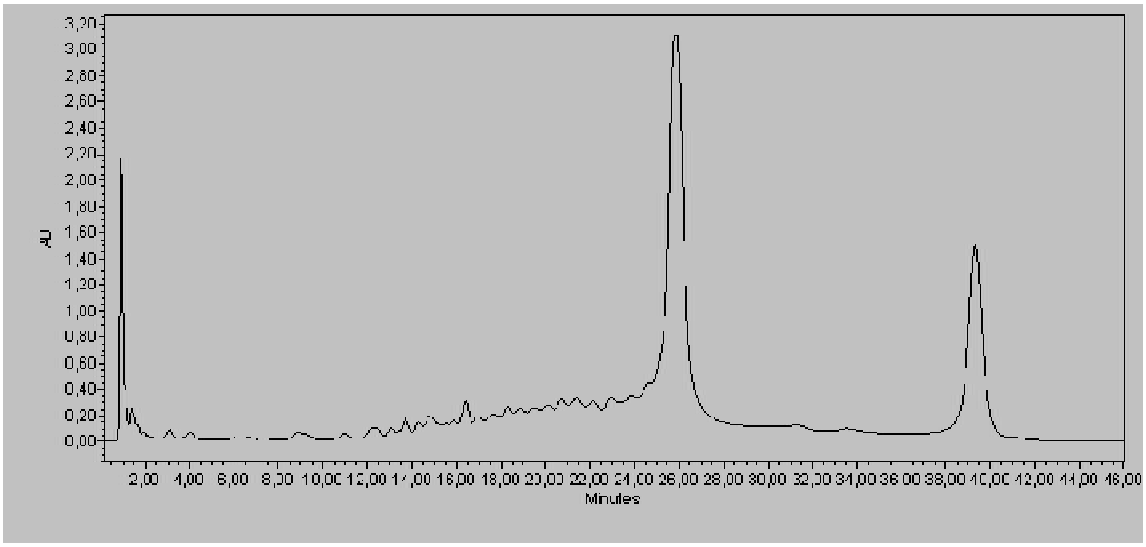

24-mer (6 adenines): from 20 % to 75 % of B in A in 35 min

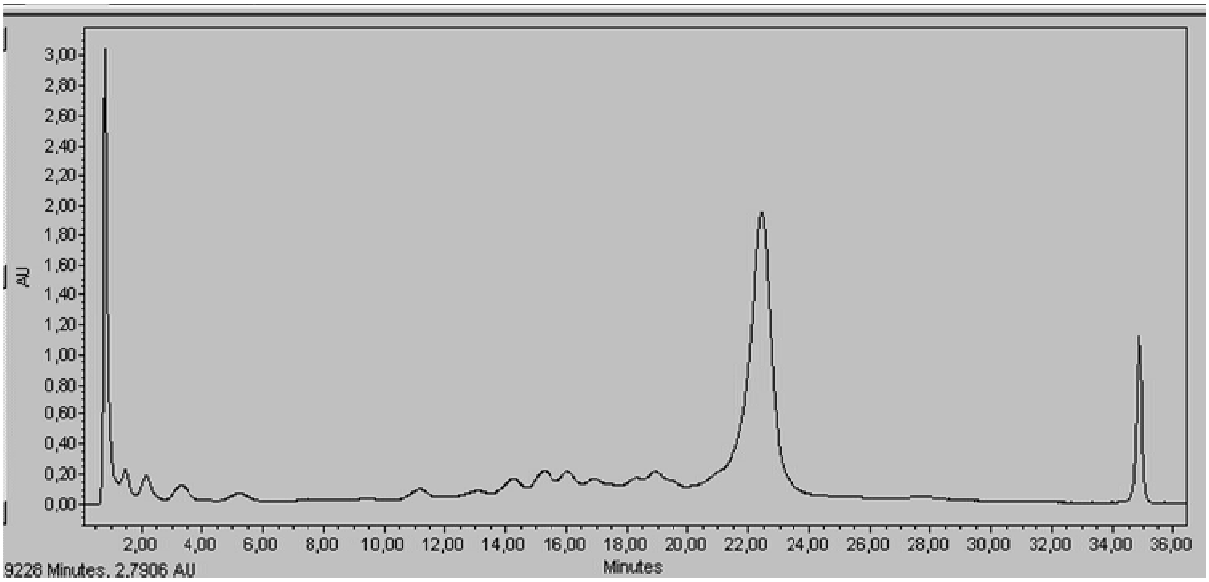

22-mer (4 adenines): from 25 % to 75 % of B in A in 25 min

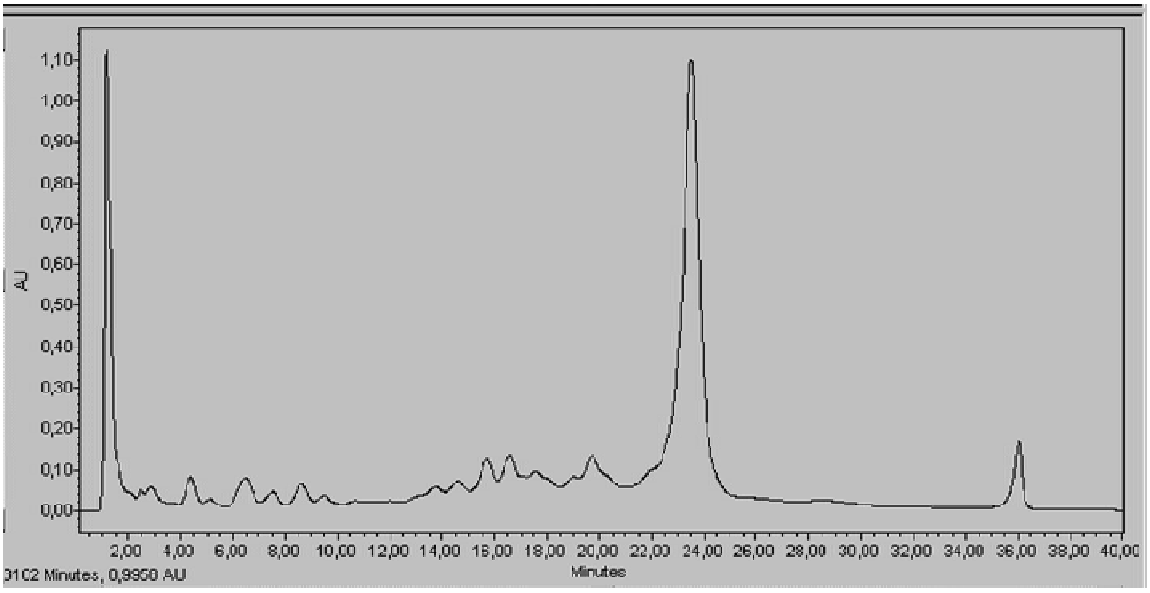

20-mer (2 adenines): from 25 % to 75 % of B in A in 30 min

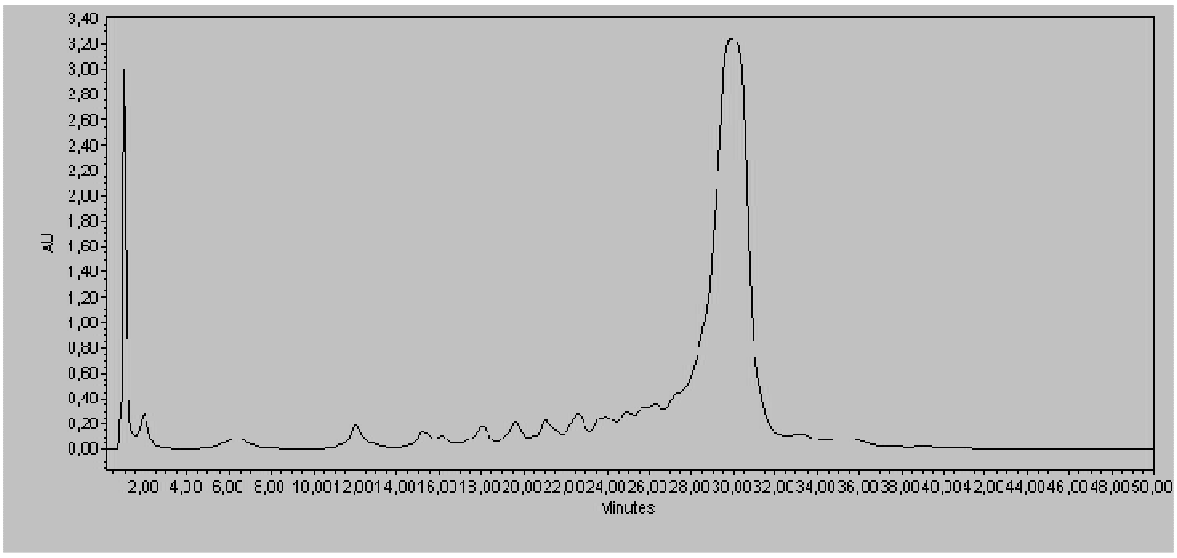

18-mer: from 25 % to 75 % of B in A in 35 min

After purification DNA oligomers were liophylised, dissolved in a known amount of milliQ water and quantified by UV measurements (T= 80 °C, Absorbance value at λ=260 nm). The epsilon used for the quantification of the oligos are calculated using molar extinction coefficients as follows: A, 15.4; T, 8.8; G, 11.7; C, 7.3 mM^{-1} and are:
24 mer, $A_8C_2G_5T_9$: ε_{260}=268900 M^{-1}
22 mer, $A_6C_2G_5T_9$: ε_{260}=244700 M^{-1}
20 mer, $A_4C_2G_5T_9$: ε_{260}=213900 M^{-1}
18' mer, $A_2C_2G_5T_9$: ε_{260}=169600 M^{-1}

18 mer, $A_9C_5G_2T_2$: ε_{260}=216100 M^{-1}
UV quantification of the oligos provided the following values:
24 mer = 310 nmol (2.30 mg, 31 % yield);
22 mer = 320 nmol (2.17 mg, 32 % yield);
20 mer = 340 nmol (2.09 mg, 34 % yield);
18'mer = 344 nmol (1.90 mg, 34% yield);
18 mer = 345 nmol (1.89 mg,35 % yield).
All DNA oligomers were characterised by MALDI-TOF MS performed on a PerSeptive Biosystems Voyager-DE MALDI-TOF mass spectrometer using 3-hydroxypicolinic acid /ammonium citrate =8/1 in water : acetonitrile= 1:1.
24 mer: Observed Mass $[M-H]^-$ = 7403.7; Calculated Mass $[M-H]^-$ = 7404.9;
22 mer: Observed Mass $[M-H]^-$ = 6778.9; Calculated Mass $[M-H]^-$ = 6778.5;
20 mer: Observed Mass $[M-H]^-$ = 6151.9; Calculated Mass $[M-H]^-$ = 6152.1;
18'mer: Observed Mass $[M-H]^-$ = 5527.0; Calculated Mass $[M-H]^-$ = 5525.6;
18 mer: Observed Mass $[M-H]^-$ = 5470.4; Calculated Mass $[M-H]^-$ = 5468.7.

1.2.4 Stability studies of bent DNA duplexes

Annealing of DNA. Equimolar amounts of complementary oligonucleotide strands were combined and dissolved in buffer (5 mM phosphate, 1mM $MgSO_4$, pH 7) to achieve DNA concentration of 2 μM . The solution was heated at 85 °C (10 min) and then allowed to cool slowly to room temperature.
The different bent DNA duplexes had to be tested for their ability to bind HMGB1 in order to find the best candidate to be used as DNA (or analogue)- based therapheutical agent against HMGB1. Stability of the free DNA duplexes was studied to find any dependence on the bulge length. Thermal stabilities for the four DNA duplexes were determined by Circular Dichroism (CD) experiments. All CD spectra were collected on a Jasco J710 spectropolarimeter equipped with a NesLab RTE111 thermal controller unity, using a quartz cylindrical cuvette with a 1-cm path length (Jasco). CD melting curves were recorded by following the decrease in ellipticity at 278 nm with a heating rate of 1 °C/min.
The Tm for the duplex 2A, 4A, 6A and 0A are reported in the following table:

	Tm (°C)
0A	48.26 ± 0.10
2A	36.99 ± 0.04
4A	34.40 ± 0.03
6A	31.40 ± 0.04

The first important consequence of the presence of the bulge is immediately evident by comparing 0A to all the other duplexes: the presence of the bulge destabilizes the duplex. This is an effect which is remarked by a Tm difference between 0A and the other duplexes ranging from 11 to 17 degrees. The effect is consistent with the data in the

literature[24], showing that even a single-base bulge has a profound destabilizing effect on the duplex. Furthermore, as predicted by the modelling, stability decreases as the number of adenine residues in the bulge increases. The most stable bent DNA duplex was that carrying two adenines (i.e. 2A, with a melting temperature of 37.0 °C). Thus, the 2A duplex adopts the most stable folding, followed by the 4A and by the 6A duplexes, respectively.
CD studies was also used to have information on the conformation and in particular on the amount of stacking for each bent duplex. For this reason, we recorded CD spectra of the DNA duplexes 0A, 2A, 4A and 6A at the same concentration at 15 °C. CD spectrum obtained for 2A (2μM, 15 °C) is reported below as an example.

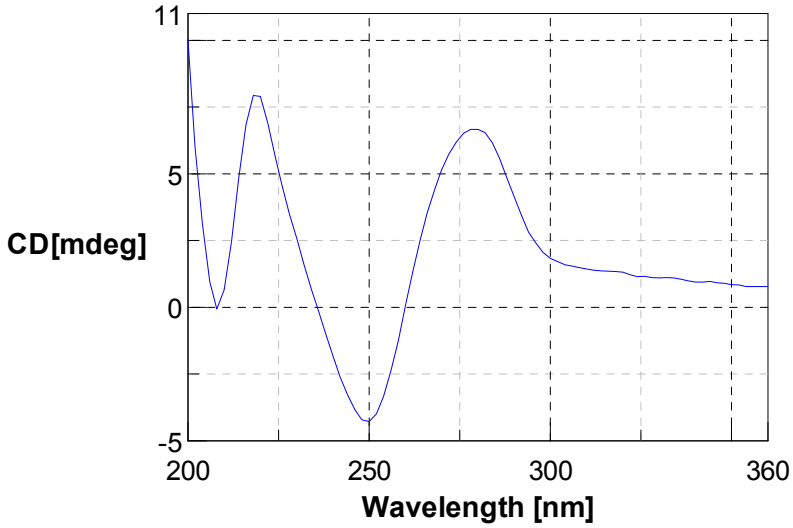

In all cases the CD spectrum confirmed the formation of the DNA duplex with an adenine loop extruding from the double helix. After transformation in the corresponding molar ellipticity spectra, the spectrum of 0A was subtracted from each bent duplex spectrum to obtain the CD contribute due only to the loop present in every bent structure. In fact this operation, assuming that the two arms flanking the central bulge have substantially the same structure in all bent duplexes (B-form DNA), eliminates the contributions coming from all the bases, except for the adenines in the central bulge, and gives the “bulge spectrum” for each bent duplex. By dividing the “bulge spectra” for the number *n* of adenines composing the corresponding bulge, it was obtained the average spectrum for the bulge adenines contained in each of the studied bent duplexes, as reported in figure 9

[24] Influence of neighboring base pairs on the stability of single base bulges and base pairs in a DNA fragment. Ke SH, Wartell RM; Biochemistry. 1995 Apr 11;34(14):4593-600.

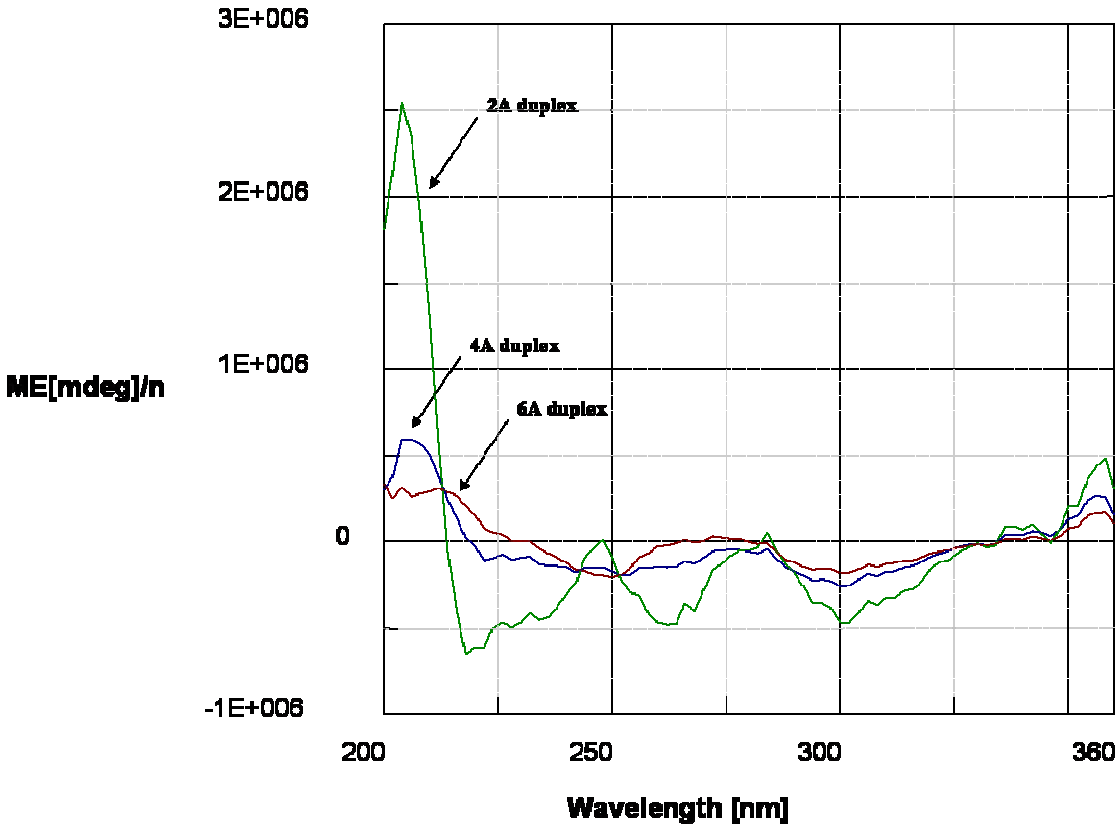

Figure 9: CD “bulge spectra” for 2A, 4A and 6A DNA duplexes.

While the molar ellipticity spectra of the adenines in the 4A and 6A duplexes are very similar in intensity and shape, the 2A spectrum is very peculiar, with a very intense CD band at 205 nm due to the stacking contribute of adenines. This observation supports the modelling studies, described before, that evidenced a bigger stacking ability for 2A duplex.

1.2.5 Stability studies of HMGB1-bent DNA complexes

Once thermal stability was found for free DNA duplexes, complexes with HMGB1 were studied. Circular dichroism (CD) spectra were obtained by using special “Tandem Mix” cells (Suprasil quartz, Hellma, showed below) which minimize errors relative to the obtainment of the exact concentration of both DNA and protein before and after the complex formation. This is particularly important when one studies by CD very little differences due to the interactions.

Light Path:	2 x 4.375 mm
Height:	46 mm
Width:	12.5 mm
Depth:	12.5 mm
Inner Dimensions: **Width:**	9.5 mm
Base Thickness:	1.5 mm

The CD spectrum obtained from the tandem mix cell before mixing corresponds to the sum of the spectrum of free HMG box B protein domain and free DNA duplex. The protein region of the spectrum (200-230 nm) changes significantly after the components are mixed, while the CD spectrum region where only DNA contributes remains almost unchanged, reflecting little conformational changes in the bent DNA (see Fig 10).

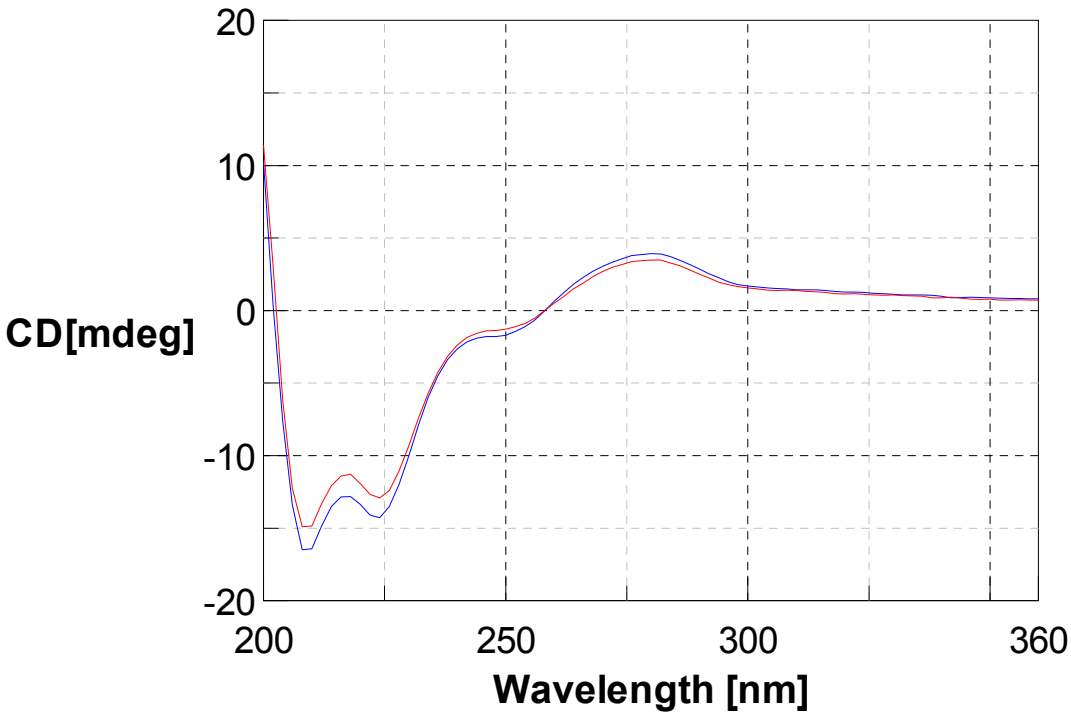

Figure 10 CD spectra of HMGB1-B Box (21 µM) and 2A (2 µM) obtained in a tandem mixing cell at 15 °C: sum spectrum (free HMG box-B domain in cell 1 and free DNA in cell 2 before mixing, blue line), complex spectrum (after mixing of the two cells, red line).

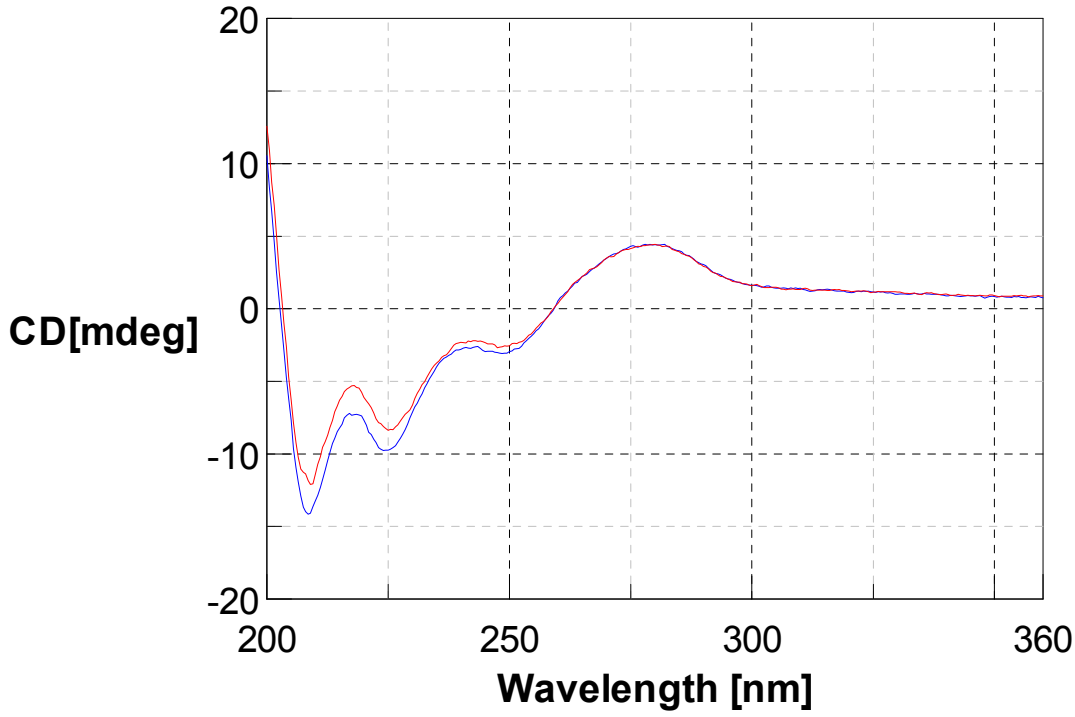

Figure 11: CD spectra of HMGB1-B Box (21 µM) / 4A (2 µM) complex (red line) and sum (blue line) at 15 °C.

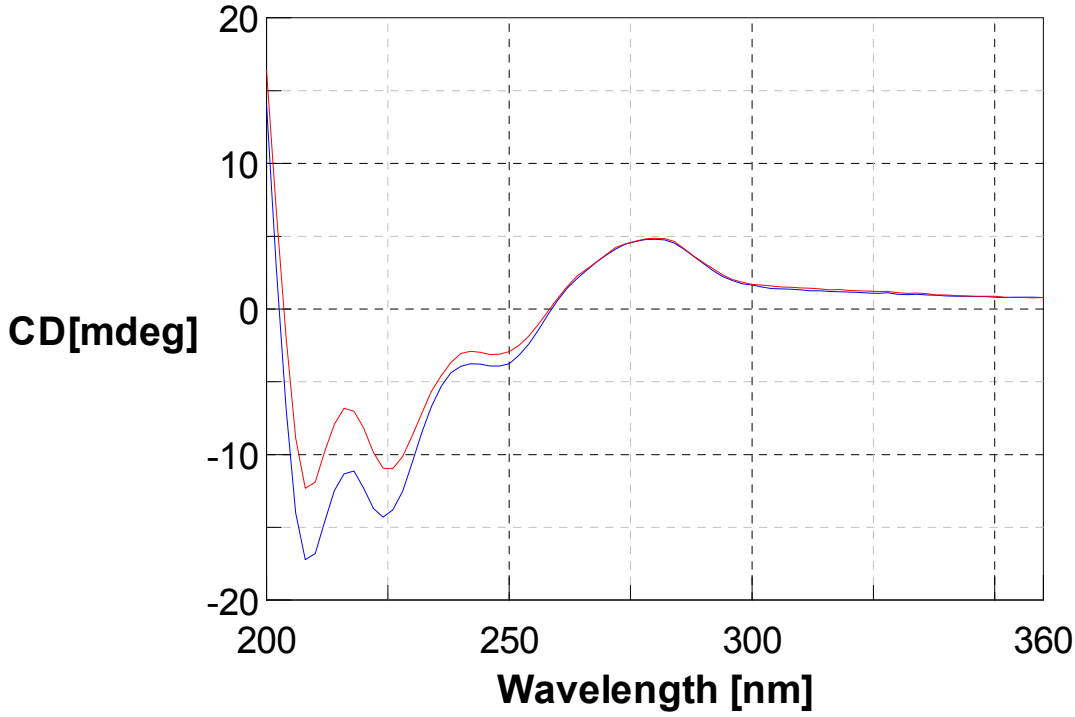

Figure 12: CD spectra of HMGB1-B Box (21 µM) / 6A (2 µM) complex (red line) and sum (blue line) at 15 °C.

"Difference spectra" were obtained in all three cases by subtracting the CD spectrum of the SUM from the complex spectrum, and confirmed the effectiveness of the HMGB1 B Box-DNA binding. The greater "difference spectrum" comes from the 6A duplex. Assuming that the CD contribution of the protein is the same for every bent-duplex, the increasing induced deformation from 2A to the 6A by the protein indicates that a bigger DNA structure deformation is needed for binding in the case of the 6A duplex. In other words, the binding of the protein to the 6A duplex requires a greater reorganization of the duplex structure, thus destabilizing the resulting complex as compared to the 4A and 2A respectively.

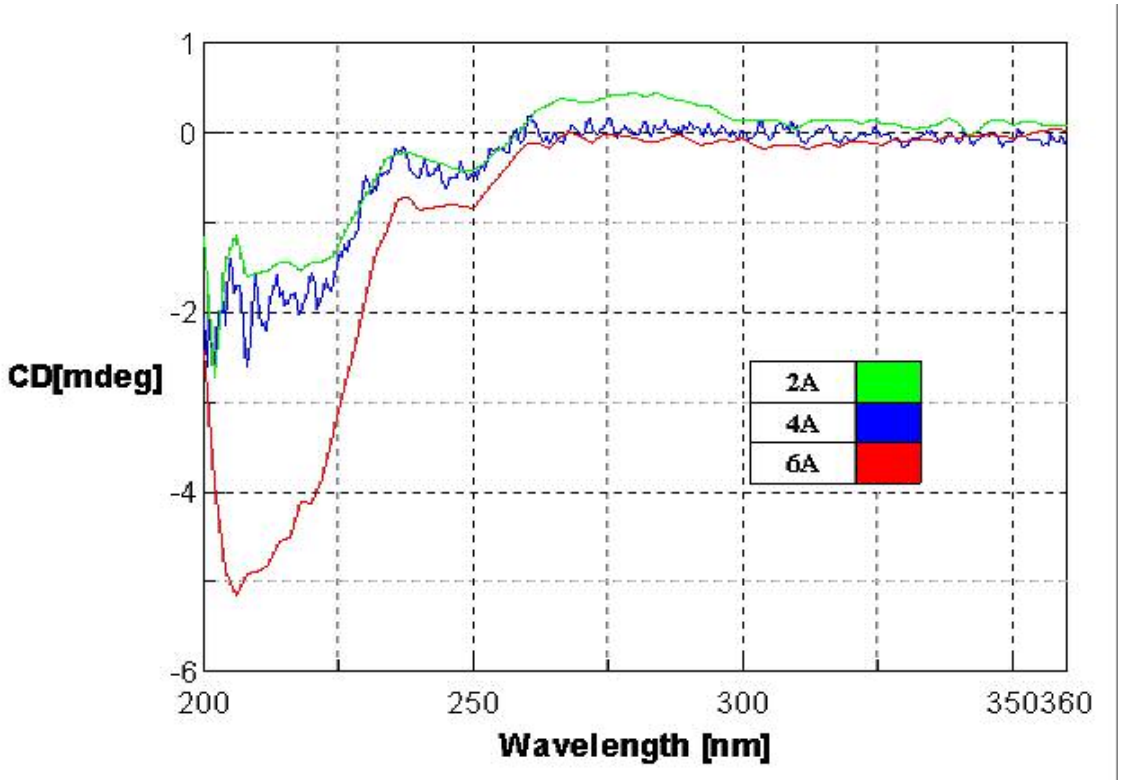

Figure 13: CD "difference spectrum" for 2A, 4A and 6A DNA duplexes.

Thermal stability of the complexes HMGB/bent DNA duplex was obtained by CD melting curves (from 4 to 60 °C) and was compared with DNA thermal stability in the free form (Figure 14). The most stable bent DNA duplex in complex with HMGB1 was 2A with a melting temperature of 40 °C. The energy differences (ΔT_m) between the bound and unbound DNA duplexes is very similar in all cases. This means that the total stabilisation due to the formation of the protein/DNA complex is comparable in all cases, giving a stability trend for the complexes which closely matches the trend observed for free DNA duplexes. Thus, the protein binds bent DNAs always in the same manner, and the

stability of the resulting complex is strongly related to the stability of the corresponding DNA duplex. The lowest complex stability is observed in the case of 6A where, as evidenced also from the CD "difference spectra" (Fig…), the binding of the protein to the 6A duplex requires a greater reorganization of the duplex structure, thus destabilizing the resulting complex as compared to the 4A and 2A respectively. This deformation is paid energetically in terms of the stability of the resulting complex, explaining the decreasing thermal stability trend observed for the protein/DNA complexes as the number of adenines into the central bulge increases.

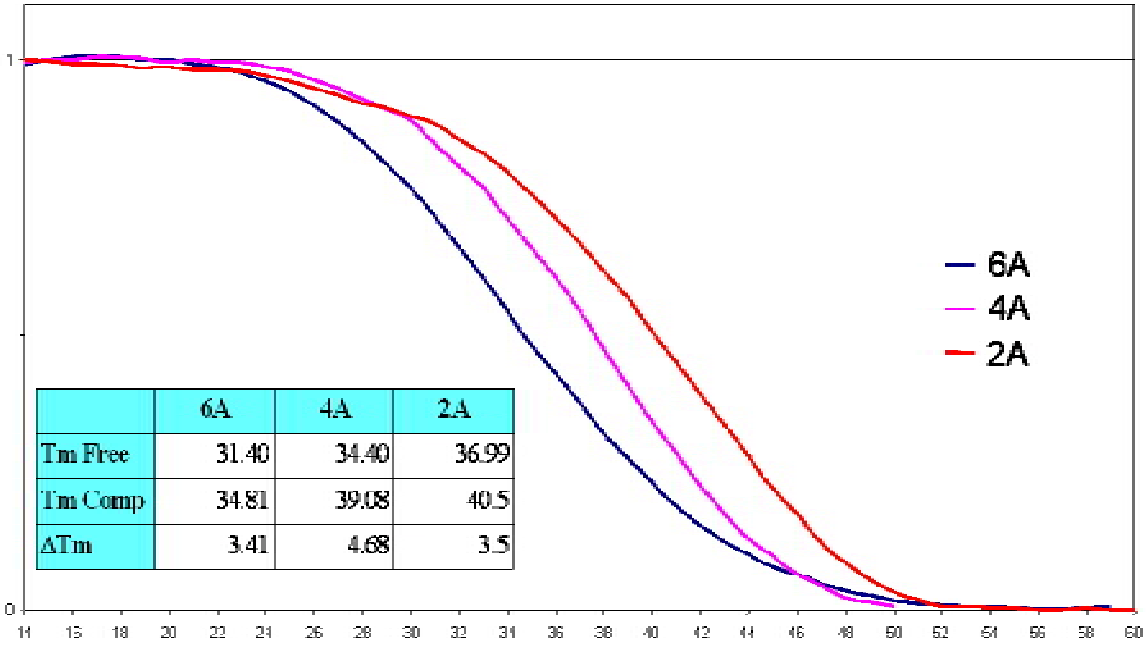

	6A	4A	2A
Tm Free	31.40	34.40	36.99
Tm Comp	34.81	39.08	40.5
ΔTm	3.41	4.68	3.5

Figure 14: Normalised CD melting curves between 0 ad 1 for DNA duplexes in complex to HMGB1 and T_m table of bent duplexes, free and in complex to HMGB1.

Affinity of HMGB1 for the most stable duplex, the 2A,was obtained performing CD titration experiments in H_2O. In a solution of 1.15 μM DNA duplex the concentration of HMGB1 was increased from 0 to 1 μM. From CD spectra collection a K_d of about 20 10^{-9} M was determined, according to an equation reported in literature[25]. Titration profiles were obtained reporting the CD variation, normalised between 0 and 1, at λ= 221nm, where both HMGB1 and DNA contribute, and 278 nm (only DNA influence) versus HMGB1 concentration (Figure 15). Binding isotherms are almost identical in both the cases and this suggests that HMGB1 protein does not modify significantly its structures when binds to DNA.

[25] C. Isernia, E. Bucci, M. Leone, L. Zaccaro, P. Di Lello, G. Digilio, S. Esposito, M. Saviano, B. Di Blasio, C. Pedone, P. V. Pedone, R. Fattorusso, *Chembiochem* 2003, *4*, 171

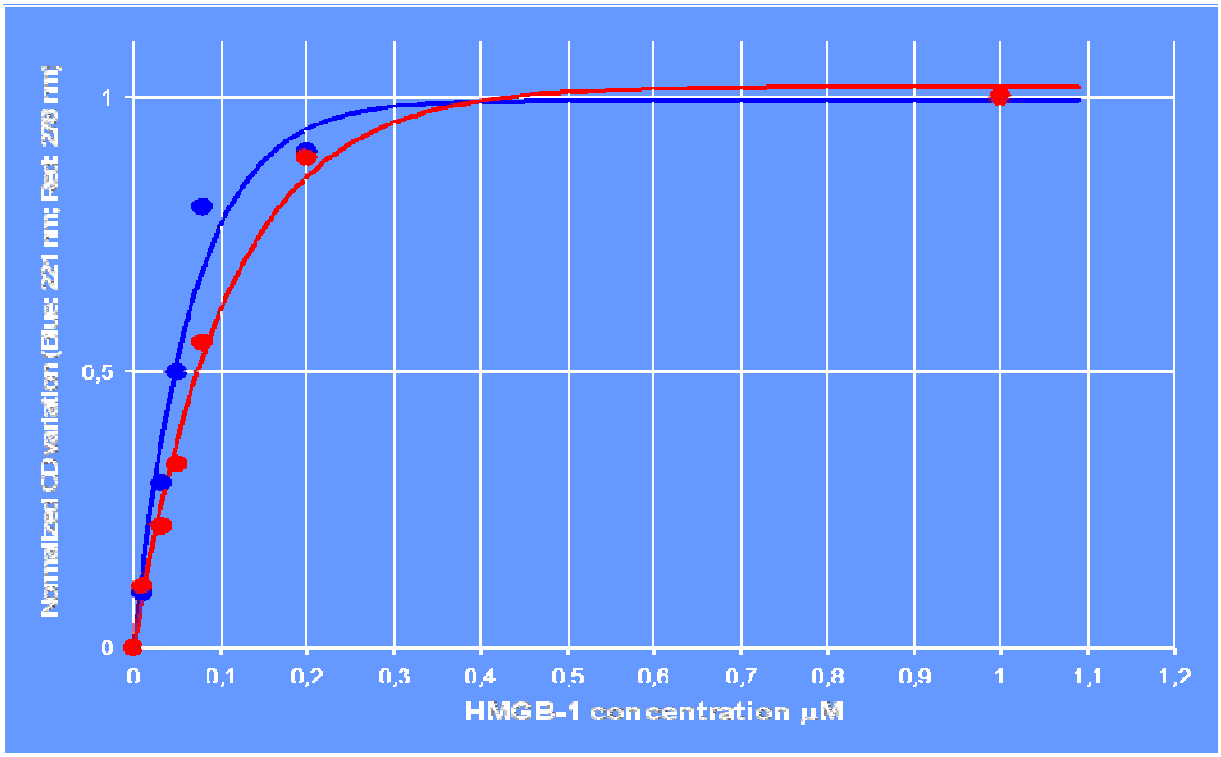

Figure 15: CD titration of 2A DNA duplex with HMGB1 in water at 15 °C (protein/DNA ratio ~ 1).

In conclusion, the most stable HMGB1-DNA complex is obtained in the case of the loop with 2 adenine residues. Consequently our attention was focused on the obtainment of the more enzymatically stable PNA-DNA chimeric duplex presenting an asymmetrical bulge of two adenines.

1.3 PNA/DNA chimeras for HMGB1 inhibition.

1.3.1 Introduction

By taking advantage of the synthetic procedures optimised in this thesis and described in the following sections it was possible to obtain PNA chimeric molecules in good amount and this allowed for their use in several in cell and *in vivo* experiments that furnished the interesting results reported in this work.
A chimeric duplex called 2A was realised with a loop of two adenines. Two chimeric strands carrying the PNA moiety at 3' end were synthesised (5'DNA-3'PNA). These kind of molecules are expected to be more resistant to enzymatic degradation than the corresponding 5'DNA-3'PNA, since *in serum* 3' exonucleases are more abundant than 5' exonucleases[22]. The nucleobase sequence for the two strands is below reported (the first three monomers at 3' terminus were PNA monomers and are indicated by small letters in both the chimeric strands):

20-mer COOH-ctt*GCATTGAATTTCTTAGG-5'OH Chim 2A
18-mer 5'OH-GAACGTAAC - - AAAGAA*tcc-COOH

The same positive characteristics in the interaction with HMGB1 already found for 2A were expected also in the case of Chim 2A. However a further improvement in the *in serum* stability was also expected for Chim 2A as a consequence of the presence of PNA moieties in the nucleotidic strands. By using these strands, a duplex chimera:chimera was obtained. UV spectroscopy and Circular Dichroism experiments were performed in order to verify the duplex formation and to determine the melting temperature.
Subsequently, the *in serum* resistance for this chimeric duplex was studied (see section 1.3.9). Other experiments were carried in cells to verify the ability of the chimeric complex to inhibit the activities of HMGB1 (see section 1.3.10). Finally the chimeric duplex was used in multiple *in vivo* experiments, in a mouse inflammation model (see section 1.3.10).

1.3.2 PNAs: useful characteristics and limits

Peptide nucleic acids (PNAs) are among the most powerful oligonucleotides analogues, with a N-(2-amino-ethyl)-glycine unit replacing the sugar-phosphate backbone[1-4]. PNAs show strong and sequence specific hybridisation to complementary DNA and RNA[5] as well as to double stranded DNA by triplex formation[6]. This type of DNA mimic is not degraded by nucleases and proteases[7] and present both good antisense and antigene activity[8-13].

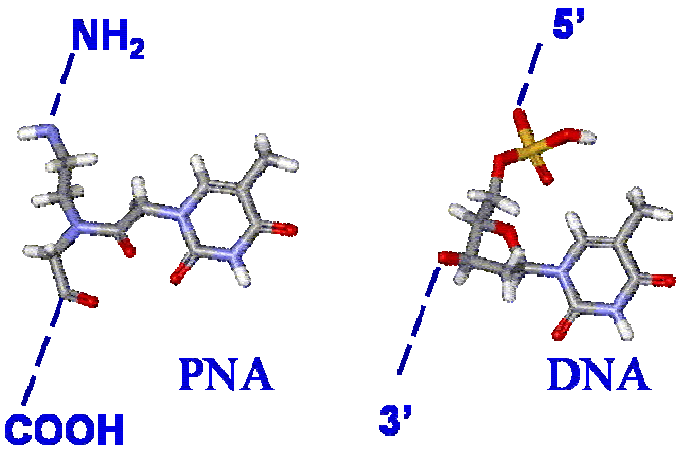

Figure 16: PNAs are DNA analogues with a pseudopeptidic backbone.

Although pure PNAs have truly remarkable binding properties, their handling during work-up, analysis and purification is often difficult because of their tendency to aggregate. Moreover, due to their neutral character the water solubility is limited[2].
Afterwards, since PNA binding to complementary oligonucleotides induces structural conformational variations with respect to natural complexes, proteins do not recognise PNA-oligonucletides complexes.

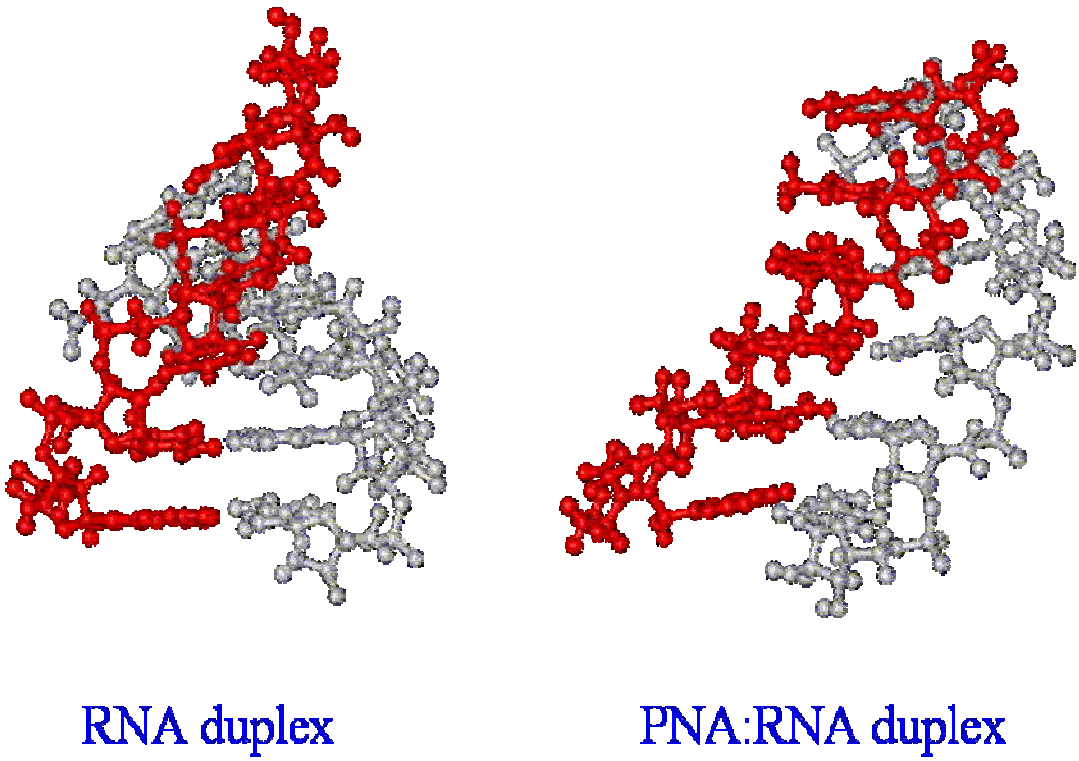

Figure 17: Structures of RNA-RNA duplex and PNA-RNA duplex: an example of conformational variation due to PNAs[27].

1.3.3 PNA-DNA chimeras

The synthesis of chimeric molecules composed of PNA and DNA is a possible approach to address PNA problems, and has been shown to improve the cellular up-take of PNAs.[14] PNA/DNA chimeras might combine the high binding efficiency and specificity of PNA, with the ability of DNA to interact with proteins, for examples with RNasi H in antisense applications,[15] or might function as a primer for DNA polymerases.[15] Preliminary experiments in cell cultures have shown that PNA/DNA chimeras used as antisense oligomers are capable of inhibiting the expression of specific target genes.[16]

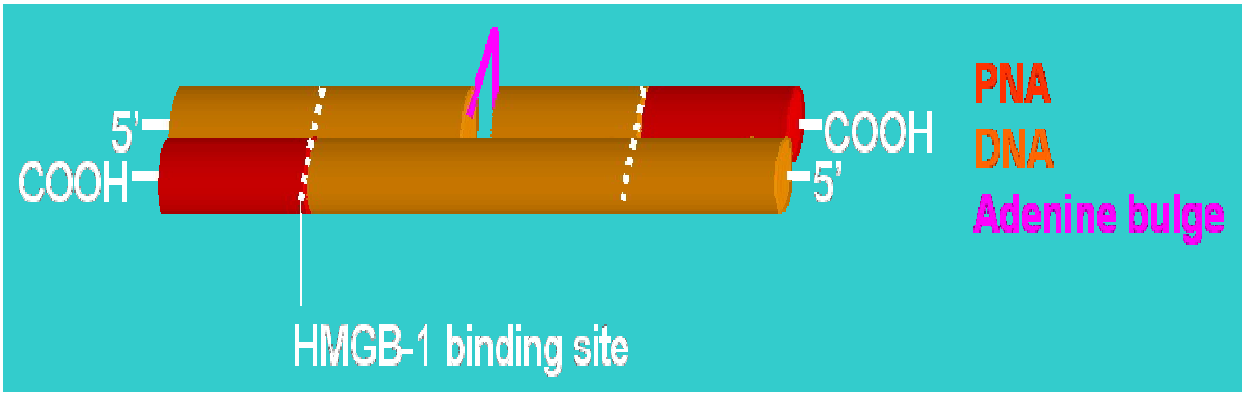

Figure 18: 5'DNA-3'PNA chimeric duplex

Furthermore, PNA parts attached to 3' and 5' ends of a DNA in a PNA/DNA chimera stabilize the molecule against degradation by 3'- and 5'-exonucleases, which are the main classes of oligonucleotide-degrading enzymes found in serum. In summary, PNA/DNA chimeras are taken up by cells, are largely nuclease-resistant, and have an excellent binding affinity to complementary oligos without having PNA drawbacks, so that they fulfil the basic requirements for antisense oligomers to be biologically active.

1.3.4 Problematic aspects in the synthesis of PNA-DNA chimeras

The step-wise "on-line" solid-phase synthesis with suitably protected monomeric building blocks has proved to be the most successful and flexible method for the synthesis of PNA/DNA chimeras and modified PNA.[17-20] Classically the automated synthesis of DNA and PNA proceeds in 3' to 5' direction for DNA and pseudo 3' to pseudo 5' for PNA, where pseudo 3' corresponds to the COOH terminus while pseudo 5' corresponds to the amino terminus of the PNA.
Commercial Fmoc/Bhoc or Boc/Cbz PNA monomers (where the first abbreviation denotes the protecting group on the backbone, while the second one that on the nucleobase) are not compatible with DNA synthetic chemistry because the deprotection of the amino group on the nucleobases from the Bhoc group (in Fmoc/Bhoc monomers) or on the backbone from the Boc group (in the Boc/Cbz monomers) is achieved by TFA

treatment, which would cause depurination of the DNA part of the chimera. Moreover, use of PNA monomers containing Fmoc group for temporary protection of the amino function in the backbone forces to utilize the 5'-DMT-O-methylated phosphoramidite instead of the less expensive standard DNA monomers (DMT-CNE- phosphoramidite) for the assembly of the DNA part in a chimera of the type PNA-DNA-PNA or 3'DNA-PNA. Furthermore it was reported that Fmoc protection in PNA backbone gives the lowest coupling yields in comparison to other protecting groups, probably because in Fmoc-PNA synthesis, where aggregation is frequently a problem, the removal of the Fmoc group becomes an issue.[21] A milder and more convenient method compatible with conditions for DNA synthesis requires utilization of PNA monomers containing the Mmt group for the temporary protection of the N-terminus and acyl protecting groups for the nucleobases.[22-25]
The lypophilic Mmt group improves the solubility of the protected monomers in polar organic solvents, such as DMF or CH_3CN. The assembly of the DNA part can be carried out with commercially available, standard DNA monomers. The temporary protecting group Mmt can be removed under mild acidic conditions (3% TCA), and the coupling efficiency, which can be determined very easily by measurement of the coloured Mmt cation release, is in the order of 95-99%.[22-25] The nucleobase protecting groups are removed at the end of the synthesis. This highly efficient and flexible strategy allows for the automated synthesis of PNA/DNA chimeras using equipment and conditions very similar to those employed in standard DNA synthesis. [22-25]

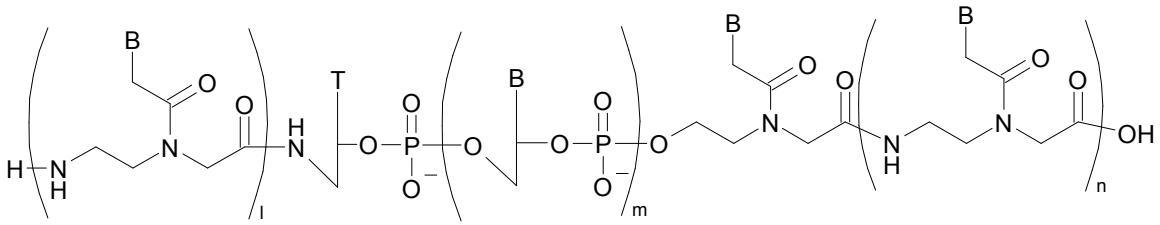

Figure 19: PNA-DNA-PNA chimera

Two linking monomers are needed to perform an automated solid phase synthesis of chimeric molecules of the type PNA-DNA-PNA.[14] The first one to pass from DNA to PNA, forming an amide bond at the 5' end of DNA, is already commercially available (5'-amino-5'-deoxythymidine phosphoramidite) (linker 1, Fig. 1). To connect the PNA part of the chimera to the DNA a 2-(hydroxyethylglycine) unit may be used to form a phosphodiester bond with the 3' end of the DNA (linker 2, Fig. 1). In particular, Mmt-O-protected nucleobase-derivatised hydroxyethylglycine is useful to this aim. Synthetic routes to Mmt PNA monomers[22-25] as well as to Mmt PNA-3'DNA linkers[25, 26] for the synthesis of PNA/DNA chimeras, have been previously reported in literature. However, the synthetic procedures for the obtainment of these useful building blocks and the corresponding yields are not yet optimal and further improvements in this regard are clearly desirable.

In this paper we present a convenient synthesis of Mmt PNA monomers and Mmt PNA-3'DNA linker which takes advantage of the introduction of the Mmt protecting group in the first step.

1.3.5 Synthesis of building blocks for PNA-DNA chimeras

MATERIALS AND METHODS

The following abbreviations are used: 4-methoxybenzoyl (An); benzhydryloxycarbonyl (Bhoc); *tert*-butoxycarbonyl (Boc); benzyloxycarbonyl (Cbz), cyanoethyl (CNE); *N,N'*-diisopropylcarbodiimide (DIC); *N,N*-dimethylformamide (DMF); di-(4-methoxyphenyl)phenylmethyl (Dmt); 9-fluorenylmethoxycarbonyl (Fmoc); 1-hydroxybenzotriazole (HOBt); (4-methoxyphenyl)diphenylmethyl (Mmt); 4-methylmorpholine (NMM); triethylamine (TEA); trifluoroacetic acid (TFA).
HOBt was purchased from Novabiochem. Solvents for chromatography were from Carlo Erba and Lab-Scan while dry solvents and all other reagents were purchased from Sigma-Aldrich-Fluka. All reactions were performed in glassware, which had been oven dried (120 °C, at least 3h) and then flame-dried under Ar atmosphere prior to use. TLC were run on silica gel Macherey-Nagel G-25 UV_{254} plates, and visualised by UV light and by a $Ce(SO_4)_2$ or ninhydrin staining solution. Column chromatography was performed using silica gel 60 (230-400 mesh).

Apparatus

^{1}H NMR and ^{13}C NMR spectra were recorded on VARIAN UNITY 400 MHz spectrometer equipped with a computer SUN ULTRA 5. Chemical shifts (δ) are quoted in parts per million (ppm), downfield from tetramethylsilane, and all coupling constants (J) are quoted in Hz. For the assignments of Mmt ^{13}C NMR signals we have used the convention showed below:

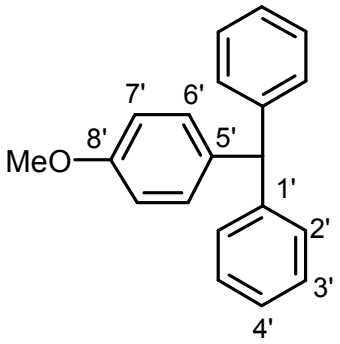

MALDI mass spectra were obtained using a Perseptive Biosystems Voyager DE spectrometer with a sinapinic acid matrix

Mmt/Acyl protected PNA monomers

For the synthesis of PNA monomers we followed a general strategy relying on the use of protected N-(2-amino-ethyl)-glycine (backbone) and protected N1/9-(methyl-carbonyl)-bases. These moieties were subsequently coupled to give the desired PNA monomers (to be used for polymer synthesis). The backbone contains Mmt group as temporary protection of the N-terminus and the nucleobases bring an acyl protection on the exocyclic NH_2.
The Mmt backbone 3 was obtained in two synthetic steps from ethylenediamine 1 with an overall yield of 65%, higher than previously obtained (Scheme 1).[22]

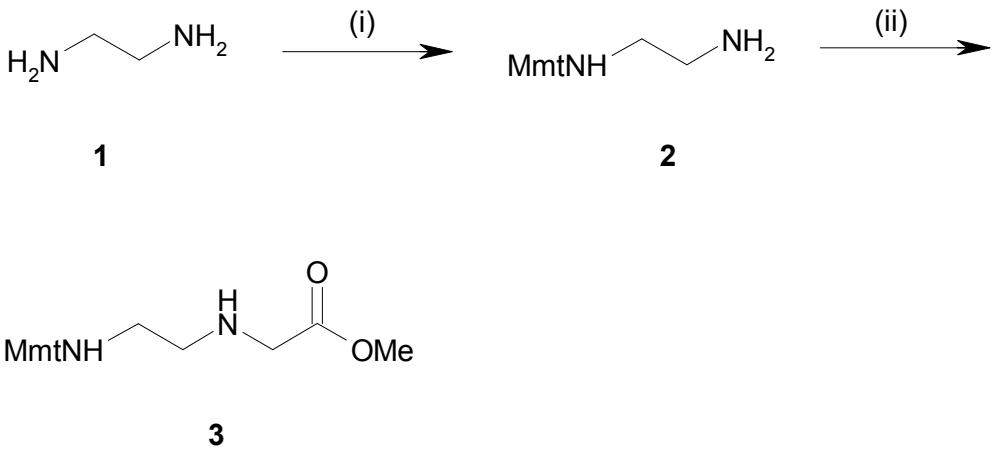

1 **2** **3**

overall yield: 65% (2 steps)

Scheme 1.

Since the introduction of the -CH_2COOMe group into the ethylenediamine complicates the separation of the product from the excess of starting material, we have chosen to introduce first the Mmt group and then the carboxymethylene moiety. In particular, the ethylenediamine was protected selectively at one of the primary amino group by reaction with MmtCl to give compound 2. Crude compound 2 was reacted without purification with methylbromoacetate to give 3. The ^1H NMR chemical shifts of the backbone 3 were in good agreement with those reported in literature.[22] The ^{13}C NMR complete assignment of 3, never reported before, is reported in the experimental part.
The synthesis of the desired protected N1/9-(methyl-carbonyl)-bases was accomplished according to reported procedures,[22] which require first the protection of exocyclic NH_2 of adenine, cytosine and guanine with An-, t-Bu-Bz- and iBu- groups respectively and then the insertion of a methylene carbonyl moiety by alkylation of the protected nucleobases with $BrCH_2COOMe$, followed by saponification, under controlled pH conditions, using aqueous NaOH and dioxane. Carboxymethylated thymine was easily synthesized according to the procedure of Kosynkina et al.[27] In the synthesis of the carboxymethylated bases (5 and 7, Scheme 2), the yields for the reactions of protected cytosine 4 and protected adenine 6 with methyl bromoacetate were of 60% and 82%, respectively. We suggest that these improved yields can be attributed to changes in the temperature during the addition of the reactants and the use of sodium hydride in mineral oil instead of the extremely reactive absolute one.

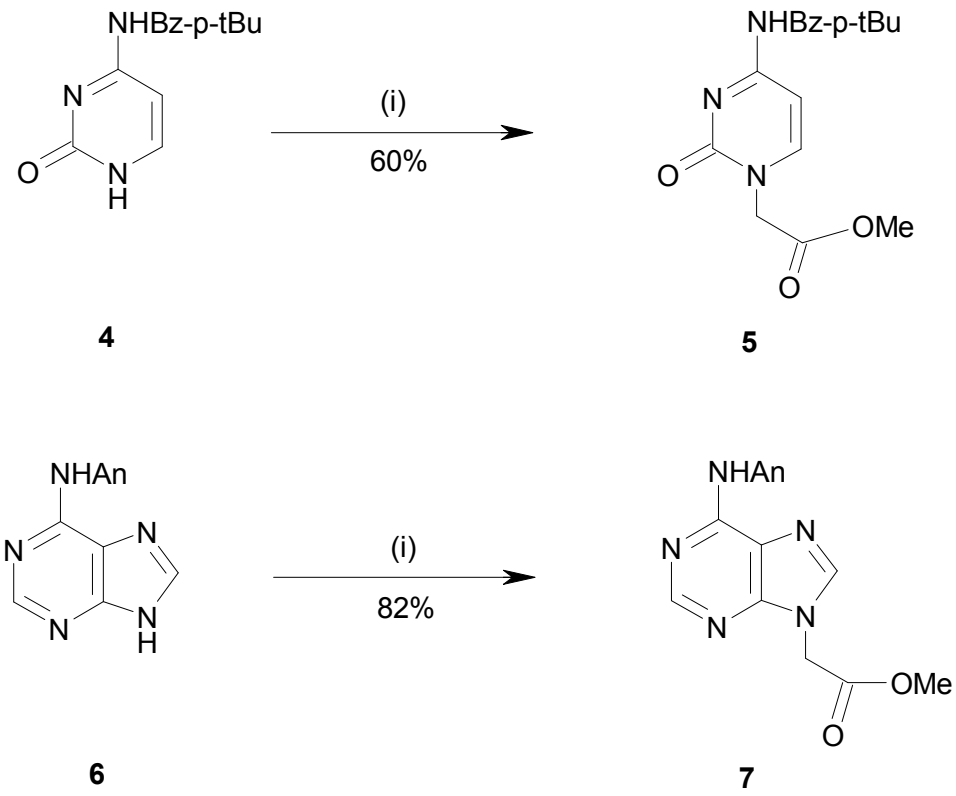

Scheme 2.

The N1/N9-carboxymethylated bases (8, 9, 10, 11, Scheme 3) were attached to the backbone under standard coupling conditions using HOBt/DIC/NMM in DMF to give the Mmt/Acyl PNA methylester monomers (12, 13, 14, 15, Scheme 3). In the condensation step, by optimisation of the reaction and work-up, we got a better yield as compared to what previously reported in the case of the coupling reactions between 9 and 10 and the backbone 3, obtaining products 13 and 14 with a 96% and 83% yield, respectively.
Finally, saponification with NBu_4OH of the resulting methylesters 12, 13, 14 and 15, under controlled pH conditions, gave the desired Mmt/Acyl PNA monomers as tetrabutyl ammonium salts in about quantitative yields.
All the PNA monomers were characterized on the basis of their NMR spectra, which were in good agreement with those reported in literature.

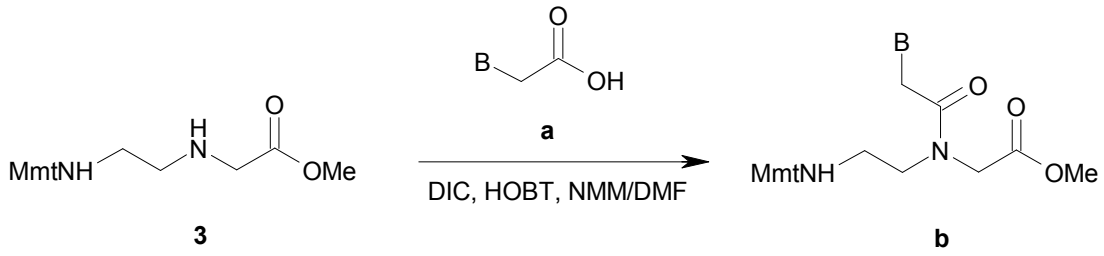

B	NHBz-p-tBu	NHAn		
a	**8**	**9**	**10**	**11**
b	**12** (92%)	**13** (96%)#	**14** (83%)#	**15** (90%)

Scheme 3.

N-(2-(4-Methoxyphenyl)diphenylmethylaminoethyl)glycine methyl ester 3 (Scheme 1).

MmtCl (1.02 g, 3.32 mmol, 1 eq), dissolved in 5 ml of pyridine, was added to a stirred solution of ethylenediamine 1 (2 ml, 29.9 mmol, 9.0 eq) in 7 ml of dry CH_2Cl_2, at 0 °C in portions over a period of 1 h. After stirring for 2 h, the reaction was quenched by adding 1 ml of methanol and evaporated to dryness. On TLC there was prevalently one spot at R_f= 0.14 (8:2 CH_2Cl_2/MeOH). Crude compound 2 was extracted by H_2O/CH_2Cl_2 (1% TEA) and the dichloromethane extracts were evaporated under reduced pressure, redissolved in dry CH_2Cl_2 and Et_3N (3.32 mmol, 462 µl, 1 eq) and directly reacted with $BrCH_2COOMe$ (336 µl, 3.65 mmol, 1.1 eq) which was added to 2 in portions at 0 °C. When the reaction was completed (2 h and 40 min) 20 ml of an aqueous solution of $NaHCO_3$ (2%) were added and the mixture was extracted by CH_2Cl_2 (3 × 15 ml). The combined organic phases were dried by $MgSO_4$, evaporated under reduced pressure and separated by silica gel chromatography using increasing amounts (15-70%) of AcOEt in hexane (1% NEt_3) as eluent, giving pure samples of 3 (872 mg, 2.16 mmol, 65% overall yield) as a yellow oil; R_f= 0.32 (98:2 CH_2Cl_2/MeOH); δ_H ($CDCl_3$) 2.27 (2 H, t, *J* 6.0, CH_2), 2.73 (2 H, t, *J* 6.0, CH_2), 3.35 (2 H, s, CH_2CO), 3.72 (3 H, s, COOMe), 3.80 (3 H, s, Mmt-OMe), 7.50-6.80 (14 H, m, Mmt); δ_C ($CDCl_3$) 43.0 ($MmtNHCH_2$), 59.8 (CH_2CO), 50.5 (CH_2NHCH_2), 51.7 ($COOCH_3$), 55.2 (Mmt-OCH_3), 70.2 (CAr_3), 113.1 (C-7'), 126.1 (C-4'), 127.8 (C-3'), 128.6 (C-2'), 129.8 (C-6'), 138.3 (C-5'), 146.4 (C-1'), 157.8 (C-8'), 173.1 (COOMe).

1-(Methoxycarbonylmethyl)-N^4-(4-tert-butylbenzoyl)-cytosine 5 (Scheme 2).

To a suspension of N^4-(4-tert-butylbenzoyl)cytosine (4, 800 mg, 2.95 mmol, 1 eq) in dry DMF (10 ml), sodium hydride (148 mg, 3.69 mmol, 1.25 eq, 60% in mineral oil) was

added in portions under stirring. After 1 h, methylbromoacetate (339 µl, 3.69 mmol, 1.25 eq) was added dropwise whilst stirring. After 2 h the reaction was quenched by adding 2 ml of methanol and removing the solvent *in vacuo*. The residue was extracted by CH_2Cl_2/water and the organic phases were evaporated *in vacuo* and crystallised from isopropanol to give compound 5 (607 mg, 1.77 mmol) as a white solid in 60% yield. R_f and ^{1}H NMR spectral data were identical to those reported in literature.[22]

N^6-(4-Methoxybenzoyl)-9-(methoxycarbonylmethyl)adenine 7 (Scheme 2).

To a suspension of *N^6*-(4-methoxybenzoyl)adenine (6, 800 mg, 2.97 mmol, 1 eq) in dry DMF (10 ml), sodium hydride (131 mg, 3.27 mmol, 1.1 eq, 60% in mineral oil) was added in portions and the mixture was stirred at room temperature. After 30 min, methylbromoacetate (300 µl, 3.27 mmol, 1.1 eq) was added dropwise whilst stirring and the mixture was further stirred at room temperature. All the reactants were added at 0 °C. After 2 h the reaction was quenched by a small amount of CO_2 in methanol and the resulting solution, concentrated to 1.5 ml, was treated with cold water. The precipitated product was filtered off, washed by a small amount of cold water and dried *in vacuo* to give compound 7 (830 mg, 2.43 mmol) as a white solid in 82% yield. R_f and ^{1}H NMR spectral data were identical to those reported in literature.[22]

N-(2-(4-Methoxyphenyl)diphenylmethylaminoethyl)-N-[(N^6-(4-methoxybenzoyl)-adenin-9-yl)acetyl] glycine methyl ester 13 (Scheme 3).

To a suspension of *N^6*-(4-methoxybenzoyl)adenine (6, 800 mg, 2.97 mmol, 1 eq) in dry DMF (10 ml), sodium hydride (131 mg, 3.27 mmol, 1.1 eq, 60% in mineral oil) was added in portions and the mixture was stirred at room temperature. After 30 min, methylbromoacetate (300 µl, 3.27 mmol, 1.1 eq) was added dropwise whilst stirring and the mixture was further stirred at room temperature. All the reactants were added at 0 °C. After 2 h the reaction was quenched by a small amount of CO_2 in methanol and the resulting solution, concentrated to 1.5 ml, was treated with cold water. The precipitated product was filtered off, washed by a small amount of cold water and dried *in vacuo* to give compound 7 (830 mg, 2.43 mmol) as a white solid in 82% yield. R_f and ^{1}H NMR spectral data were identical to those reported in literature.[22]

N-(2-(4-Methoxyphenyl)diphenylmethylaminoethyl)-N-[(N^2-(isobutanoyl)-guanin-9-yl) acetyl] glycine methyl ester 14 (Scheme 3).

To a solution of [(*N^2*-(isobutanoyl)-9-(carboxymethyl)guanine (10, 155 mg, 0.556 mmol, 1 eq) in dry DMF (2 ml), HOBt (83 mg, 0.612 mmol, 1.1 eq) was added followed by NMM (122 µl, 1.11 mmol, 2 eq) and a solution of the backbone 3 (289 mg, 0.722 mmol, 1.3 eq) in 2 ml of dry DMF. Finally, DIC (103 µl, 0.667 mmol, 1.2 eq) was added whilst stirring. After 64 h the reaction mixture was quenched by addition of few drops of water and was evaporated *in vacuo*. The residue, dissolved in AcOEt, was washed by water and the organic extract, evaporated under reduced pressure, was purified by chromatography on a silica gel column eluted with increasing amounts of MeOH in CH_2Cl_2 (1% TEA), to give 305 mg (0.461 mmol, 83%) of 14. R_f and ^{1}H NMR spectral data were identical to those reported in literature.[22]

Synthesis of Mmt PNA-3'DNA linker

The Mmt-O-protected, nucleobase-derivatised hydroxyethylglycine is a useful monomer to connect the PNA part of a PNA-DNA chimera to the 3' end of the DNA. The reported synthesis of a protected (Dmt) hydroxyethylglycine backbone to be coupled to the protected carboxymethylated nucleobases brings to the desired backbone in three synthetic steps with an overall yield of 41%.[25] We obtained the corresponding Mmt backbone with an overall yield of 80% in only two synthetic steps. We have chosen the Mmt protection because of its greater stability in comparison to the Dmt, used in previous works.[25,26] The hydroxyl function of commercially available 2-aminoethanol as chlorhydrate salt (16, Scheme 4) was protected by treatment with Mmt-Cl in DMF and pyridine to give compound 17. A small amount of crude product 17 was purified to check its identity by NMR. The ^{13}C NMR chemical shift value (86.1 ppm) of the quaternary carbon $C(Ar)_3$ is diagnostic for a $(Ar)_3C$-O as compared to the chemical shift value of $(Ar)_3C$-N, which is around 70 ppm. Compound 17 was monoalkylated using methyl-bromoacetate in CH_2Cl_2/TEA to give N-(2-(4-methoxyphenyl)diphenylmethoxyethyl)glycine methyl ester 18 (Scheme 4).

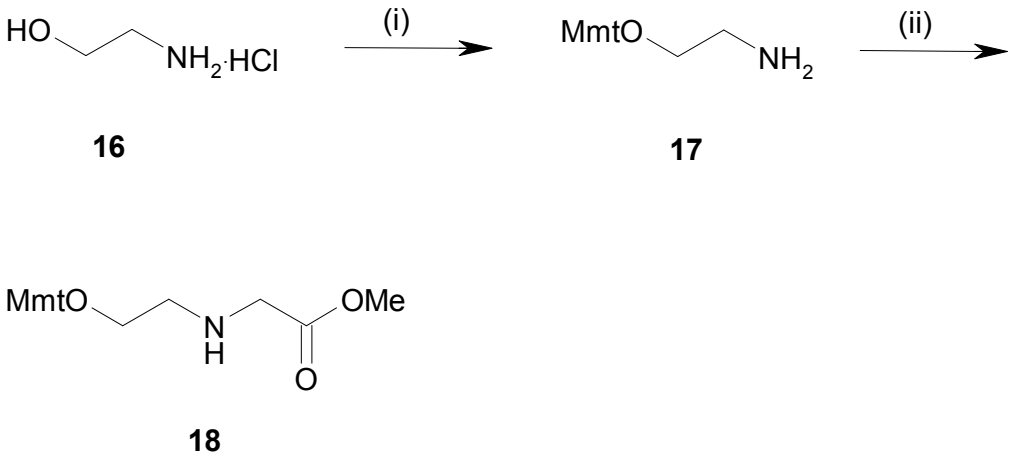

16 **17** **18**

overall yield: 80% (2 steps)

Scheme 4.

The synthesis of the linker monomers requires the coupling between the protected N-(2-hydroxyethyl) glycine (backbone 18) and protected N1/9-(methyl-carbonyl)-bases. As an example we report here the synthesis of the Mmt thymine linker (Scheme 5), obtained by coupling the new backbone 18 with carboxymethylated thymine 11 to give 19, followed by saponification in standard conditions, which afforded the desired Mmt-t linking monomer 20 with an overall yield of 80%. Considering the Mmt-Cl amount used in the first step of the synthetic strategy, the overall yield of Mmt-t linking monomer 20 resulted to be 65%, higher than previously obtained.[25,26] The new O-Mmt backbone 18

can be easily used also to synthesize PNA-3'DNA linkers containing the other bases in analogy to Mmt/acyl PNA monomers (12, 13, 14).
The new linking backbone 18 and the corresponding t linker monomer 19 were characterized on the basis of their ^{1}H and ^{13}C NMR spectra.

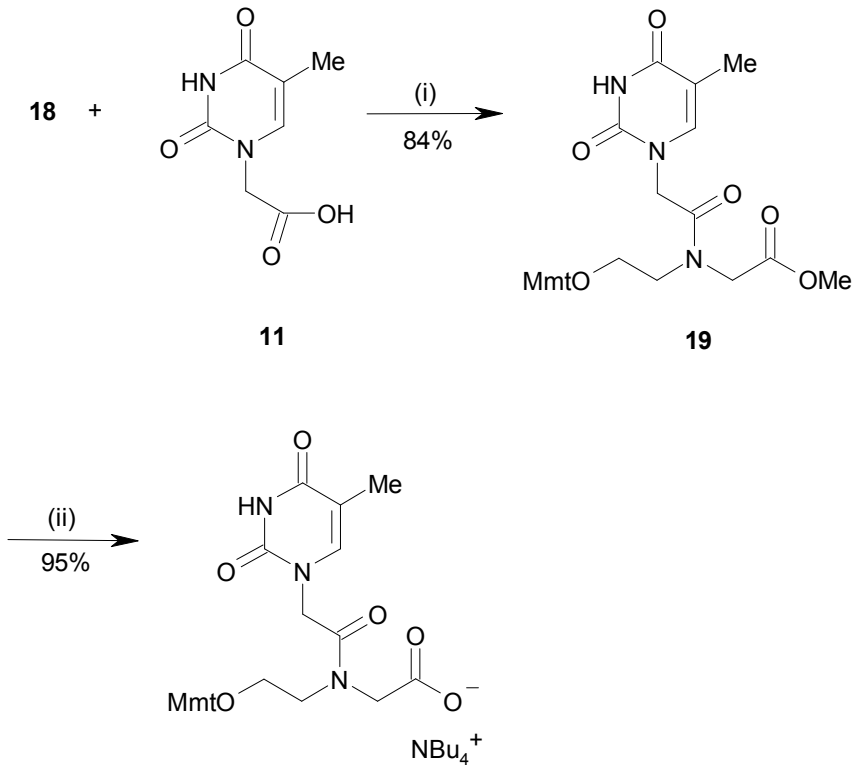

Scheme 5.

N-(2-(4-Methoxyphenyl)diphenylmethoxyethyl)glycine methyl ester 18 (Scheme 4).

Chlorohydrate salt of 2-aminoethanol (16, 120 mg, 1.28 mmol, 4 eq) was dissolved in dry DMF (2 ml) and cooled at 0 °C. Mmt-Cl (99 mg, 0.32 mmol, 1 eq) in dry pyridine (1 ml) was added under stirring in portions and the solution was allowed to warm to room temperature. After 16 h, the reaction was quenched by adding few drops of methanol, evaporating to dryness and extracting with H_2O/CH_2Cl_2 (1% TEA). A small amount of crude product (2-(4-methoxyphenyl)-diphenylmethoxy)ethylamine 17 was loaded on a chromatographic column and eluted with increasing amounts (15-20%) of AcOEt in CH_2Cl_2 (1% NEt_3) as eluent to check for the identity by NMR; yellow oil; R_f =0.14 (85:15 CH_2Cl_2/MeOH); δ_H ($CDCl_3$) 2.87 (2 H, t, *J* 5.2, CH_2), 3.14 (2 H, t, *J* 5.2, CH_2), 3.78 (3 H, s, Mmt-OMe), 7.19-7.46 (14 H, m, Mmt); δ_C ($CDCl_3$) 42.3 (CH_2NH_2), 55.2 (Mmt-OCH_3), 65.6 (CH_2O), 86.1 (CAr_3), 113.0 (C-7'), 126.8 (C-4'), 127.7 (C-3'), 128.4 (C-2'), 130.3 (C-6'), 135.9 (C-5'), 144.6 (C-1'), 158.5 (C-8'); The remaining crude product 17 was dissolved in dry CH_2Cl_2 and Et_3N (535 µl, 3.85 mmol, 12 eq) and directly reacted with

$BrCH_2COOMe$ (35 µl, 0.384 mmol, 1.2 eq). After 2 h the reaction was complete and was quenched by adding water. Crude material was extracted by H_2O/CH_2Cl_2 (1% TEA) and separated by silica gel chromatography using increasing amounts (15-20%) of AcOEt in CH_2Cl_2 (1% NEt_3) as eluent, giving pure sample of 18 (103 mg, 0.256 mmol, 80% overall yield) as a yellow oil; R_f =0.22 (8:2 CH_2Cl_2/AcOEt); δ_H ($CDCl_3$) 2.03 (1 H, s, NH), 2.82 (2 H, t, *J* 5.4, CH_2), 3.21 (2 H, t, *J* 5.4, CH_2), 3.42 (2 H, s, CH_2CO), 3.73 (3 H, s, COOMe), 3.79 (3 H, s, Mmt-OMe), 7.46-6.81 (14 H, m, Mmt); δ_C ($CDCl_3$) 49.2 (*C*H_2CO), 50.7 (*C*H_2NHCH_2), 51.7 (COO*C*H_3), 55.1 (Mmt-O*C*H_3), 62.8 (Mmt*O*CH_2), 86.2 (*C*Ar_3), 113.3 (C-7'), 127.0 (C-4'), 128.0 (C-3'), 128.6 (C-2'), 130.5 (C-6'), 136.0 (C-5'), 144.8 (C-1'), 158.7 (C-8'), 173.0 (*C*OOMe); *m/z* (MALDI-TOF) found 406 (M + H^+), $C_{25}H_{27}NO_4$ + H^+ requires 406.5.

N-(2-(4-Methoxyphenyl)diphenylmethoxyethyl)-N-((1-thyminyl)acetyl glycine methyl ester 19 (Scheme 5).

To a solution of carboxymethyl thymine (11, 55 mg, 0.30 mmol, 1.2 eq) in dry DMF (2 ml), HOBt (40 mg, 0.30 mmol, 1.2 eq) was added followed by NMM (60 µl, 0.55 mmol, 2.2 eq) and a solution of the backbone 18 (100 mg, 0.250 mmol, 1.0 eq) in 2 ml of dry DMF whilst stirring. Finally, DIC (50 µl, 0.325 mmol, 1.3 eq) was added whilst stirring. After 20 h the reaction mixture was quenched by adding few drops of water and evaporating *in vacuo*. The residue, dissolved in AcOEt, was washed by water and the organic extract, evaporated under reduced pressure, was purified by chromatography on a silica gel column eluted with increasing amounts of AcOEt in CH_2Cl_2 (1% TEA), to give 119 mg (0.210 mmol, 84%) of 19 as a yellow oil; R_f = 0.46 (96:4 CH_2Cl_2/MeOH); δ_H ($CDCl_3$) 1.81 and 1.90 (3 H, 2xs [2 rotamers], H-5 T), 3.31 and 3.41 (2 H, 2xm [2 rotamers], NCH_2), 3.54 (2 H, m, Mmt*O*CH_2), 3.67 (3 H, s, COOMe), 3.79 (3 H, s, Mmt-OMe), 3.98 and 4.35 (2 H, 2xs [2 rotamers], CH_2COOMe), 4.42 and 4.72 (2 H, 2xs [2 rotamers], CH_2CON), 6.64-7.39 (15 H, m, Mmt, H-6 T), 8.77 and 8.86 (2 H, 2xs [2 rotamers], H-3 T); δ_C ($CDCl_3$) 12.27 and 12.29 (thymine CH_3), 47.4 and 47.5 (*C*H_2N(CO)CH_2), 47.9 and 48.5 (N(CO)*C*H_2CO), 48.3 and 50.4 (N(CO)*C*H_2N), 52.3 and 52.6 (COO*C*H_3), 55.2 (Mmt-O*C*H_3), 61.0 and 62.6 (Mmt*O*CH_2), 87.0 and 87.7 (*C*Ar_3), 110.5 and 110.6 (thymine C5), 113.2 and 113.3 (C-7'), 127.0 and 127.3 (C-4'), 127.9 and 128.1 (C-3'), 128.2 and 128.4 (C-2'), 130.3 and 130.4 (C-6'), 134.8 and 135.2 (C-5'), 140.8 and 140.9 (thymine C6), 143.7 and 144.2 (C-1'), 150.89 and 150.94 (thymine C2), 158.6 and 158.8 (C-8'), 164.1 and 164.2 (thymine C4), 167.2 and 167.4 (N(*C*O)CH_2N), 169.0 and 169.6(*C*OOMe); *m/z* (MALDI-TOF) found 594 (M + Na^+), $C_{32}H_{33}N_3O_7$ + Na^+ requires 594.6.

Tetrabutylammonium N-(2-(4-methoxyphenyl)diphenylmethoxyethyl)-N-((1-thyminyl)acetyl) glycinate 20 (Scheme 5).

To a solution of compound 19 (119 mg, 0.210 mmol) in dioxane (3 ml) a solution of tetrabutyl ammonium hydroxide (2 M) was added dropwise until the solution reached pH 12. After 2 h the solution was adjusted to pH 7 by the dropwise addition of 2 M aqueous $KHSO_4$. After evaporation the residue was resuspended in CH_2Cl_2 and filtered. The filtrate evaporated under reduced pressure resulted to be the desired compound 20 (158

mg, 0.199 mmol) in 95% yield; R_f =0.44 (9:1 CH_2Cl_2/MeOH); δ_H ($CDCl_3$) 0.97-1.64 (28 H, m, butyl), 1.82 and 1.85 (3 H, 2xs [2 rotamers], H-5 T), 2.34 and 2.41 (2 H, 2xm [2 rotamers], NCH_2), 3.19 (8 H, m, butyl NCH_2), 3.43 and 3.56 (2 H, 2xm [2 rotamers], $MmtOCH_2$), 3.78 (3 H, s, Mmt-OMe), 3.90 and 4.01 (2 H, 2xs [2 rotamers], CH_2COO^-), 4.45 and 4.88 (2 H, 2xs [2 rotamers], CH_2CON), 6.77-7.44 (15 H, m, Mmt, H-6 T), 8.64 (1 H, s, H-3 T); *m/z* (MALDI-TOF) found 580 (M + Na^+), $C_{31}H_{31}N_3O_7$ + Na^+ requires 580.6.

In conclusion in this section we described a new synthetic strategy to synthesize a Mmt protected PNA-3'DNA linker useful for connecting the PNA part of PNA/DNA chimeras to 3' end of the DNA one.
Mmt protected hydroxyethylglycine 18 (Scheme 4), conveniently obtained in two synthetic steps starting from chlorohydrate salt of 2-aminoethanol, was coupled to the carboxymethyl thymine 11 to give the monomer 19 in a very good overall yield (Scheme 5).
Furthermore, a convenient method for the preparation of PNA monomers with monomethoxytrityl (Mmt) group as temporary protection of the backbone amino function and acylic protection on the nucleobases was employed. We followed a general strategy that relies on the coupling between Mmt protected N-(2-amino-ethyl)-glycine ester (backbone) and protected N1/9-(methyl-carbonyl)-bases. The Mmt protected backbone 3 was obtained from ethylenediamine 1 in two synthetic steps with an overall yield (65%) higher than previously obtained (Scheme 1).[22]
The synthesis of the desired protected N1/9-(methyl-carbonyl)-bases was accomplished according to reported procedures.[22] However, we have obtained an improvement in the reactions between protected cytosine 4 and protected adenine 6 with methyl bromoacetate in respect to those previously reported in literature.[22] We got better yields as compared to those reported in literature[22] also in the condensations between the N1/N9-carboxymethylated bases 9 and 10 and the backbone 3 to give the monomers 13 and 14 (Scheme 3).
The main advantage of the synthetic procedures to obtain both the Mmt backbone 3 and the Mmt hydroxyethylglycine 18 is the introduction of the acid labile Mmt protecting group in the first step.
The strategies described herein thus easily allows a cheap and large scale preparation of the monomers for the automatic synthesis of PNA/DNA chimeras using the convenient Mmt chemistry.

1.3.6 Synthesis of PNA/DNA chimeras

The PNA/DNA chimeras oligomers were assembled with the PNA section at the 3'-end (C-terminus, Fig. 2) and the DNA part at the 5'-end. A glycine residue was loaded on a Controlled-Pore Glass (CPG, loading 49µmol/g) resin by using DIC/DMAP as activating system (R.T., 16 h). Glycine loading was checked by UV detection of removed Fmoc group and was always more than 95%. Subsequently PNA monomers were added manually and swelling of the resin during each synthetic step was provided by means of a vibrating shaker. PNA monomer coupling was carried out in DMF/MeCN solution using NMM as base and PyBOP as activating reagent (two couplings of 20 min). The modified PNA thymine linker monomer bearing the monomethoxytrityloxyethyl group has been

used to connect the PNA part to the DNA one (22). After each coupling, capping of unreacted amino groups was achieved using a mixture of acetic anhydride (5%) and lutidine (6%) in DMF. Coupling efficiency was evaluated by spectroscopic measurements of monomethoxytrityl cation release after deprotection with 3% TCA in DCM (yields between 90-95%). The assembly of DNA part was performed on an Expedite 8909 automated DNA/PNA synthesiser on the 15 µmol scale by a standard synthetic cycle, consisting of double coupling with the 5'-DMT-nucleoside-3'-phosphoramidite, capping of the unreacted 5'-OH functionalities and oxidation of the P(III) to P(V) with final DMT removal. DNA coupling efficiency was automatically monitored by the measurement of 4,4'-dimethoxytrityl cation released by the acid treatment of each deblock step. Deprotection of the nucleobase protecting groups and detachment of the chimeric oligomers from the solid support were achieved by treatment with a solution of KOH (0.4 M) in MeOH:H_2O (4:1) for 17 h at R.T. The supernatant was filtered and the support washed with H_2O (3x4 ml). The combined filtrate and washings were concentrated in vacuo and redissolved in water.

1.3.7 HPLC purification of PNA-DNA chimeras

The crude chimeric oligomers were analysed and purified by HPLC on a Nucleogel SAX column (Machery Nagel SAX 1000-8 4.6x50 mm, SAX 1000-10 25x150 mm) eluted with linear gradients of KCl (0-70%) in 20 mM K_2HPO_4, pH 7.0, 20% CH_3CN.
Analytical HPLC for Chim 18 mer (crude material):

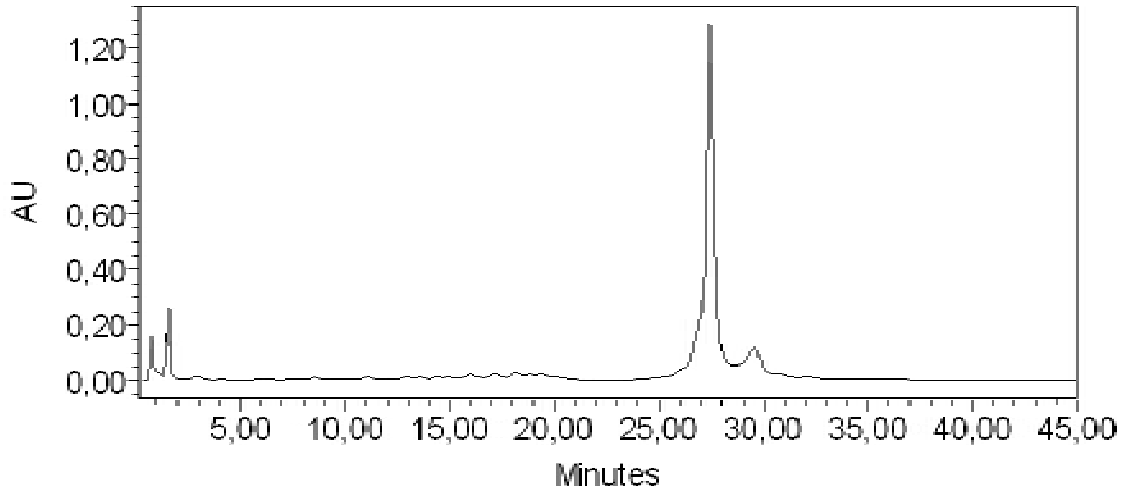

0-100% B 40 min (analytical SAX column)

Analytical HPLC Chim 20 mer (crude material):

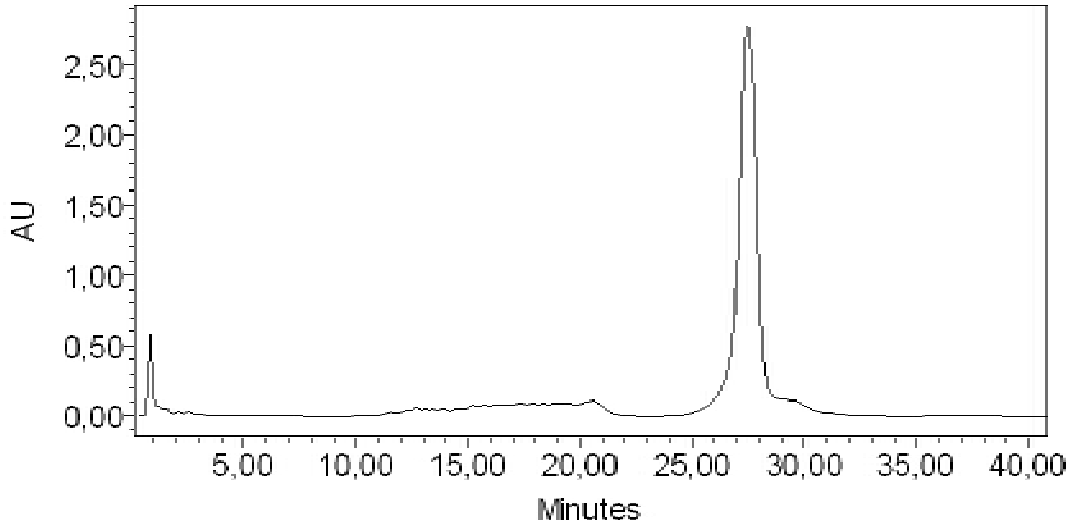

0-100% B 40 min (analytical SAX column)

The isolated oligomers (20 mer and 18 mer) having both a retention time of about 27 min, were desalted by Sephadex gel filtration on NAP^{TM}-25 columns eluted with water and analysed by LC ESI-MS (experiments performed on Finnigan Surveyor MSQ™ LC/MS Mass Spectrometer). Around 25 mg of chimeric oligomer were recovered in both cases after this procedure corresponding to a ~20 % yield. Chim 20: *m/z* (ESI) found 1521.4 $[M + 4H]^{4+}$, 1215.9 $[M + 5H]^{5+}$ require 1520.6 $[M + 4H]^{4+}$, 1216.7 $[M + 5H]^{5+}$; Chim 18: *m/z* (ESI) found 1844.6 $[M + 3H]^{3+}$, 1384.3 $[M + 4H]^{4+}$, 1107.7 $[M + 5H]^{5+}$ require 1845.4 $[M + 3H]^{3+}$, 1384.3 $[M + 4H]^{4+}$, 1107.6 $[M + 5H]^{5+}$. By HPLC analysis on analytical column the isolated oligomers resulted to be more than 98% pure.

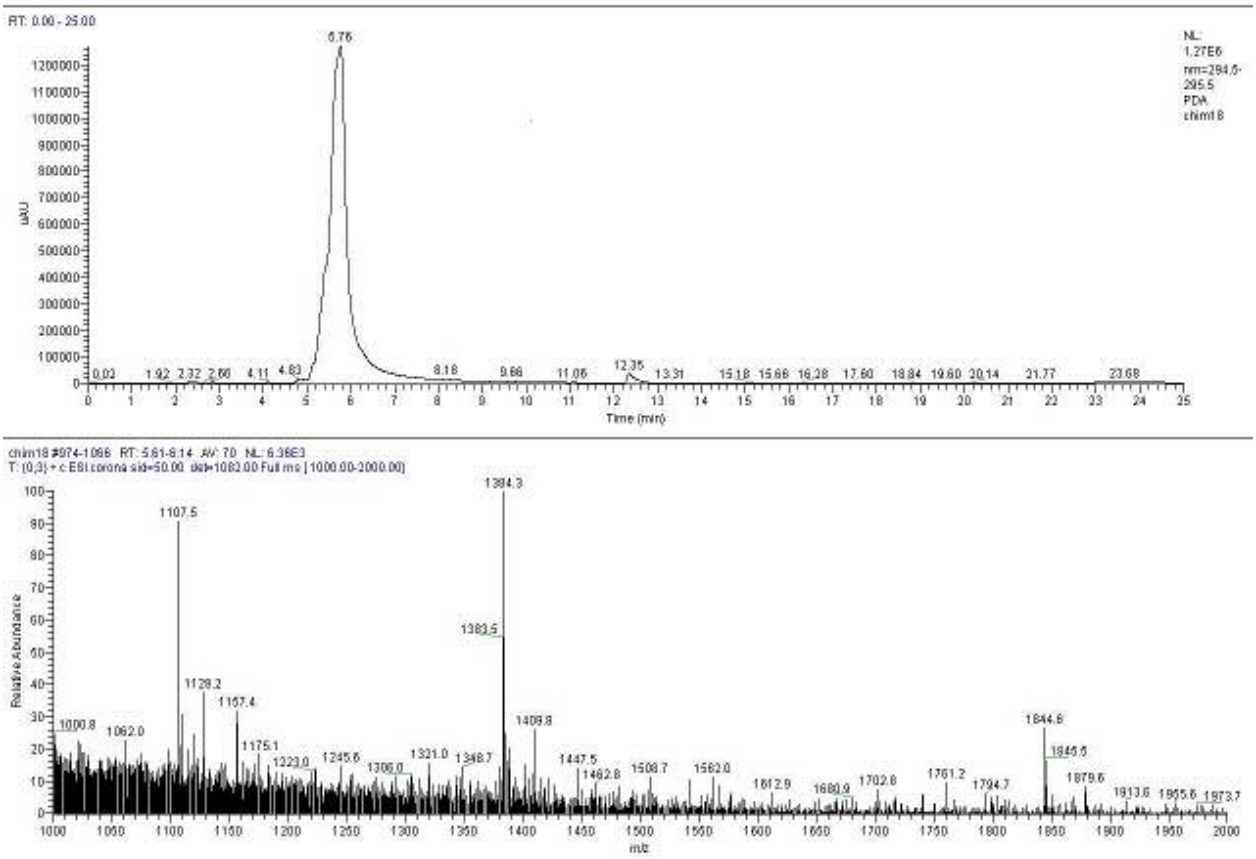

Figure 20: LC-ESI MS allows for checking identity of chimeras

1.3.8 UV melting studies of the chimeric duplex

The chimeric molecules were annealed in a solution consisting of 100 mM NaCl (pH 7.0) by heating the mixture at 90 °C for 5 min and allowed to cool at R.T overnight. Ultraviolet melting temperatures (T_m) at λ= 260 nm on this solution were determined using a JASCO V-550 UV/VIS spectrophotometer equipped with a Peltier block. A heating rate of 0.5 °C/min was used throughout.

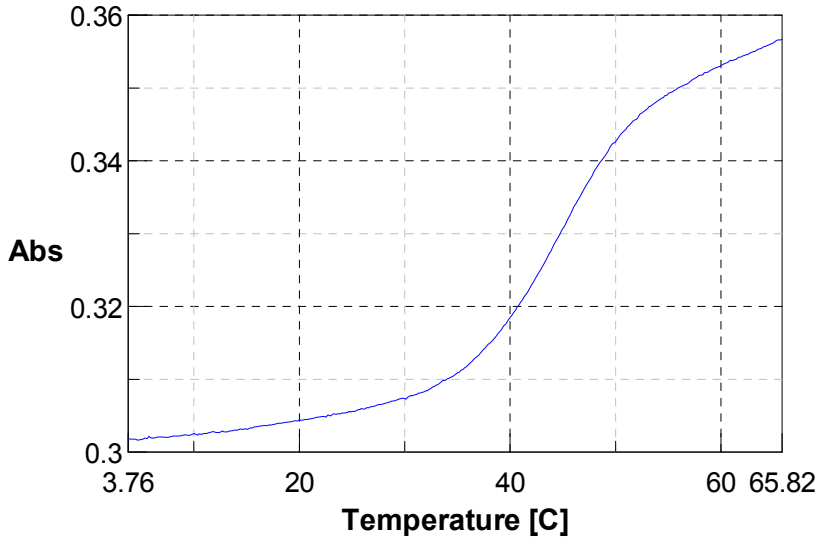

Figure 21: UV Melting (0.5 °C/min) of duplex Chim 2A (10 μM), 100 mM NaCl, cuvette 1mm.

Experiments were repeated until three values within 0.5 °C of each other were obtained. Molar extinction coefficients used for DNA bases were as follows: A, 15.4; T, 8.8; G, 11.7; C, 7.3 mM^{-1}. Molar extinction coefficients used for PNA bases were T, 8.6; C, 6.6 mM^{-1}. T_m value (43.9 °C) was determined from the maximum of the first derivative of the plot of A_{260} versus temperature.
CD profile for the chimeric duplex is reported below. Parameters used in this experiment were: scanning speed = 50 nm/min; cell Length= 1 cm; concentration= 2 μM; solvent= tamp 5mM pH7 0.5mM Mg Temperature = 15 °C.

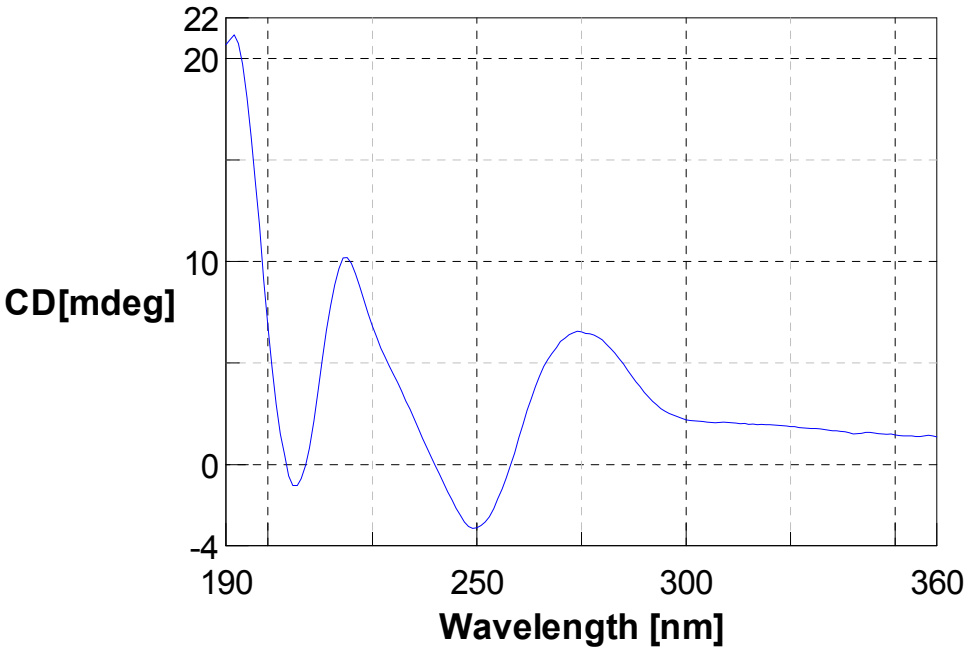

1.3.9 Stability of bent Nucleic Acids and PNA-DNA chimeras in Human Serum at 37 °C

The stability of the double-stranded PNA-DNA chimera molecule with 2 adenines in the bulge (chim 2A) was tested in human serum in comparison with 2A, the double-stranded DNA.
7 µM Chim 2A (as checked by UV absorption) was incubated at 37 °C in 100% fresh human serum and 10 ul of the solution was injected on Sax analytical column in HPLC experiments (A = 20 mM K_2HPO_4, pH 7.0, 20% CH_3CN; B = KCl 1M, 20 mM K_2HPO_4, pH 7.0, 20% CH_3CN). The diminution of the area of the HPLC peak corresponding to the undegraded molecule after different incubation times in serum was checked in order to follow the degradation of 2A.

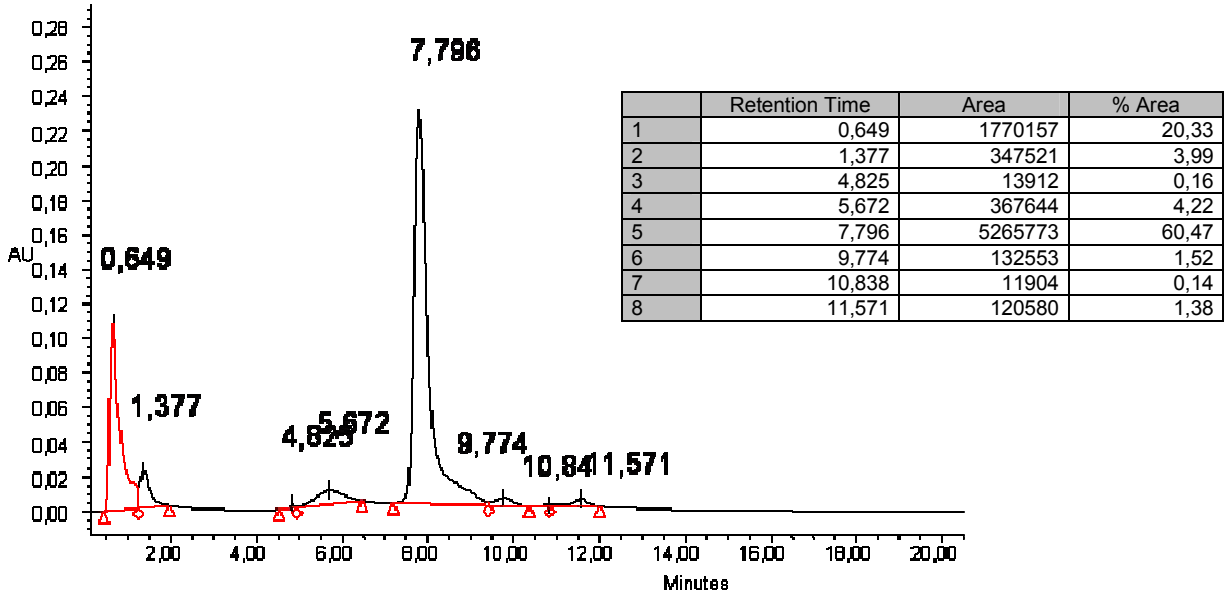

	Retention Time	Area	% Area
1	0,649	1770157	20,33
2	1,377	347521	3,99
3	4,825	13912	0,16
4	5,672	367644	4,22
5	7,796	5265773	60,47
6	9,774	132553	1,52
7	10,838	11904	0,14
8	11,571	120580	1,38

Figure 22: HPLC profile of 100% fresh human serum (analytical Sax column, 0-100% B in A in 25 min).

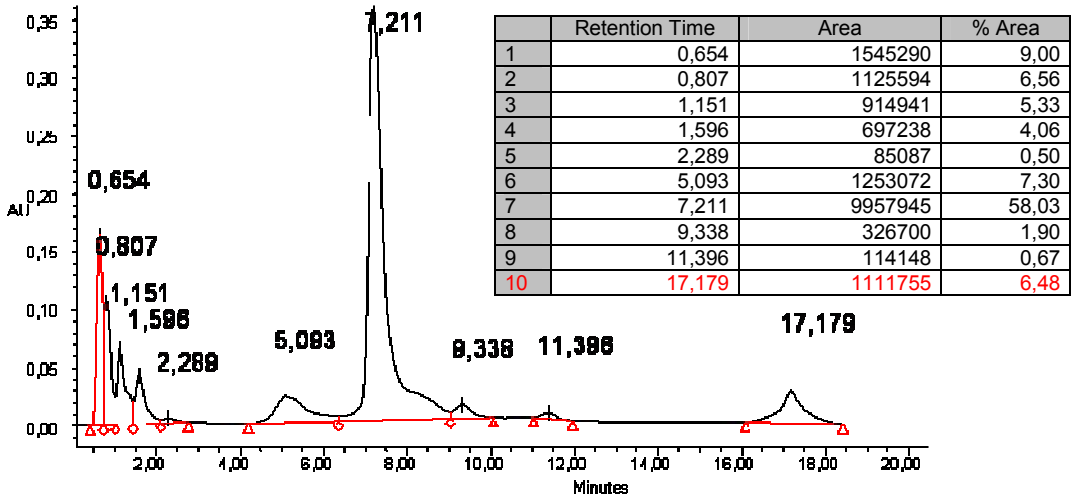

	Retention Time	Area	% Area
1	0,654	1545290	9,00
2	0,807	1125594	6,56
3	1,151	914941	5,33
4	1,596	697238	4,06
5	2,289	85087	0,50
6	5,093	1253072	7,30
7	7,211	9957945	58,03
8	9,338	326700	1,90
9	11,396	114148	0,67
10	17,179	1111755	6,48

Figure 23: HPLC profile of 7 µM Chim 2A incubated at 37 °C in 100% fresh human serum (t = 30 min).

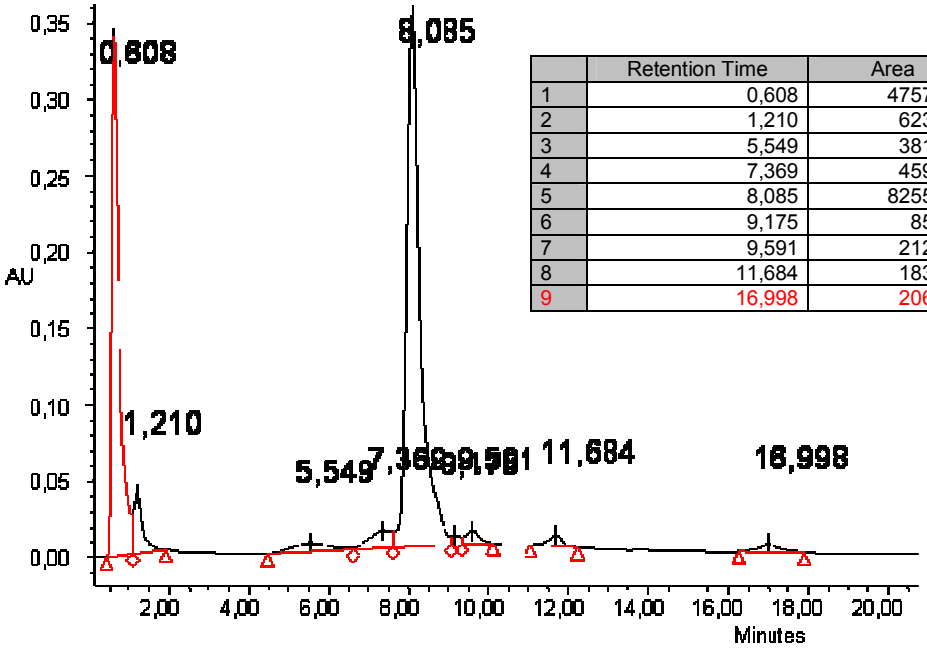

	Retention Time	Area	% Area
1	0,608	4757473	31,37
2	1,210	623890	4,11
3	5,549	381956	2,52
4	7,369	459964	3,03
5	8,085	8255918	54,43
6	9,175	85241	0,56
7	9,591	212881	1,40
8	11,684	183174	1,21
9	16,998	206395	1,36

Figure 24: HPLC profile of 7 µM Chim 2A incubated at 37 °C in 100% fresh human serum (t = 24 h).

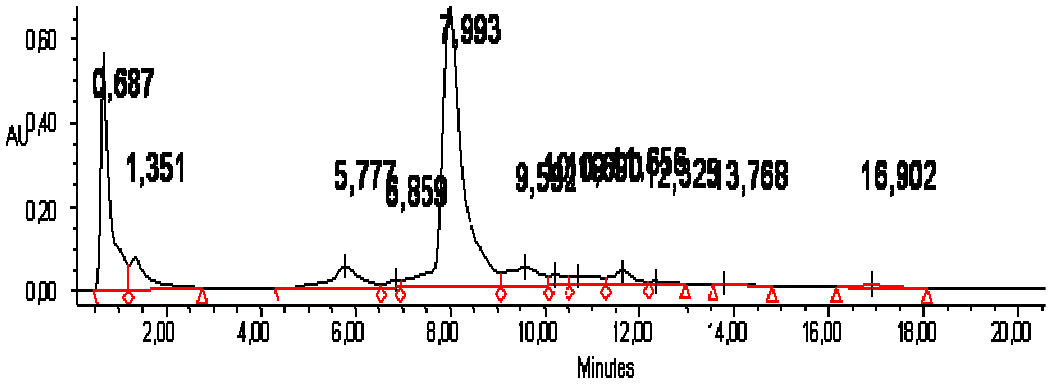

	Retention Time	Area	% Area
1	0,687	7341081	19,70
2	1,351	2011804	5,40
3	5,777	2275586	6,11
4	6,859	338108	0,91
5	7,993	20249236	54,35
6	9,592	2067249	5,55
7	10,197	602727	1,62
8	10,690	880515	2,36
9	11,656	981639	2,63
10	12,325	144454	0,39
11	13,768	34508	0,09
12	16,902	305438	0,82

Figure 25: HPLC profile of 7 µM Chim 2A incubated at 37 °C in 100% fresh human serum (t = 40 h).

The HPLC peak areas relative to the Chim 2A, expressed as percentage of the total HPLC profile area to avoid inaccuracies due to different injection volumes, was reported in function of the incubation times (see Fig. 26). The non-linear regression analysis curve (R^2 = 0.99) gave, by interpolation, a 50% degradation time of 9 h. On the other hand, 2A DNA duplex has a 40 min half-life, and was completely degraded after 1h 35 min.

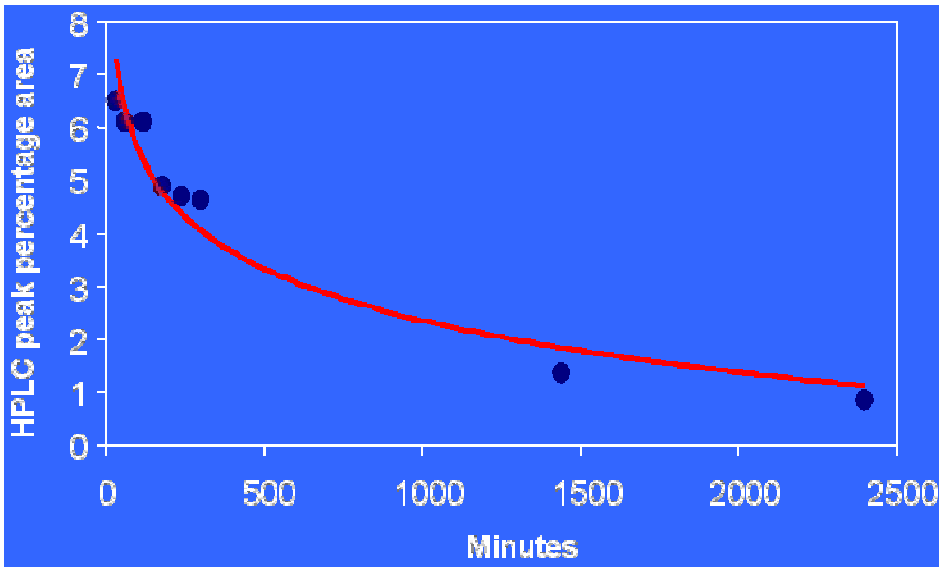

Figure 26: Serum degradation curve for Chim 2A in human fresh serum.

1.3.10 Biological Assays: proliferation assay, migration assay and *in vivo* test

To investigate whether the chimeric bent duplex was able to inhibit *in vitro* the HMGB1 induced proliferation and migration activities of bovine aortic endothelial cells (BAEC), two biological assays were performed: the proliferation and the chemotaxis assays.

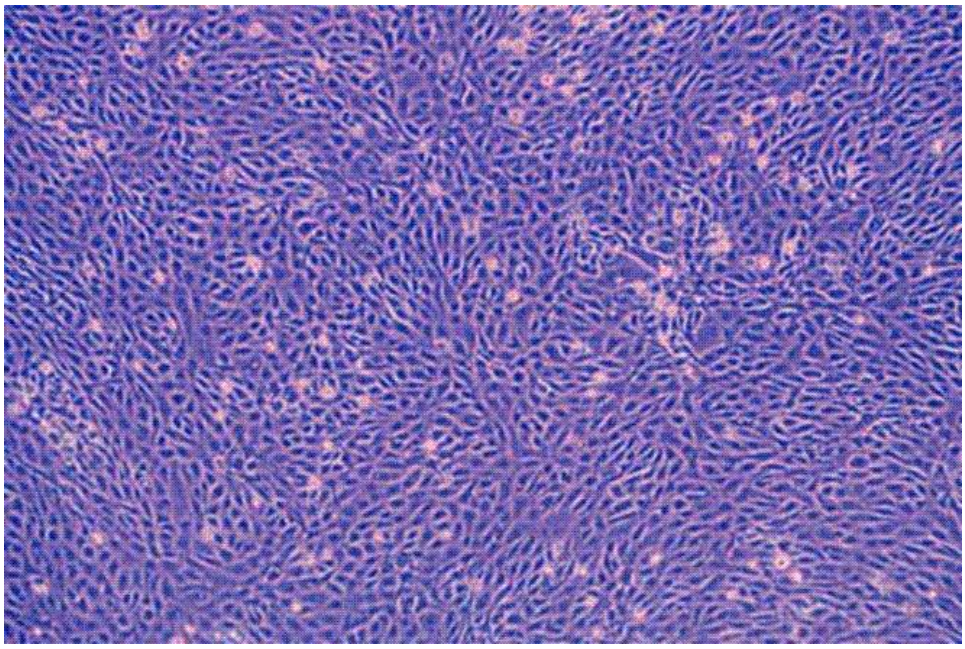

Figure 27: Bovine Aortic Endothelial Cells (BAEC).

Proliferation Assay

The proliferation assay was performed as described by Palumbo et al., (2004). BAEC cells (bovine aortic endothelial cells) were seeded in 6-well plates (10^5 cells/well) and grown in RPMI medium supplemented with 20% FCS. After 24 h, the medium was replaced with serum-free RPMI and cells were then starved for 16 hours to synchronize the cell population. Vehicle (negative control or basal proliferation) or 30 ng/mL (1 nM) of HMGB1 (bacterially made) were added in the presence or in the absence of 100 nM of the test compounds (dissolved and diluted in serum-free medium).

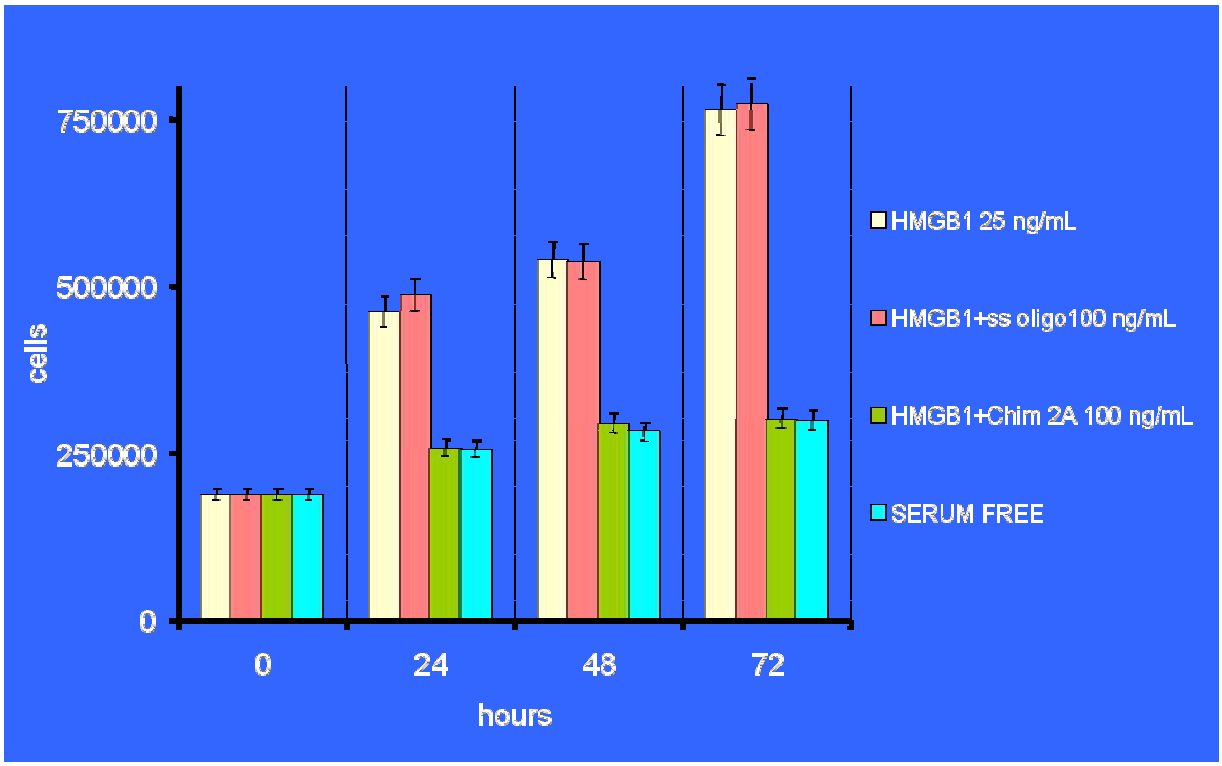

Figure 28: Effect of HMGB1-Chimeric duplex interaction on cellular (BAEC) proliferation

The assay performed with the bent Chim 2A was also carried out with a control linear oligo DNA (indicated as ss oligo in the legend of Figure 28), consisting of the 20 mer strand. The experiment was repeated three times. BAEC cell proliferation was determined by detaching the cells from the plate at the indicated times, and counting the Trypan-blue excluding cells under the microscope. The inhibition of the HMGB1-induced proliferation activity of BAEC cells by the bent chimeric compound are shown in Figure.
In a further assay according to the protocol as described above, it was demonstrated that the bent chimeric duplex concentration-dependently inhibit/antagonize the proliferation of BAEC cells induced by HMGB1.
The highest proliferation effect was recorded in serum free cells treated with HMGB1 (25 ng/mL) after 72 hours. When serum free cells are treated with HMGB1 (25 ng/mL) and Chim 2A (100 ng/mL) the proliferation effect is basal and similar to that showed by serum free untreated cells.
The Chim 2A exhibited an IC_{50} of ~10 nM, while control linear duplex DNA does not (Figure 10/Table 1). In a further experiment , proliferation of BASMC (bovine aortic smooth muscle cells) in the presence of the specific compounds of the present work was tested (protocol described in Palumbo et al., 2004, not shown data). BASMC cells were seeded in 6-well plates (10^5 cells/well) and grown in RPMI medium supplemented with 20% FCS. After 24 h, the medium was replaced with serum-free RPMI and cell were then starved for 16 hours to synchronize the cell population. Vehicle (negative control or basal proliferation) or 25 ng/mL (1 nM) of HMGB1 (bacterially made) were added in the presence or in the absence of the compounds dissolved as described above. Each

experimental point represents the mean +/- SD of triplicate determinations. The experiment was repeated three times. BASMC cell proliferation was determined by detaching the cells from the plate at different times (on days 1, 2, 3 and 4 of culturing) and counting the Trypan-blue excluding cells under the microscope. A concentration dependent inhibition of proliferation of BASMC was observed for the bent duplex (IC_{50} ~ 10 nM). The linear control compounds had no effect.

Chemotaxis Assay

Chemotaxis assays were performed using well-known protocols, in particular as described by Palumbo et al., (2004).
Modified Boyden chambers were used with filters having 5-8 µm pore size and treated with gelatine type A from porcine skin 5 µg/mL. BAEC cells were resuspended in serum-free DMEM (Dulbecco's Modified Eagle's Medium) and a sample of 40,000 cells was added to the upper well of a Boyden chamber.

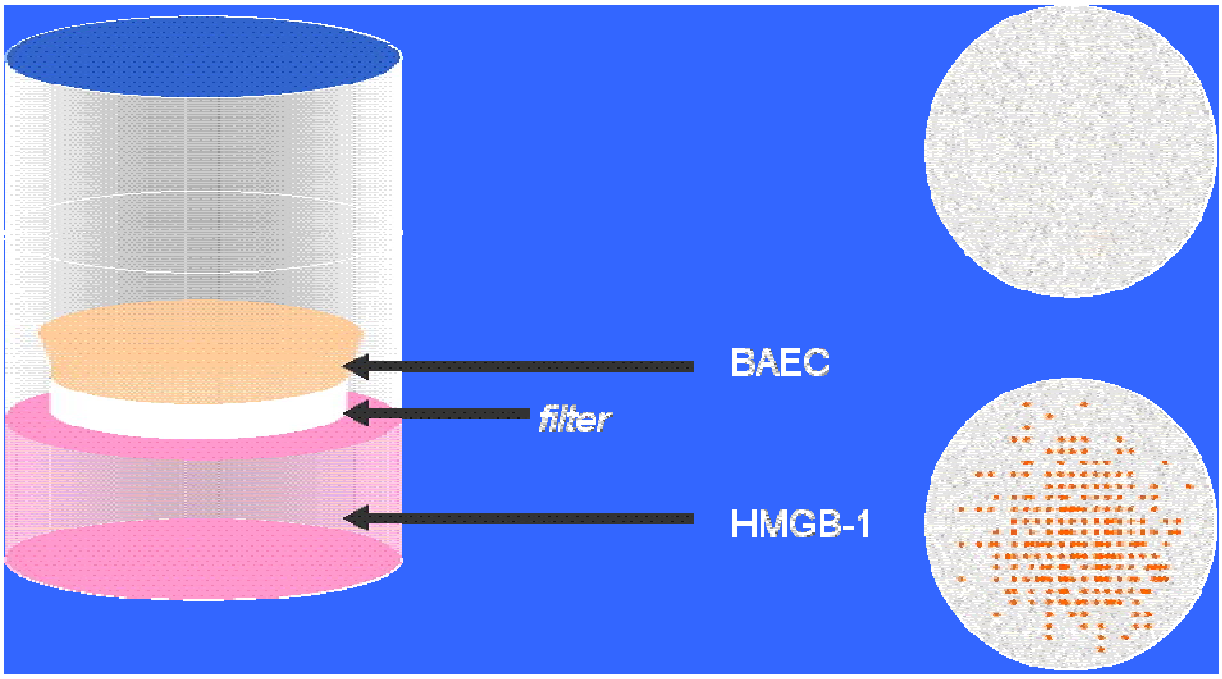

Figure 29: Boyden chamber for chemotaxis assays

The molecules to be tested were dissolved and diluted in the same serum-free medium and added to the lower well of the chamber; HMGB1 (bacterially made) concentration was 25 ng/mL, for test compounds it was 3-100 nM. The assay performed with bent Chim 2A was also carried out with a single strand (20 mer) as indicated above as control compound. Cell migration was allowed at 37 ± 0.5 °C for 4 hours, then cells were scraped off the upper surface, and filters were fixed in ethanol and stained in a solution of modified Giemsa stain (Accustain, Sigma).

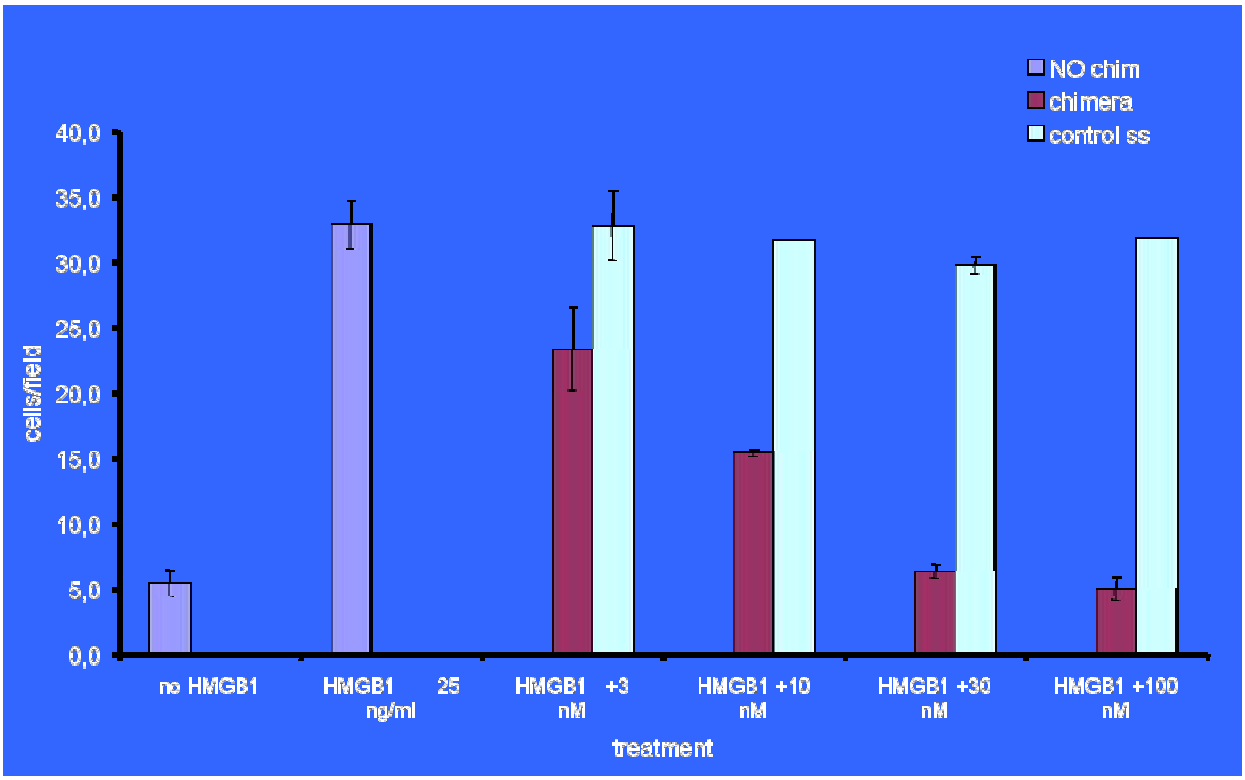

Figure 30: Effect of HMGB1-Chimeric duplex interaction on cellular migration

All experiments were performed at least twice in triplicate. The inhibition of HMGB1-induced migration activity of BAEC cells by the bent chimeric compound is shown in Figure 6. Results are the mean +/- SD of the number of cells counted in 10 high power fields per filter. In absence of HMGB1 cell migration was only basal (migration index~ 5,0 cells/field). When HMGB1 is present at a concentration of 25 ng/mL, cells migrate significantly (~30 cells/field). A similar migration is observed when cells are treated with 25 ng/mL HMGB1 and different amounts (3/10/30/100 nM) of control single strand. In this case, since single strand does not present the same ability of Chim 2A bent structure to interact with HMGB1, no effect was expected. On the other hand, when cells, incubated with HMGB1 (25 ng/mL), are treated by Chim 2A, a concentration dependent inhibition of migration of BAEC cells is observed (IC_{50} ~10 nM).

In vivo tests

Several in vivo tests based on the reversal of LPS-induced endotoxemia in mice are in progress and preliminary results show that mortality significantly decreases as a consequence of the treatment with PNA/DNA chimeras.

1.3.11 Conclusions and perspectives

This thesis shows that it is possibile to use oligonucleotidic ligands to target pro-inflammatory cytokines like HMGB1. By improving the synthesis and purification of both

monomers and chimeric oligomers, it was possible to obtain enzymatically stable 5'DNA-3'PNA chimeras in large scale and high purity. The obtained quantities of pure chimeras allowed us to use these molecules for the first time *in vivo* in experiments that showed that chimera-chimera duplexes are able to interact with HMGB1 blocking its important pro-inflammatory effects.
Future efforts will be focused on improving this strategy by shortening chimeric sequences. Another approach to be explored will deal with duplexes having two different nucleobases in the bulge or an abasic. Subsequently, other DNA analogues different from PNA will be used for realising new chimeric structures to be used for the same biotechnological application described in this thesis.

1.3 - REFERENCES

1. Peter E. Nielsen, Michael Egholm, Rolf H. Berg, and Ole Buchardt. *Sequence-Selective Recognition of DNA by Strand Displacement with a Thymine-Substituted Polyamide*. Science, 254: 1497--1500, 1991.
2. Egholm M, Buchardt O, Nielsen PE, Berg RH: Peptide nucleic acids (PNA). Oligonucleotide analogs with an achiral peptide backbone. *J Am Chem Soc* 1992, 114: 1895-1897.
3. Nielsen PE, Egholm M, Buchardt O: Peptide Nucleic Acid (PNA). A DNA Mimic with a Peptide Backbone. *Bioconjugate Chemistry* 1994, 5: 3-7. Uhlmann, E.; Peyman, A.; Breipohl, G.; Will, D. W. Angew Chem Int Ed 1998, 37, 2796.
4. Egholm, M.; Buchardt, O.; Christensen, L.; Behrens, C.; Freier, S. M.; Driver, D. A.; Berg, R. H.; Kim, S. K.; Norden B.; Nielsen, P. E. Nature 1993, 365, 566.
5. Nielsen, P. E.; Egholm, M.; Buchardt, O. J Mol Recognit 1994, 7, 165.
6. Demidov, V. V.; Potaman, V. N.; Frank-Kamenetskii, M. D.; Egholm, M.; Buchard, O.; Sonnichsen, S. H.; Nielsen, P. E. Biochem Pharmacol 1994, 48, 1310-3.
7. Buchardt, O.; Egholm, M.; Berg R. H.; Nielsen, P. E. Trends in Biotechnology 1993, 11, 384-6.
8. Nielsen, P. E.; Egholm, M.; Berg, R. H.; Buchardt, O. Anti-Cancer Drug Design 1993, 8, 53.
9. Nielsen, P. E.; Egholm, M. Curr Issues Mol Biol 1999, 1, 89.
10. Gambari, R. Curr Pharm Des 2001, 7, 1839.
11. Nielsen, P. E. Curr Opin Mol Ther 2000, 2, 282.
12. Ray, A.; Norden, B. Faseb J 2000, 14, 1041.
13. Uhlmann, E.; Will, D. W.; Breipohl, G.; Langner, D.; Ryte, A. Angew Chem Int Ed 1996, 35, 2632.
14. Uhlmann, E. Biol Chem 1998, 379, 1045.
15. Borgatti, M.; Lampronti, I.; Romanelli, A.; Pedone, C.; Saviano, M.; Bianchi, N.; Mischiati, C.; Gambari, R. J. Biol Chem 2003, 278, 7500.
16. Bergmann, F.; Bannwarth, W.; Tam, S. Tetrahedron Lett 1995, 36, 6823.
17. Kuwahara, M.; Arimitsu, M.; Sisido, M. J Am Chem Soc 1999, 121, 256.
18. Kuwahara, M.; Arimitsu, M.; Shigeyasu, M.; Saeki, N.; Sisido, M. J Am Chem Soc 2001, 123, 4653.

19. Kovács, Gy.; Timár, Z.; Kupihár, Z.; Kele, Z.; Kovács, L. J Chem Soc Perkin Trans 1, 2002, 1266-1270.
20. Kofoed, T.; Hansen, H. F.; Orum, H.; Koch, T. J. Pept Sci 2001, 7, 402.
21. Will, D. W.; Breipohl, G.; Langner, D.; Knolle, J.; Uhlmann, E. Tetrahedron 1995, 51, 12069.
22. Stetsenko, D. A.; Lubyako, E. N.; Potapov, V. K.; Azhikima, T. L.; Sverdlov, E. D. Tetrahedron Lett 1996, 37, 3571.
23. Finn, P. J.; Gibson, N. J.; Fallon, R.; Hamilton, A.; Brown, T. Nucleic Acids Res 1996, 24, 3357.
24. Breipohl, G.; Will, D. W.; Peyman, A.; Uhlmann, E. Tetrahedron 1997, 53, 14671.
25. Petersen, K. H.; Jensen, D. K.; Egholm, M.; Nielsen, P. E.; Buchardt, O. Bioorganic & Medicinal Chemistry Letters 1995, 5, 1119.
26. Kosynkina, L.; Wang, W.; Liang, T. C. Tetrahedron Lett 1994, 35, 5173.
27. Brown, SC, SA Thomson, JM Veal & DG Davis: NMR solution structure of a peptide nucleic acid complexed with RNA. Science 265, 777-780 (1994)

PART 2

New nucleoamminoacids useful for applications of PNA/DNA chimeras in the diagnostic field

2.1 Introduction

The unambiguous and fast detection of oligonucleotide sequences *in vitro* and *in vivo* still is a major market especially since more and more diseases are linked to their genetic origin. In 1996 Kramer introduced the concept of a molecular beacon (Figure 1A)[1] as one of many diagnostic methods for DNA single strand sequence detection as well as mismatch identification known so far.[2] The molecular beacon is a DNA single strand composed of a loop region having a length of around 20 nucleotides with a sequence complementary to the target DNA and a stem region in which the terminal nucleotides (around 10) are paired in a double strand.[3] On the 5'- or 3'-terminus, respectively, a fluorophore and a quencher are linked. Fluorescence is quenched as long as the stem region is paired in a double strand. Recognition of the target DNA by formation of a rigid helical double strand leads to separation of the termini which can be easily detected by fluorescence. Next to genetic analysis[4] and detection of point mutations, the molecular beacon concept is also of use in real time PCR,[1] RNA detection in living cells,[5] and in the identification of protein-DNA interactions.[6] The introduction of single molecule detection for the interaction of a molecular beacon with DNA leads to an increase in sensitivity from about 10^{-7} M to 10^{-11} - 10^{-12} M.[7] Nevertheless, the sensitivity based on this detection is limited due to the solvent accessibility of the fluorophore.

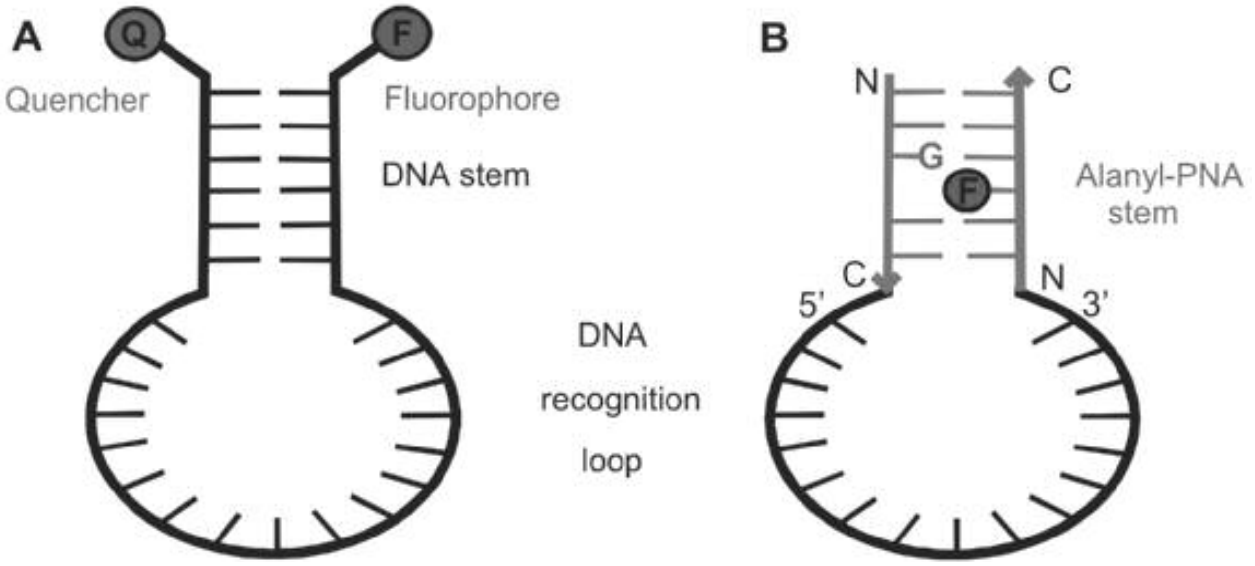

Figure 1. A. Concept of a molecular beacon as described by Kramer;[1] B. Molecular beacon composed of an alanyl-PNA stem hiding the fluorophore (F) within the nucleobase stack and DNA recognition loop.

2.2 The molecular beacon approach for DNA single strand sequence detection

In order to gain even higher sensitivity for DNA detection, we propose to use an alanyl-PNA double strand as the stem of a molecular beacon keeping the DNA recognition loop (Figure 1B). Alanyl-PNA is an artificial oligomer that forms specific and stable double strands based on nucleobase recognition.[8] The alanyl-PNA pairing system is orthogonal to oligonucleotides with respect to double strand formation and provides a possibility to hide the fluorophore from polar solvents.[9]

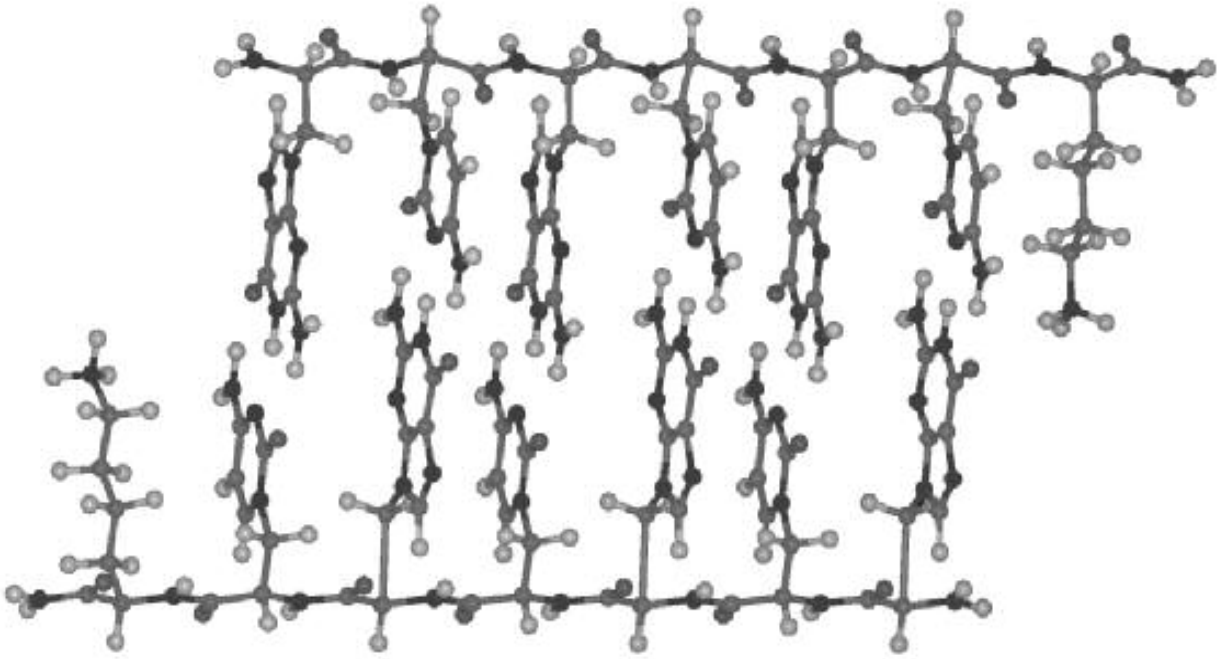

Figure 2. Linear alanyl-PNA double strand: a fluorophore can be hidden within the nucleobase stack covalently linked to an alanyl side chain instead of a nucleobase.

An alanyl-PNA oligomer is based on a regular peptide backbone composed of alanyl amino acids that carry covalently linked nucleobases in the β-position of the side chain (Figure 2).[10] Oligomerization of the nucleo amino acids allows for the formation of rigid and well defined double strands with linear topology based on base pair recognition, stacking, and solvation. Base pairs are stacking with a distance of about 3.5 Å providing a completely extended peptide backbone. Nevertheless, intercalation can be made possible by creating oligomers with a missing base pair by introduction of glycines in opposite positions.[11] Evidence for a non-polar environment within the basestack of alanyl-PNA is derived from a stabilizing effect from incorporation of aromatic amino acids in alanyl-PNA.[9] Shielding of the fluorophore from the water environment when intercalated within the alanyl-PNA duplex should be a major advantage of the chimeric alanyl-PNA/DNA molecular beacon. To ensure for a stoichiometrically well defined system, the fluorophore will be covalently linked to the peptide backbone. Guanine nucleobases in the complementary alanyl-PNA strand will function as quenchers.[7]
A molecular beacon composed of an alanyl-PNA stem and a DNA recognition part requires the preparation of alanyl-PNA/DNA/alanyl-PNA chimeras (Figure 3A). They might be obtained either by ligation of two alanyl-PNA fragments to the 3'- and 5'-termini of the DNA single strand, respectively,[12,13] or by solid phase synthesis of the whole chimeric strand under DNA synthesis conditions.[14] Uhlmann and van Boom already reported the

stepwise solid phase synthesis of aminoethylglycine-PNA/DNA chimeras (Figure 3B)[15,16] adapting the protecting group strategy for nucleo amino acids to DNA synthesis conditions. The protecting groups of the nucleo amino acids need to be compatible with the DNA phosphoramidite chemistry: the acid labile monomethoxytrityl (Mmt) protection and the acyl protecting groups on the exocyclic amino functions of the nucleobases are suitable for this purpose. The Mmt-protected monomers show good solubility in the polar organic solvents (e.g. DMF) used for the synthesis of the oligomers and the conditions for removing the Mmt protecting group (3% trichloroacetic acid) are mild and do not cause depurination in the DNA portion of the chimeras. Moreover, in the peptide synthesis by Mmt-chemistry every coupling can be monitored by measuring the absorbance of Mmt^+ ion released in acid (ε_{478}=65000) allowing the evaluation of the coupling yield.

2.3 Alanyl-PNA double strand as the stem of a molecular beacon

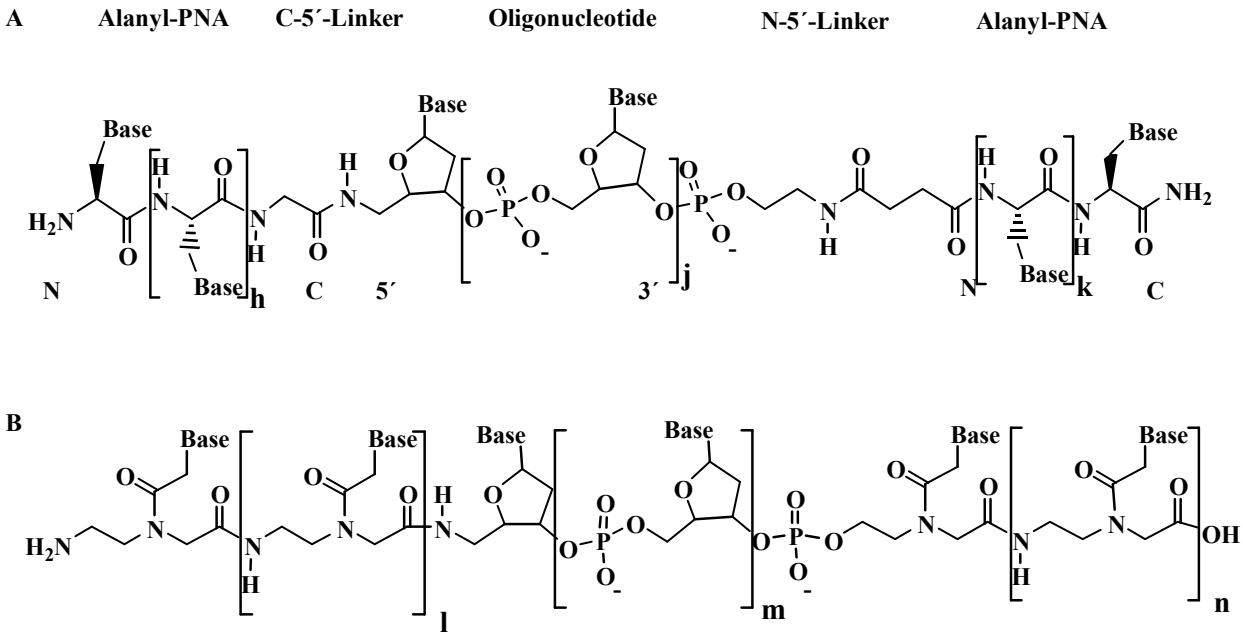

Figure 3. A. Alanyl-PNA/DNA/Alanyl-PNA chimera and B. aminoethylglycine-PNA/DNA/aminoethylglycine-PNA chimera as described by Uhlmann.[15]

In this work the enantioselective preparation of Mmt-protected nucleo amino acids 1–4 (Figure 4) was provided by the syntheses of Boc-alanyl nucleo amino acids[17,18] followed by a substitution of the terminal amino protecting group. Nevertheless, the need for acyl protection of the nucleobases afforded a reinvestigation of the Boc-amino acid synthesis with the respective nucleobase.

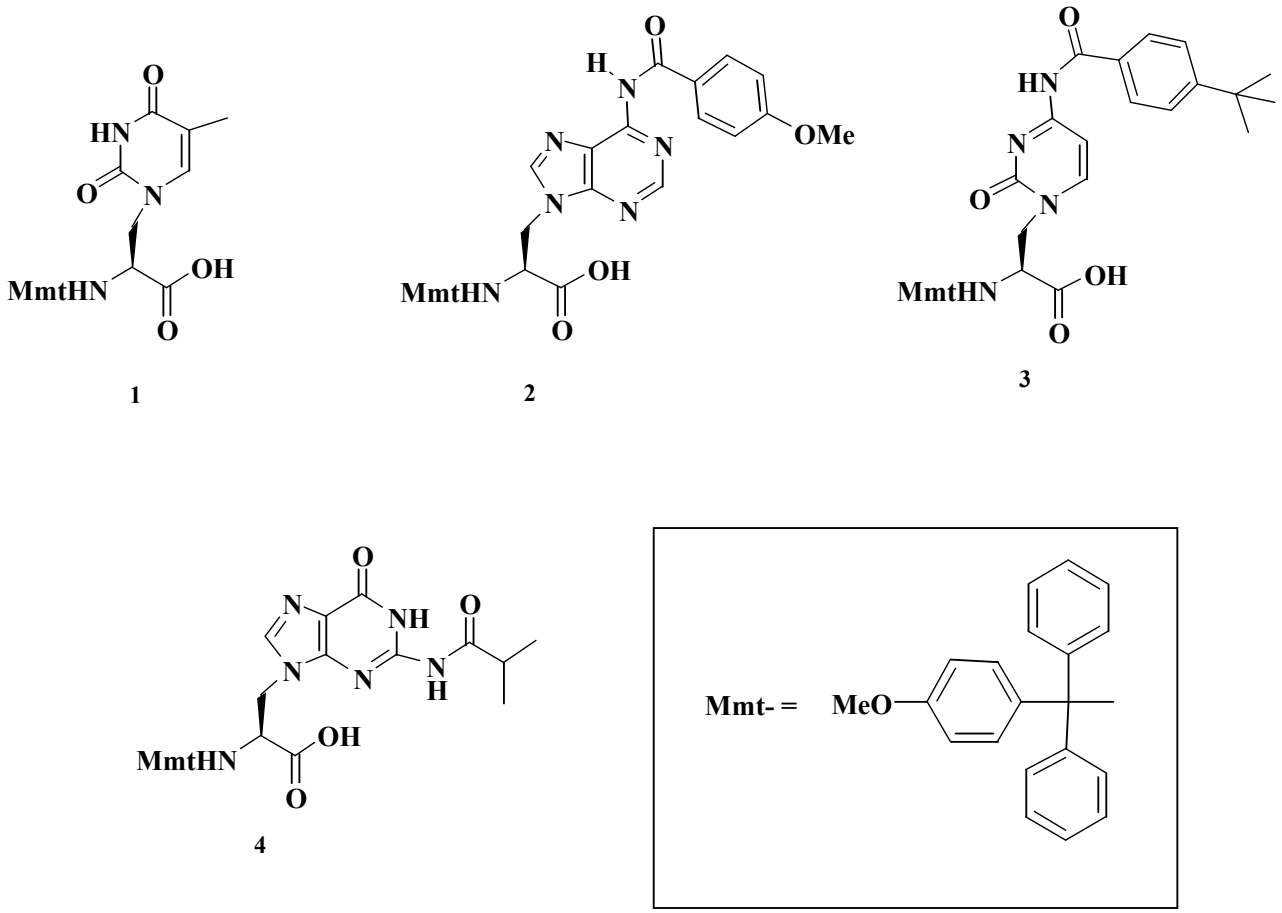

Figure 4. Mmt/acyl-protected nucleo amino acids for the synthesis of alanyl-PNA/DNA chimeras.

2.4 Synthesis of Mmt-protected alanyl nucleo amino acids.

Boc-protected alanyl nucleo amino acids are obtained by ring opening of Boc-serine lactone (5)[19] with the respective nucleobase (Scheme 1).[17,18] Since thymine is the only nucleobase that does not require protection, nucleo amino acid 6 was obtained as described in literature.[17] The acyl-protected nucleobases 8, 9 and 11 were synthesised according to the procedure described by Will et al.[15] N_α-Boc-β-[N^6-(Anisoyl)adenin-9-yl]alanine (7) was provided in 32% yield by ring opening of Boc-serine lactone 5 with N^6-anisoyladenine (8) in DMSO with DBU as a base. As known already for the reaction with the unprotected nucleobases, the yield of the serine lactone ring opening with nucleobases is quite low (22% in case of adenine)[18] because of their low solubility, regioselectivity problems (N7 vs. N9 alkylation and S_N2 vs. carbonyl attack on the serine lactone), polymerization of the serine lactone, and racemization. Nevertheless, despite intensive studies for improvement in the yield for this reaction, this route turned out to be most efficient. The enantiomeric purity was investigated for nucleo amino acid 7 (92% ee) as well as for all other derivatives described herein by Boc-deprotection followed by dipeptide formation with the Boc-L-Ala-OSu active ester and HPLC analysis of the respective diastereomers. N^4-(4-*tert*-Butylbenzoyl)cytosine (9) was also converted to the N_α-Boc-β-[N^4-(4-*tert*-butylbenzoyl)cytosin-1-yl]alanine (10) in DMSO in presence of DBU with moderate yield (42%) but excellent enantiomeric purity (99% ee).
N_α-Boc-β-[*N2*-(isobutyryl)guanin-9-yl]alanine (11) was provided with an optical purity of 96% ee in 29% yield by ring opening of Boc-serine lactone 5 with N^2-(isobutyryl)guanine (12) in DMSO and DBU as base.

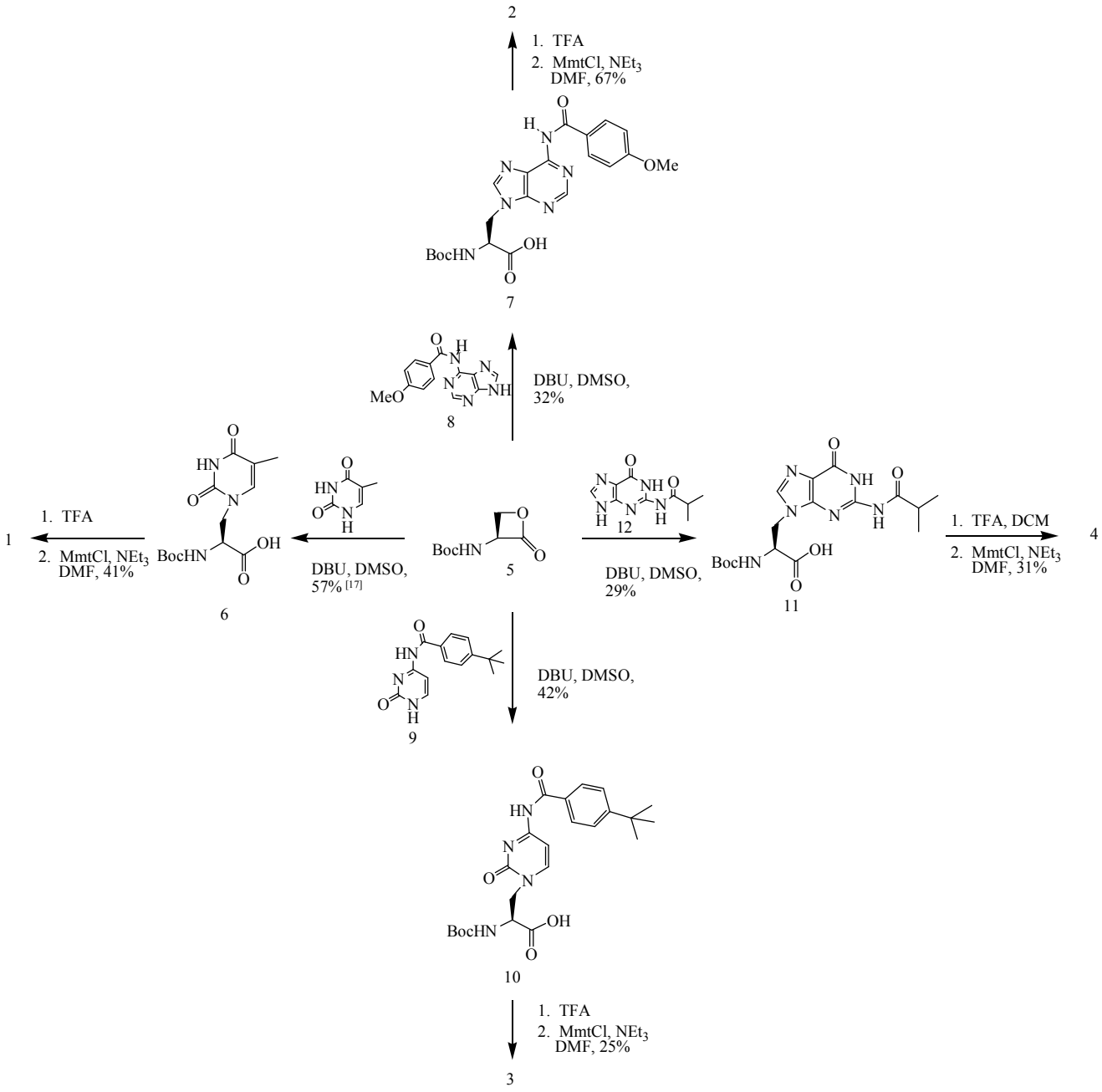

Scheme 1. Synthesis of Boc and Mmt protected nucleo amino acids with acyl protected nucleobases.

Mmt-protected nucleo amino acids 1–4 were obtained starting from the respective Boc-derivatives 6, 7, 10 and 11 by Boc-deprotection with TFA and immediate tritylation of the free nucleo amino acids with monomethoxytrityl chloride (MmtCl) in DMF in presence of triethylamine (Scheme 1). The desired protected monomers were directly obtained by precipitation from diethyl ether at -28 °C. This straightforward route was chosen even because silica gel chromatography of the Mmt-amino acids making use of acidic eluents for protonating the carboxylate moiety causes the deprotection of the acid labile trityl protection. Experimental procedures for this synthetic route are described by Roviello et al[20].

2.5 Conclusions and perspectives

The enantioselective preparation of all canonical alanyl nucleo amino acids with Mmt-protected α-amino groups and acyl-protected exocyclic amino functions of the nucleobases was presented in this work. It was made possible by the synthesis of the respective *N*-Boc nucleo amino acids carried out by adapting the synthetic routes to the Boc-protected alanyl amino acids in the case of the acyl-protected nucleobases. These derivatives will be advantageous in the solid phase synthesis of alanyl-PNA/DNA chimeras which might serve as tools for very sensitive DNA detection following the molecular beacon concept. Oligomer synthesis and functional evaluation are currently under investigation.

REFERENCES - PART 2

[1] a) S. Tyagi, F. R. Kramer, *Nat. Biotechnol*. 1996, *14*, 303. b) S. Tyagi, D. Bratu, F. R. Kramer, *Nat. Biotechnol*. 1998, *16*, 49.
[2] a) G. P. Pfeifer, *Technologies for Detection of DNA damage and mutations*, Plenum, New York, 1996; b) G. R. Taylor, *Laboratory methods for the detection of mutations and polymorphisms in DNA*, CRC Press, Boca Raton, Fla, 1997; c) V. V. Didenko, *In situ detection of DNA damage: Methods and protocols*, Humana Press, Totowa, New Jersey, 2002.
[3] a) W. Tan, X. Fang, J. Li, X. Liu, *Chem. Eur. J.* 2000, *6*, 1107.
[4] L. G. Kostrikis, S. Tyagi, M. M. Mhlanga, D. D. Ho, F. R. Kramer, *Science* 1998, 279, 1228.
[5] T. Matsuo, *Biochim. Biophys. Acta* 1998, *1379*, 178.
[6] J. J. Li, X. Fang, S. M. Schuster, W. Tan, *Angew. Chem. Int. Ed.* 2000, *39*, 1049.
[7] J. P. Kneymeyer, M. Sauer, *Anal. Chem*. 2000, *72*, 3717.
[8] U. Diederichsen, in "Bioorganic Chemistry - Highlights and New Aspects" Eds. U. Diederichsen, T. K. Lindhorst, L. A. Wessjohann, B. Westermann, Wiley-VCH, Weinheim, 1999.
[9] U. Diederichsen, D. Weicherding, *Synlett* 1999, *S1*, 917.
[10] U. Diederichsen, *Angew. Chem. Int. Ed. Engl*. 1996, *35*, 445.
[11] U. Diederichsen, *Bioorg. Med. Chem. Lett.* 1997, *7*, 1743.
[12] U. Diederichsen, H. Guthmann, S. Cortekar, manuscript in preparation.
[13] a) N. J. Ede, G. W. Tregear, J. Haralambidis, *Bioconjugate Chem.* 1994, *5*, 373; b) K. Arar, A. M. Aubertin, A. C. Roche, M. Monsigny, R. Mayer, *Bioconjugate Chem.* 1995, *6*, 573; c) E. Vives, B. Lebleu, *Tetrahedron Lett.* 1997, *38*, 1183; d) J. G. Harrison, S. Balasubramanian, *Nucleic Acids Res.* 1998, *26*, 3136; e) D. L. McMinn, M. M. Greenberg, *Biorg. Med. Chem.* 1999, *9*, 547; f) D. Forget, D. Boturyn, E. Defrancq, J. Lhomme, P. Dumy, *Chem. Eur. J.* 2001, *7*, 3970; g) T. S. Zatsepin, D. A. Stetsenko, A. A. Arzumanov, E. A. Romanova, M. J. Gait, T. S. Oretskaya, *Bioconjugate Chem.* 2002, *13*, 822; h) N. Ollivier, C. Olivier, C. Gouyette, T. Huynh-Dinh, H. Gras-Masse, O. Melnyk, *Tetrahedron Lett.* 2002, *43*, 997.
[14] a) F. Bergmann, W. Bannwarth, *Tetrahedron Lett.* 1995, *36*, 1839; b) J. C. Truffert, U. Asseline, A. Brack, N. T. Thuong, *Tetrahedron* 1996, *52*, 3005; c) M. Antopolsky, A. Azhayev, *Helv. Chim. Acta* 1999, *82*, 2130; d) A. Sakakura, Y. Hayakawa, *Tetrahedron* 2000, *56*, 4427; e) M. Antopolsky, A. Azhayev, *Tetrahedron Lett.* 2000, *41*, 9113; f) M. Antopolsky, E. Azhayeva, U. Tengvall, A. Azhayev, *Tetrahedron Lett.* 2002, *43*, 527; g) D. A. Stetsenko, A. D. Malakho, M. J. Gait, *Org. Lett.* 2002, *4*, 3259; h) D. Musumeci, G. N. Roviello, M. Valente, R. Sapio, C. Pedone, E. M. Bucci, *Biopolymers* 2004, *76*, 535.

[15] a) E. Uhlmann, B. Greiner, G. Breipohl, in *Peptide Nucleic Acids, Protocols and Applications* (Eds. Nielsen, P. E., Egholm, M.), Horizon Scientific Press, Norfolk, 1999, 51; b) R. Vinyak, in *Peptide Nucleic Acids, Protocols and Applications* (Eds. Nielsen, P. E., Egholm, M.), Horizon Scientific Press, Norfolk, 1999, 71; c) E. Uhlmann, A. Peyman, G. Breipohl, D. W. Will, *Angew. Chem. Int. Ed.* 1998, *37*, 2797; d) D. W. Will, G. Breipohl, D. Langner, J. Knolle, E. Uhlmann, *Tetrahedron* 1995, *51*, 12069.
[16] a) A. C. van der Laan, N. J. Meeuwenoord, E. Kuyl-Yeheskiely, R. S .Oosting, R. Brands, J. H. van Boom, *Recl. Trav. Chim. Pays-Bas*. 1995, *114*, 295; b) A. C. van der Laan, A. C. Brill, R. Kuimelis, E. Kuyl-Yeheskiely, J. H. van Boom, *Tetrahedron Lett*. 1997, *38*, 2249.
[17] P. Lohse, B. Oberhauser, B. Oberhauser-Hofbauer, G. Baschang, A. Eschenmoser, *Croatica Chim. Acta* 1996, *69*, 535.
[18] U. Diederichsen, D. Weicherding, N. Diezemann, *Org. Biomol. Chem.* 2005, *3*, 1058.
[19] L. D. Arnold, T. H. Kalantar, J. C. Vederas, *J. Am. Chem. Soc*. 1985, *107*, 7105.
[20] G. Roviello, S. Gröschel, E. Benedetti, U. Diederichsen, *Eur. J. Org. Chem.* In preparation for the submission

Experiences in foreign laboratories

During my PhD training, I attended for four months the laboratory of Institut für Organische und Biomolekulare Chemie, directed by the professor Ulf Diederichsen, at the Georg-August-Universität Göttingen (Germany).

Pubblications Index:

A short PNA targeting coxsackievirus B3 5'-nontranslated region prevents virus-induced cytolysis. Musumeci D, Valente M, Capasso D, Palumbo R, Gorlach M, Schmidtke M, Zell R, Roviello GN, Sapio R, Pedone C, Bucci EM. Journal of Peptide Science (in press) Published Online: 24 Aug 2005.

New synthesis of PNA-3'DNA linker monomers, useful building blocks to obtain PNA/DNA chimeras. Musumeci D., Roviello G.N., Valente M., Sapio R., Pedone C., Bucci E.M. Biopolymers (Peptide Science). 2004 Nov;76 (6) 535-542.

The oxidation of Δ^2, $\Delta^{2,4}$ and $\Delta^{4,6}$ steroids with RuO_4. Musumeci D., Roviello G.N., Sica D. Steroids. 2004 Mar;69(3):173-9.

Communications Index:

Optimal recognition of the lenght of DNA insertion/deletion patterns by HMGB1". Bucci E., Musumeci D., Roviello G., Sapio R., Valente M., Fumero S., Barone D., Bianchi M. "32° Congresso Nazionale della Società Italiana di farmacologia", Napoli 1-4 June, 2005.

Strategies for oligonucleotide sequence detection: Oligonucleotides-gold Nanocrystals Conjugates. Bucci E., Massa R., Messere A., Milano G., Moggio L., Musumeci D., Roviello G. N., Sapio R., Valente M., Pedone C. and Di Blasio B. (poster). From chemistry to technology. Belvedere di San Leucio, Caserta (Italy). November 11-13, 2004.

Targeting of PNA to a cytoplasmic virus. Musumeci D., Roviello G., Valente M., Bucci E., Pedone C., Palumbo R., Capasso D., Schmidtke M., Zell R. (poster). Journal of Peptide Science. 3rd International and 28th European Peptide Symposium. Prague (Czech Republic). September 5-10, 2004. Supplement to volume 10:196.

PNA/DNA Chimeras: New Strategies for the synthesis of PNA monomers. Roviello G., Musumeci D., Bucci E. and Pedone C. (poster and oral communication). 3th Sigma Aldrich Young Chemists Symposium. Riccione (Italy). May 19-21, 2003.

Antiviral PNA in the targeting of Coxsackievirus B3 genomic RNA. Valente M., Bucci E., Musumeci D., Roviello G., Sapio R., Capasso D., Palumbo R., Schmidtke M., Häfner S., Pedone C. (poster). 9th Naples Workshop on Bioactive Peptides. Villa Orlandi di Anacapri, Capri (Italy). May 8-11, 2004.

Strategies for oligonucleotide sequence detection: insertion of gold nanocrystals into oligonucleotides by Serinol moieties. Roviello G. N., Bucci E. M., Messere A., Musumeci D., Valente M., Sapio R., Pedone C. (poster). The Organic chemistry and the Nanotechnologies. Parco Scientifico e Tecnologico Vega, Marghera, Venice (Italy). April 1–4, 2004.